A Zebrafish Model of Uveal Melanoma

A Zebrafish Model of Uveal Melanoma

A dissertation presented

by

Kristin Melissa Rose

to

The Division of Medical Sciences

in partial fulfillment of the requirements

for the degree of

Doctor of Philosophy

in the subject of

Biological and Biomedical Sciences

Harvard University

Cambridge, Massachusetts

April 2015

Dissertation Advisor: Professor Leonard I. Zon Kristin Melissa Rose

A Zebrafish Model of Uveal Melanoma

Abstract

Uveal melanoma is the most common primary intraocular tumor in adults, and is often characterized by poor prognosis and few effective therapeutic options. The typical site of metastasis for uveal melanoma is the liver, and over 80% of patients with metastatic disease will die within one year of metastasis diagnosis. The vast majority of human uveal melanomas contain activating somatic mutations in the GPCR alpha subunits GNAQ or GNA11. To directly observe the *in vivo* effects of GNA11 Q209L (constitutively active) overexpression, I used a zebrafish cancer model in which plasmids can be injected into transgenic fish and melanoma formation can be assessed. Surprisingly, zebrafish injected with a construct overexpressing *mitfa*:GNA11 Q209L developed a significant incidence of uveal melanomas. A mini-screen of HOX genes using this system revealed a novel role for HOXB7, which also functioned as an inducer of uveal melanomas in our zebrafish model. Other plasmids containing oncogenes do not lead to uveal tumors, suggesting a specificity for GNA11 and HOXB7. Cell lines were derived from GNA11 Q209L-overexpressing zebrafish tumors and uveal melanoma cells were sensitive to PKC inhibition, which has been observed in human uveal melanoma cells as well. Additionally, RNAseq analysis of zebrafish uveal melanoma cell lines revealed high expression of genes such as *cyr61* and *ctgf*, YAP pathway genes that are known to be induced by GNAQ in human uveal melanomas. I found that overexpression of catalytically inactive BAP1, a chromatin factor whose function is frequently lost in metastatic uveal melanomas, led to a significant acceleration of overall melanoma onset but did not induce a uveal melanoma phenotype in our model. Morpholino experiments showed that knockdown of either zebrafish *gna11* or *bap1*

affected the spatial expression of *hoxb7a*, with a combined knockdown of *gna11* and *bap1* suggesting that *bap1* is epistatic to *gna11*. My studies demonstrate the first known instance of spontaneous uveal melanoma formation in response to overexpression of a human uveal melanoma oncogene, and that the resulting uveal melanomas share genetic features and drug response tendencies with human uveal melanomas. This model is a useful new tool for the study of uveal melanoma pathogenesis, genetics, and therapeutics.

Table of Contents

ACKNOWLEDGEMENTS

I would like to first thank my husband, Jamon, who has witnessed the ups and downs of my years in graduate school firsthand, has supported me unwaveringly, and has always put my happiness above all else. I also have to thank my mom for truly believing that I can do anything and be anything I want, and that I can be the best at it. Few people know that my mom and I talk three times a day on average, and I would like to thank her for the roughly 4000 phone calls exchanged while I have been in graduate school; I never had to feel too far from home.

I have to give a special thanks to Len for his support during my time in his lab. He put me onto a great project that any graduate student or post-doc would be lucky to have. He has also stuck by me through hard times personally and professionally, and never once threatened to kick me out of the lab! He really does care that everyone in his lab is happy and thriving, and his enthusiasm for science can be infectious (I think I will say "Should be good!" for the rest of my life).

I don't think this thesis would have been possible without the support of my technician, Rachel, and I can't thank her enough on paper. Aside from the fact that she is an essentially flawless scientist, Rachel is also an essentially flawless human being. She handles every task, big or small, with alacrity and grace. Aside from being the resident expert at countless lab techniques, Rachel always somehow knows just what kind of flowers or tasty treats will make my day, and just when I need them. She is truly one of a kind.

I am going to miss my other labmates-turned-family: Papa Chuck, Sister Julie, Brothers David and Justin. Chuck, whose family I've loved seeing grow over the years and who keeps me up to date on the latest science; Julie, who is a bottomless pit of motivation and is an inspiration to watch; David, for always knowing how to put life in perspective; and Justin, for answering a

million “quick questions” and spreading his deep appreciation for food. To everyone else in the Zon lab, thank you for always being happy to see me, and always wanting to see me happy. You are the reason I was the first person in my year to join a lab.

Many thanks as well to my dissertation advisory committee: Dave Langenau, Levi Garraway, and Yang Shi. Their input over the years has really moved my project forward in leaps and bounds. Their encouragement has been invaluable, and it has always been obvious that they truly want to see me succeed in science and beyond.

To the BBS office – Kate, Maria, and Danny – and my BBStars – Laura, Daisy, Stéphane, Kaitlin, Silvia, Niroshi, Ben, *et al.* – you all have made this program so much more than just a path to a doctorate. I didn’t know I could actually have so many friends at once, and so many ears willing to listen. Thank you all for some fantastic times, and whenever you “get low,” please think of me.

To anyone I forgot – my apologies, and thank you, too!

This dissertation is dedicated to the memory of my father,

Albert Edward Rose (June 28, 1935 – January 1, 2013).

"Give them hell, Kris."

CHAPTER 1: Introduction

Attributions

Richard White and I co-authored a review entitled “Zebrafish cancer – the state of the art and the path forward” (White RM, Rose KM, and Zon LI, Nat Rev Cancer. 2013 13:624-36). Excerpts from this review are included in the introduction chapter.

Overview

The zebrafish is a recent addition to animal models of human cancer, but is rapidly contributing major insights. Zebrafish develop cancer spontaneously, after mutagen exposure, and via transgenesis. The tumors resemble human cancers at the histological, gene expression and genomic level. Its combination of in vivo imaging, chemical and genetic screens, and high-throughput transgenesis offers a unique opportunity to functionally characterize the cancer genome in the post-TCGA era. Moreover, increasing sophistication at modeling combinations of genetic and epigenetic alterations will allow the zebrafish to complement what can be achieved in other models such as mouse and human cell culture systems.

The cancer biology field is rapidly heading towards a post-genomic state, in which the majority of human cancers will have been extensively sequenced. The next decade will witness a concerted effort to study the functional implications of this new sequencing data using human cell lines and animal models. No single model will fully capture the heterogeneous and evolving complexity of cancer, so we must rely on the strengths of a variety of systems to contextualize this information. Although mouse models will remain a cornerstone, recent years have now pointed to the unique capabilities of the zebrafish to help us understand cancer biology *in vivo*.

This chapter highlights key insights that have been gained from studying cancer in zebrafish, how cancer biologists can leverage technologies unique to zebrafish and what the key roles that the zebrafish will play in the coming decade. Specific review of uveal melanoma biology, genetics, and animal models is provided as uveal melanoma is the particular disease focus of this thesis.

Introduction to the zebrafish

The zebrafish emerged as a model organism for developmental genetics in the 1960s, described by George Streisinger as a "phage with a backbone". Its advantages for genetic studies were its high fecundity, the generation of transparent embryos that developed outside the mother, and the conservation of vertebrate organs that allow comparison to humans. The true utility of the model was established as a result of several large forward genetic screens [G] (Driver et al., 1996; Haffter et al., 1996) which identified mutants in virtually every organ or cell type, the majority of which are shared with mammals (**Figure 1.1**), demonstrating that the fish could be used to identify genetic mutants for essentially any phenotype.

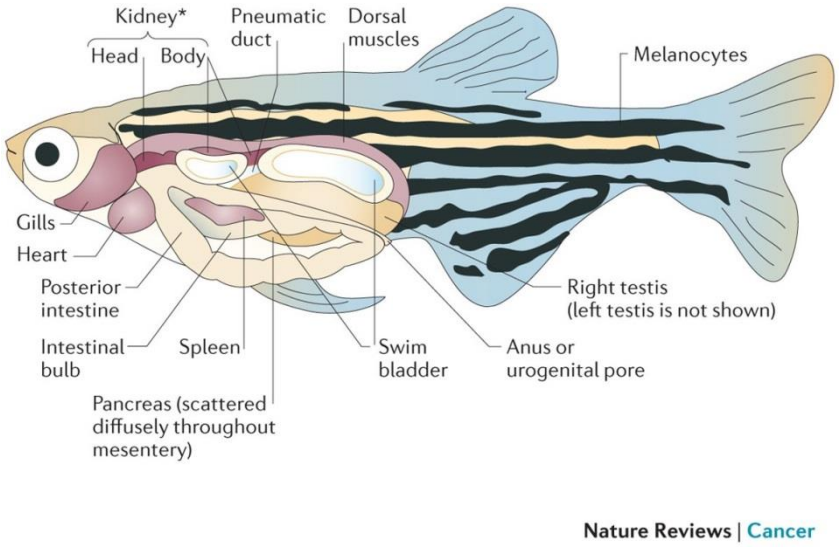

Figure 1.1. Zebrafish anatomy. An adult zebrafish is shown with the anatomical structures labelled. Zebrafish share most of their organs with mammalian counterparts, including the brain, heart, liver, spleen, pancreas, gallbladder, intestines, kidney, testis and ovaries. *The kidney is also the site of hematopoiesis in zebrafish.

Zebrafish as a cancer model

Fish have been known to develop cancer for well over a century. *Xiphophorus* species develop spontaneous melanoma, which was found to be due to activating mutations of the

tyrosine kinase *xmrk* (xiphophorus melanoma related kinase; Dimitrijevic et al., 1998). That zebrafish could be useful as a model for cancer was suggested in 1982, when it was found that exposure to carcinogens such as dimethylnitramine caused low penetrance tumor formation in zebrafish (Pliss et al., 1982). By 2000, it was recognized that zebrafish exposed to more common mutagens such as ethylnitrosourea (ENU), dimethylbenz(a)threcene (DMBA) and N-methyl-nitrosoguanadine (MNNG) develop a variety of neoplasms including skin papillomas, hepatic adenomas, rhabdomyosarcoma and seminoma (Beckwith et al., 2000; Spitsbergen et al., "DMBA," 2000; Spitsbergen et al., "MNNG," 2000). However, it was with the emergence of rapid transgenic technology in the zebrafish that the field jumped forward. Langenau and Look demonstrated that expression of the mouse oncogene *Myc* under the zebrafish recombination activating gene 2 (*rag2*) promoter resulted in the rapid onset of adult leukemias that emerged from the thymus, quickly spread, and were fully transplantable as seen by green fluorescent protein (GFP)-labeling of the tumor cells (Langenau et al., 2003). Since that time, numerous zebrafish models of cancer using transgenic expression of dominant acting oncogenes have been created (reviewed in Berghmans et al., "Making waves," 2005, and Stoletov and Klemke, 2008) (**Table 1.1**). Aside from oncogenes, the isolation of a zebrafish strain with mutant *tp53* (which encodes the tumor suppressor p53), which developed malignant peripheral nerve sheath tumors (Berghmans et al., "tp53 mutant," 2005), demonstrated that both oncogenes and tumor suppressors retained their evolutionarily conserved role in tumorigenesis. As increasing attention has come to the role of immune and microenvironmental regulation of cancer, it remains to be seen whether these aspects are also conserved in zebrafish. Advantages and disadvantages of using zebrafish to study cancer are summarized in **Table 1.2**.

Table 1.1. Transgenic models of cancer in the zebrafish.

Cancer	Oncogene	Tumour suppressor	Use in cancer biology	Refs
Melanoma	*mitfa–BRAF*^{V600E}	*tp53*$^{-/-}$	Genetic and chemical modifier screens	27, 30,31
	mitfa:EGFP:*NRAS*^{Q61K}	*tp53*$^{-/-}$		
	kita–Gal4 × *uas-HRAS*			
Pancreatic	*ptf1a–KRAS*^{G12V}–GFP		Genetic modifier screens	22,97
	ptf1a:Gal4–VP16 × *uas–KRAS*^{G12V}–GFP			
T cell lymphoma or leukaemia	*rag2–myc*		Cancer modelling and *in vivo* imaging	14,98
	rag2–lox–dsRED2–lox–EGFP–mMyc × *hsp70*–cre		Inducible cancer model	99
	rag2–NOTCH1		NOTCH1 interaction with Bcl-2	100,101
	rag2–myc × *rag2–bcl2*		Mechanisms of leukaemia dissemination	39
B cell leukaemia	*Xenopus* Spp. EF1α or zebrafish B actin–TEL–AML1 (ETV6–RUNX1)		Initiating events in B cell leukaemia	34
Numerous	b-actin–lox–GFP–lox–*KRAS*^{G12D} × *hsp70*–cre		Inducible cancer model	102
	krt4:Gal4VP16;14 × *uas:smoa1*–EGFP × *uas:myrAKT1*		Cooperation of hedgehog and AKT pathways	103
Rhabdomyosarcoma	*rag2–KRAS*^{G12D}		Identification of tumour-initiating cell populations	29
Neuroblastoma	dβh:EGFP–*MYCN*		Cooperation of MYCN and ALK	23
	dβh:EGFP and dβh:*ALK*^{F1174L}		Cooperation of MYCN and ALK	23
AML	*pu1–MYST3/NCOA2*–EGFP		First model of AML in zebrafish	104
MPNST		*tp53*$^{-/-}$	Conservation of tumour-suppressor pathways in zebrafish	17
			Major tumour type found in p53-deficient zebrafish	
Lipoma	*krt4*–myr*AKT1*		Platform for the study of drugs to treat lipoma and/or obesity	105
Ewing's sarcoma	*hsp70* or β-actin–*EWSR1–FLI1*	*tp53*$^{-/-}$	Conserved function of EWS–FLI1 fusion protein from human to fish	106
Liver	*fabp10*:LexPR; LexA:EGFP × cryB:mCherry; LexA:EGFP–*kras*^{G12V}		Inducible KRAS-G12V hepatocellular cancer model	36
	fabp10:TA; TRE:*xmrk*; *krt4*:GFP		Inducible EGFR-homologue hepatocellular cancer model	107
Pancreatic neuroendocrine	*zmyod–MYCN*		Pancreatic neuroendocrine model as a platform for downstream MYCN targets	108
Myeloproliferative neoplasms	*sp1–NUP98–HOXA9*		NUP98–HOXA9-induced oncogenesis from defects in haematopoiesis and aberrant DNA damage response	109
Corticotroph adenoma and neoplasm	*POMC–PTTG*		Identification of CDK inhibitors as possible treatment of corticotroph tumours	110
Testicular germ cell tumour	*fugu flck*–SV40 large T		Platform for modifier screens of testicular tumours	35

ALK, anaplastic lymphoma kinase; AML, acute myeloid leukaemia; CDK, cyclin-dependent kinase; EF1α, elongation factor 1α; EGFP, enhanced green fluorescent protein; *fabp10, fatty acid-binding protein 10, liver basic*; GFP, green fluorescent protein; *hsp70, heat shock protein 70*; *krt4, keratin 4*; *mitfa, microphthalmia-associated transcription factor a*; MPNST, malignant peripheral nerve sheath tumour; *myr, myristoylated*; *POMC*, pro-opiomelanocortin; *ptf1a, pancreas transcription factor 1 subunit a*; *PTTG*, pituitary tumour-transforming gene; *rag2, recombination-activating gene 2*; *smoa1, activated smoothened mutant*; *uas, upstream activating sequence.*

Table 1.2. Positives and negatives of using zebrafish for cancer research.

Advantages	Disadvantages
Large numbers of transparent embryos that develop outside the female and that grow rapidly. A single adult mating pair can produce 200 embryos or more per week.	Low incidence of spontaneous tumorigenesis, necessitating the use of mutagens and/or transgenic techniques.
Embryonic phenotypes are strongly predictive of adult phenotypes in most organs, allowing for the screening of relevant adult phenotypes using space-efficient embryos.	Short-lived when compared with humans, which makes direct comparison of age-related cancer phenotypes limited.
As vertebrates, zebrafish share nearly all organs with mammals, including the brain, eyes, heart, intestines, pancreas, kidneys and liver.	Organs are typically simpler than mammalian counterparts. For example, the kidneys resemble the mesonephric rather than the metanephric stage.
Fish have a complex immune system with a full range of immune effectors, such as T cells and B cells, macrophages and monocytes.	Some mammalian organs are not conserved, including the mammary and prostate glands.
Highly amenable to transgenic approaches. Mosaic (F0) transgenics can be created at a rate of 500–1,000 animals per day, and stable transgenic founders can be found in 50% of injected F0 animals using transposon-based systems.	The genome size is approximately one-half the size of the human genome, making comparisons outside genic regions difficult.
Both forward genetic (using ethylnitrosourea) and reverse genetic (using TAL-like effector nuclease and CRISPRs) techniques are well characterized and highly scalable.	The genome underwent a genome duplication event, so many genes have redundant copies, which complicates loss-of-function studies of tumour-suppressor genes.
Transparent adult strains (that is, casper) allow for detailed in vivo imaging of tumour growth, migration and metastasis.	Zebrafish grow at 28.5 °C, rather than at 37 °C, and are poikilothermic, limiting studies in which mammalian homeostatic temperature may be important to oncogenic phenotypes.
Large numbers of fluorescently tagged transgenic lines marking cells such as vascular endothelium, red and white blood cells, platelets and stroma are available.	Limited range of antibody reagents, making protein-based analysis more difficult.
There is high conservation of oncogenes such as BRAFV600E and NRASQ61K in zebrafish models of cancer. Microinjection of human genes under tissue-specific promoters leads to tumours that are similar to the human disease.	
Tumours in zebrafish strongly resemble human tumours at the histological, gene expression and genomic levels.	
Demonstrated success of chemical screening in zebrafish, which has led to clinical trials in patients with melanoma.	

There are several technologies available in the fish that have made it a unique contributor to the cancer field (**Figure 1.2**). In particular, cancer can be uniquely studied throughout the life of the animal, each stage with attendant experimental advantages that make zebrafish a powerful complement to other more traditional model systems. Below, we highlight some of the key

techniques that have emerged using zebrafish, particularly those with direct relevance to human cancer pathogenesis.

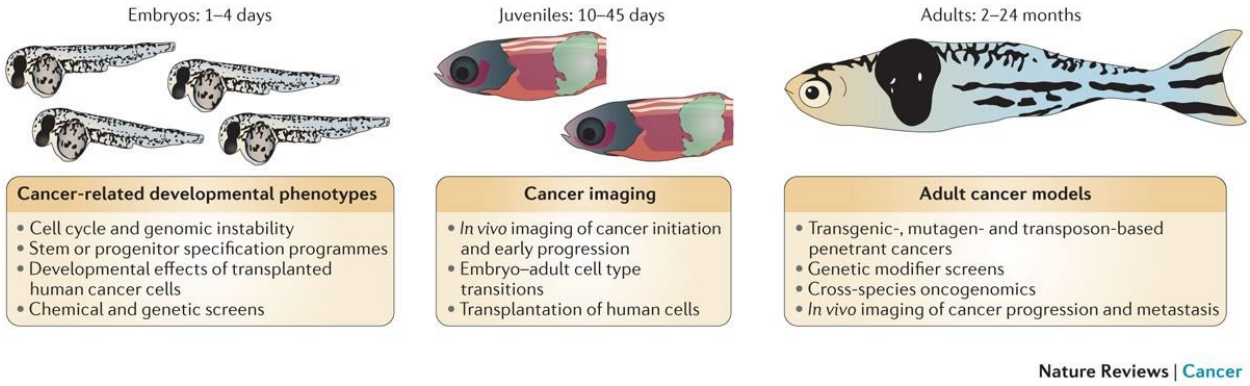

Figure 1.2. Studying cancer in the zebrafish. Differently aged animals each offer distinct advantages for cancer-relevant phenotypes. Embryos can be used to identify phenotypes that are highly relevant to cancer biology, such as defects in the cell cycle or genomic instability. Other embryo phenotypes may include stem or progenitor cells that act as cell of origin of the tumor or changes in embryo morphology on transplantation of human cells. Any of these phenotypes can then be used as the basis of chemical or genetic screens to find modifiers, which can be tested for their relevance to human cancer. Juvenile fish have the capacity for modelling early tumorigenesis and remain optically fairly translucent, lending themselves to detailed *in vivo* imaging. These cancers can be either from transgenic models or can arise via transplantation of tumor cells, and confocal imaging can be used to assess the tumor–stroma interaction at single-cell resolution. Adult fish develop fully penetrant and advanced cancers, both through transgenic techniques and through the transplantation of either zebrafish or human tumor cells. These animals are ideally suited to cross-species oncogenomics, either by directly testing candidate human genomic changes in the fish (by rapid transgenesis) or by comparing the profiles (DNA or RNA) of the mature tumor in the fish to that of the human to look for evolutionarily conserved events. Both the wild-type fish and the transparent casper model add improved capacities compared to mouse models for *in vivo* imaging and analysis of tumor stem cells and tumor progression and metastasis.

Cross-species oncogenomics

The zebrafish can be used to functionally characterize the large number of changes seen in human cancer, a major challenge that has emerged from projects such as The Cancer Genome Atlas (TCGA). This can be done in two primary ways: 1) by identifying changes in human cancer, and then testing these candidate changes in transgenic zebrafish models (**Figure 1.3a**), or

2) by comparing genomic alterations found in human cancers to those found in zebrafish models of cancer to find evolutionarily conserved "drivers" (**Figure 1.3b-d**). Both approaches have been successfully applied as outlined in **Figure 1.3**.

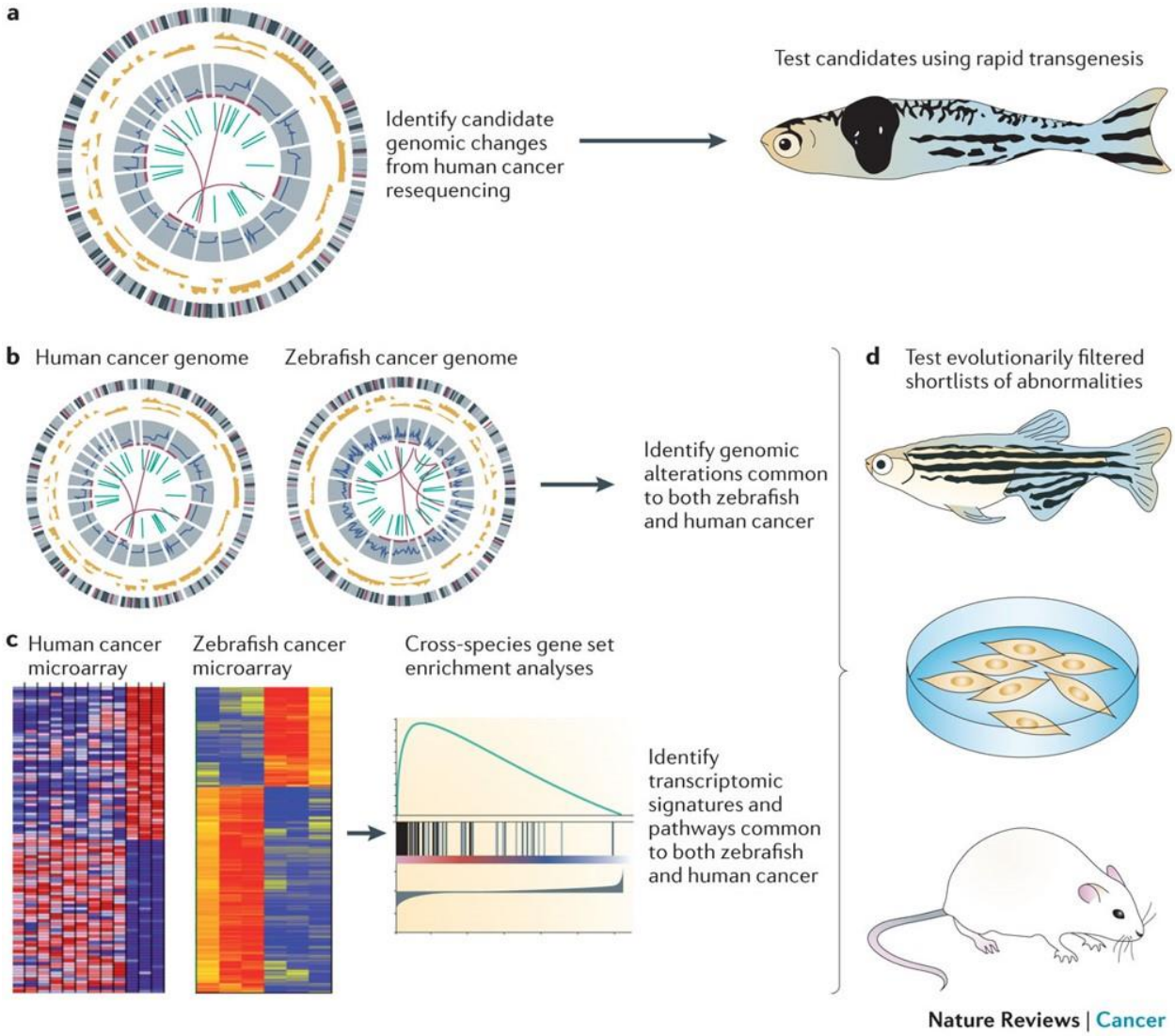

Figure 1.3. Cross-species oncogenomics provides a powerful way to identify highly evolutionarily conserved events in tumorigenesis. Candidate genomic changes in human cancers (**a**) are being identified through consortiums such as The Cancer Genome Atlas and the International Cancer Genome Consortium (ICGC), which have revealed thousands of potential mutations, copy number changes and structural variants, most of which have not been functionally analyzed *in vivo*. By testing a proportion of the high-confidence, recurrent events in transgenic zebrafish models, a direct readout of their effect on actual tumor biology can be rapidly achieved. This type of analysis can be carried out in the transient transgenic setting,

Figure 1.3 Continued. allowing for thousands of animals or variants to be tested in a single experiment. Because there are now numerous models of cancer in the zebrafish (**b, c**), the genomic profile of these fish tumors can be directly compared with that of the human tumors to look for events that are common between the two species. This can be done either at the level of DNA (**b**) by looking for common copy-number changes, mutations and structural variants, or at the RNA level (**c**) by looking for transcriptomic commonalities. This will essentially act as a 'filter' to provide much shorter lists of highly penetrant changes that are conserved across millions of years of evolution. These abnormalities can then be efficiently tested in cell culture, zebrafish and mouse models (**d**). Part **c** is reproduced, with permission, from Mizgirev, I. & Revskoy © (2011) Macmillan Publishers Ltd. All rights reserved.

Human melanoma is amongst the most genomically abnormal of all cancers, likely in part due to the accumulation of large numbers of UV-induced passenger mutations. Although common genetic alterations, such as $BRAF^{V600E}$ and $NRAS^{Q61K}$ mutations, are well documented in human cancer, these are insufficient to explain the aggressive behavior of the disease, and they likely cooperate extensively with other somatic changes during the course of tumorigenesis. Analyses of human melanoma samples using the GISTIC algorithm [G] had identified a number of regions of chromosomal amplification, and a subset of these were also overexpressed at the RNA level (Lin et al., 2008) but there was no immediate method to find which of these changes were biologically significant. Focusing on a region of chromosomal gain at 1q21 comprising ~30 genes, Houvras, Ceol and Zon developed an assay called miniCoopR to rapidly identify which are the key genes in this region (Ceol et al., 2011). Zebrafish harboring a transgene overexpressing human *BRAF*^{V600E} under the melanocyte-specific **microphthalmia-associated transcription factor a** (*mitfa*) promoter and in the context of p53 loss of function were bred to the nacre mutant, which encodes an inactivating mutation of *mitfa*. These animals are devoid of melanocytes and never develop melanoma. However, when embryos were injected with a rescuing miniCoopR plasmid encoding a *mitfa* minigene (again under the *mitfa* promoter), the

resulting mosaic adults had partially restored melanocyte stripes and rapidly developed melanoma. This assay was then adapted so that the injected plasmid could contain not only the *mitfa* minigene, but also any other gene of interest. They then systematically tested each of the 30 human genes in the 1q21 region. Over 3000 adult animals were screened, and a single gene, SET domain, bifurcated 1 (*SETDB1*), was found to cooperate with BRAF-V600E in mediating melanoma growth. SETDB1 induces this effect in part by overcoming BRAF-V600E mediated senescence, and tumors co-expressing both BRAF and SETDB1 exhibited signs of increased aggressiveness. SETDB1, a histone methyltransferase, was found to target a broad range of transcriptional targets, particularly those of the HOX family. Other groups have since identified the 1q21 interval as a novel melanoma-susceptibility locus for familial melanoma (Macgregor et al., 2011), solidifying the notion that SETDB1 is a bona fide oncogene in human melanoma. This study provides one key example of how the zebrafish can be rapidly used to 'filter' the vast number of genetic alterations that are found by sequencing human tumor samples, and identify the potential driver effects of such changes. Although similar approaches could be envisioned in human xenograft or mouse models (with shRNA or cDNA screens), the number of observed zebrafish provides a powerful incentive to utilize the fish as an initial screening tool. Furthermore, the power of this assay is that it directly reads out tumor incidence, providing an immediate *in vivo* context for any genetic hit.

Introduction to uveal melanoma

Uveal melanoma is the most common primary intraocular malignant tumor in adults (Chang et al., 1998). Uveal melanomas arise in the iris, ciliary body, or choroid of the eye, which together make up the uvea. This disease is difficult to treat and has a strong pattern of metastasis

to the liver. Approximately half of uveal melanoma patients will develop liver metastases, resulting in a poor prognosis of 87% mortality at one year (Gragoudas et al., 2003). Uveal melanomas are genetically and biologically distinct from more common cutaneous melanomas, and no effective therapies exist for metastatic uveal melanoma. Because uveal melanoma is an altogether rare disease, diagnosed in 5 people per million each year in the U.S. (Kumar et al., 2009), primary patient samples can be difficult to obtain and cell lines are not as prolific as other more common cancers. Additionally, much progress remains to be made in the area of animal models of uveal melanoma.

Uveal melanoma genetics

In 2005 it was determined that uveal melanomas frequently exhibit activation of the mitogen activated protein kinase (MAPK) pathway, but that this generally did not occur through mutated BRAF or RAS, as it does in cutaneous melanoma (Zuidervaart et al., 2005). This observation was partially explained a few years later when oncogenic mutations in guanine nucleotide-binding protein subunit alpha q (GNAQ) were identified to occur early in uveal melanomas (Onken et al., 2008). In fact, over 80% of uveal melanomas harbor activating mutations in the stimulatory alpha G-protein subunits GNAQ or guanine nucleotide binding protein alpha 11 (GNA11), typically a constitutively activating Q209L mutation (van Raamsdonk et al., 2010). GNAQ/11 have been shown to activate the MAPK pathway, with canonical downstream signaling that includes protein kinase C (PKC) activation. Mutations in GNAQ/11 occur early in neoplastic transformation and cooperate with loss of function in tumor suppressors, such as p53, to promote tumorigenesis (Onken et al., 2008). These mutations are

also mostly mutually exclusive with other mutations that are more common in cutaneous melanoma, such as BRAF, KIT, and others (Onken et al., 2008).

Although constitutive activation of the MAPK pathway is known to stimulate cell growth, GNAQ/11 mutations alone are insufficient to transform primary human melanocytes into melanomas (van Raamsdonk et al., 2009). More work is needed to identify the genetic signaling events that take place downstream of GNAQ/11 activation in uveal melanoma. More recently, GNAQ/11 activation has been shown to stimulate the Yes-associated protein (YAP) pathway in human embryonic kidney 293 (HEK293) cells transfected with GNAQ Q209L (Feng et al., 2014). This stimulation occurred through Trio-Rho/Rac circuitry that promotes actin polymerization, and occurred independently of phospholipase Cβ and the canonical Hippo signaling pathway (Feng et al., 2014). In these studies, constitutively active GNAQ promoted the expression of endogenous YAP-regulated genes connective tissue growth factor (*CTGF*) and cysteine-rich angiogenic inducer 61 (*CYR61*) and promoted YAP-dependent uveal melanoma cell growth. While these findings further our understanding of the roles of GNAQ/11 activation in uveal melanoma, the specific oncogenic signaling that arises from Gαq family members is not fully understood.

The most common site of metastasis in uveal melanoma is the liver, and about half of uveal melanoma patients will die of metastatic disease even with early diagnosis and proper treatment (Kujala et al., 2003). As many as 84% of uveal melanoma metastases contain inactivating somatic mutations in BRCA-1 associated protein 1 (BAP1; Harbour et al., 2010). BAP1 is a deubiquitinase that mediates deubiquitination of histone 2A (H2A) and host cell factor 1 (HCF-1; Scheuermann et al., 2010; Machida et al., 2009). When BAP1 pairs with the Polycomb group protein additional sex combs like transcriptional regulator 1 (ASXL1), they

form the catalytic component of the Polycomb repressive deubiquitinase (PR-DUB) which controls H2A ubiquitination levels and regulates expression of homeobox genes (Jensen et al., 1998; Scheuermann et al., 2010). Interestingly, there is no correlation between the activating GNAQ/11 mutations that are common in primary uveal melanoma and the inactivating BAP1 mutations found in metastatic uveal melanoma (Harbour et al., 2010). The most important genetic alteration for predicting poor prognosis in patients with uveal melanoma is inactivation of BAP1, which occurs most commonly through mutation of one allele and subsequent loss of the wild-type allele by complete loss of chromosome 3 (Monosomy 3; Harbour et al., 2010). More work remains to be done to elucidate the molecular events downstream of BAP1 loss of function in uveal melanoma.

Interestingly, gene expression profiling of primary uveal melanomas revealed that these tumors cluster naturally into two classes that are strongly correlated with risk of metastasis, class 1 being low-grade and class 2 being high-grade (Onken et al., 2004). As few as three genes were able to correctly predict the class labels of all uveal melanoma samples with no errors, and these genes were pleckstrin homology-like domain, family A, member 1 (*PHLDA1*), frizzed class receptor 6 (*FZD6*), and ectonucleotide pyrophosphatase/phosphodiesterase 2 (*ENPP2*). This three-gene signature also accurately predicted metastatic death. This study emphasizes the clinical importance of gene expression analysis and of the establishment of gene signatures in uveal melanoma.

Animal models of uveal melanoma

In 1981, an early effort at modeling uveal melanoma involved viral induction of ocular tumors in cats. Previously, McCullough et al. had determined that the Gardner strain feline

sarcoma virus, isolated from cats with sarcoma, could induce malignant melanomas in cats. To model uveal melanoma, this virus was injected into the anterior chamber of newborn kittens, a fluid-filled space between the iris and the cornea (Albert et al., 1981). The ocular tumors that arose in this study had a similar ultrastructural appearance to that of human ocular tumors. However, there was a high rate of mortality in infected animals, and tumor cells were found to have virus particles budding from the cell membrane, which is in striking contrast to human uveal melanoma. Another attempt to virally induce uveal melanoma involved introducing another oncogenic virus, simian virus 40, into hamster eye tissue grown *in vitro* before injecting this tissue subcutaneously into hamsters; tumors arising from this method were not melanocytic and therefore not melanomas (Albert et al., 1968). In addition to the caution required to work with oncogenic viruses, these studies produced tumors that most likely were not genetically similar to human uveal melanomas.

A common method for modeling uveal melanoma in animals is to inoculate animal eyes or embryos with tissue culture melanoma cells. The establishment of human uveal melanoma cell lines was an important step for this particular method. A proof of principle was shown in 1993 when *in vitro* cultured human uveal melanoma cells were injected into the chicken embryonal eye before the immune system had matured (Luyten et al., 1993). Twenty percent of embryos developed tumors and most survived embryogenesis. More recently in 2014, primary and metastatic human uveal melanoma cell lines were injected into the yolks of zebrafish embryos; these cells proliferated, and more migration and proliferation was observed in cells derived from metastases (van der Ent et al., 2014). This model was amenable to screening for metastasis inhibitors. Numerous studies have involved injecting suspension of human uveal melanoma cells into the eyes of immune-compromised rabbits or mice, and these models have been used to better

understand the nature of liver metastases in uveal melanoma, the pathology and vasculature of uveal melanomas, and the role of the immune system in metastasis of these tumors (Hu et al., 1994; Blanco et al., 2005; Yang et al., 2008; Mueller et al., 2002; Ma et al., 1995). However, all of these xenograft models required immature or suppressed immune systems. This is a disadvantage due to some of the important functions of the innate and adaptive immune system in the tumor microenvironment, in addition to the fact that biological differences in the host and recipient species could confound the behavior of these tumors. Also, cultured cells may acquire adaptive changes while growing *in vitro* that distinguish them from tumor cells *in vivo*.

Beyond the xenograft models described above, attempts have been made to generate engineered models of uveal melanoma that spontaneously develop these tumors. One such transgenic model uses a human tyrosinase enhancer/promoter fusion element to drive melanocyte-restricted expression of activated human *HRAS* in mice lacking the Ink4a/Arf tumor suppressor (Tolleson et al., 2005). Fifteen percent of these animals spontaneously developed uveal melanomas within 6 months. These tumors shared histopathological characteristics with human uveal melanomas. Another group assessed a melanoma mouse model that used the mouse dopachrome tautomerase promoter (dct) to drive melanocyte-specific expression of glutamate receptor 1 (Grm1; Schiffner et al., 2014). The Grm1 promoter had previously been implicated in melanoma after being found to contain multiple insertional mutagenesis events in a melanoma-prone insertional mouse mutant (Pollock et al., 2003). Schiffner and colleagues observed uveal melanocytic neoplasms in these mice and went on to find higher levels of Grm1 in human uveal melanomas than in normal eyes. With these models, however, the shortcomings with these models include the fact that *HRAS* mutations are not observed in human uveal melanoma (Zuidervaart et al., 2005), and GRM1 was only found to be upregulated in human uveal

melanoma by qRT-PCR in a small sample size (9 samples; Schiffner et al., 2014), with no studies implicating oncogenic properties of GRM1 in uveal melanoma.

Much work has been done to create a suitable animal model of uveal melanoma and animal models are highly valuable for this disease where patients and patient samples are rare. Progress in this area has provided a better understanding of this disease, but many caveats exist in current models. Work remains to be done in finding a satisfactory animal model that accurately reflects the genetics and therapeutic responses of uveal melanoma. I believe that the model I present in this thesis serves to advance existing animal models by providing the first instance of spontaneously-occurring uveal melanomas driven by a human uveal melanoma oncogene in an animal model.

Additional cancer modeling in zebrafish

Chemical genetics comes into focus

The term chemical genetics has come to encompass two overlapping concepts. First is the idea of using small molecules to uncover a basic biological process, roughly analogous to what can be achieved by using genetic mutants. The second is to use the *in vivo* capabilities of screening chemicals in a whole animal in order to find molecules with potential therapeutic relevance. Although a seemingly artificial separation, the choice of particular library, assay and downstream assessment of a chemical hit will largely determine the outcome of such approaches.

The zebrafish embryo is an ideal system on which to perform such screens (**Figure 1.4**). The embryo develops externally and one can obtain thousands of embryos per day, especially with the use of mass-mating chambers such as the iSpawn (Adatto et al., 2011). Phenotypes can be screened using brightfield, *in situ* hybridization or fluorescent approaches, and can be treated in 96 well format. Finally, one can vary the time of chemical exposure, so that modifiers of

virtually any cell type can be found if the chemical is applied at the correct developmental window. This is in contrast to genetic mutants, where the expression of a given phenotype is controlled solely by the period in which maternal RNA and protein contribution runs out during embryonic development and the strength of the particular allele.

The zebrafish has long been used to assess the teratogenic effects of chemicals (van Leeuwen et al., 1990). But it was the pioneering work of Schreiber and Peterson who first performed an unbiased "chemical screen", in which they tested several thousand small molecules for their effects on developmental endpoints (Peterson et al., 2000) such as central nervous system (CNS), melanocyte, heart and ear development, and demonstrated that careful regulation of the timing of drug administration and washout could affect specific organs.

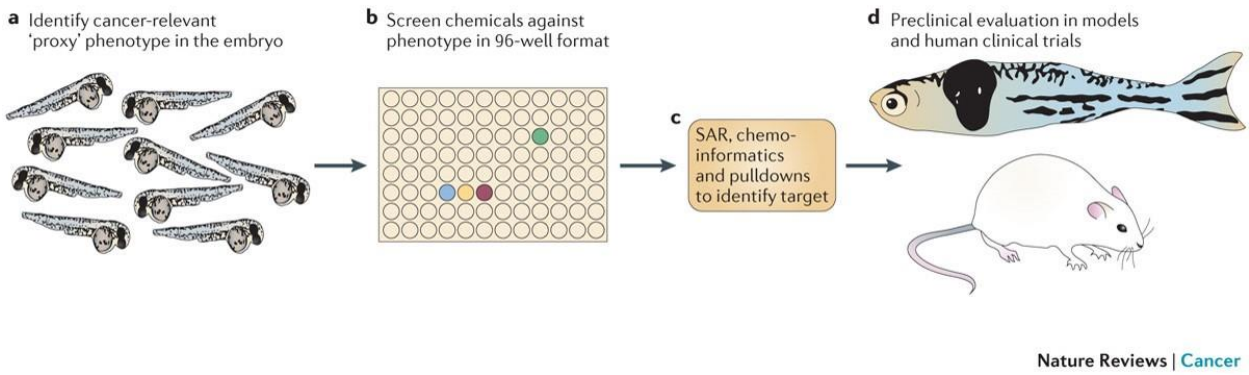

Figure 1.4. Chemical screening in the zebrafish. These types of screens are most efficiently carried out on embryos, given their amenability to large-scale, high-throughput manipulation and analysis. (**a**) Identification of an embryonic phenotype that is highly relevant to cancer is a key step in this process. An embryo stained for the neural crest marker crestin is shown; neural crest cells give rise to pigmented melanocytes but also to melanoma in the zebrafish. (**b**) After a relevant embryo phenotype is found, the embryos can be distributed in their chorions to plates, most typically the 96-well format. Each well will receive a distinct small molecule, either manually or with the aid of a liquid-handling robot. This method has been applied to screens ranging from 1,000 to 26,000 molecules. (**c**) Identifying the mechanism of hits is shown. This will primarily depend on the nature of the library used. Molecules with unknown function may require methods such as structure–activity relationships (SARs), chemoinformatics (using algorithms and databases such as PubChem, ChemBank or DiscoveryGate) or pulldowns using tagged versions of drugs and mass spectrometry. For libraries biased towards chemicals with US

Figure 1.4 Continued. Food and Drug Administration-approved or known mechanisms, this step can often be rapid, whereas for molecules of unknown function it can take up to 1 year or more. (**d)** While mechanistic evaluation is ongoing, chemicals can be tested for their effects on cancer in multiple downstream assays, including zebrafish cancer models or mouse transgenic and xenograft models. Depending on potency and safety, some of these hits will be amenable to testing in clinical trials in humans.

An early attempt to apply this approach to cancer was performed by Murphey and Zon, who screened for molecules that could rescue the cell cycle defect in a mutant called crash and burn (crb), which is mutated for the transcriptional regulator b-myb (also known as mybl2; Stern et al., 2005; Saville et al., 1998). They screened a library of 16,000 molecules (primarily of unknown function) and found a single hit, persynthamide, that almost completely normalized the mutant phenotypes. Unfortunately, the effects of this molecule could not be generalized to mammalian cancer cells.

Building on this experience, we performed a chemical screen to identify suppressors of the neural crest progenitors that give rise to melanoma (White et al., 2011). Transcriptional profiling of melanomas from the mitfa-BRAF;p53-/- model (Patton et al., 2005) revealed an upregulation of genes such as *crestin* and SRY-box containing gene 10 (*sox10*) that are normally only expressed in the embryonic neural crest, the cell type that ultimately gives rise to pigmented melanocytes. Reasoning that these neural crest programs are important in melanoma growth, we designed a screen using a library of ~2000 chemicals in zebrafish embryos to find suppressors of the *crestin*$^{+}$ lineage using *in situ* hybridization. We found that inhibitors of the metabolic enzyme dihydroorotate dehydrogenase (DHODH), such as leflunomide (which is used for patients with rheumatoid arthritis; Golicki et al., 2012), completely suppressed the expression of crestin and downstream genes such as *sox10* and *mitfa*. Leflunomide acts primarily at the level of the neural crest stem cell and not on differentiated derivatives and inhibition of DHODH was shown to

interfere with the transcriptional elongation of key genes that are required for neural crest development (such as *mitfa*) as well as myc target genes known to be required for neural crest development (Hong et al., 2008). Leflunomide inhibits the growth of human melanoma cells both *in vitro* and in mouse xenografts, and a phase I/II clinical trial of leflunomide in combination with the BRAF inhibitor vemurafenib has been initiated in patients with melanoma. This is the first example of a zebrafish screen directly leading to a clinical trial in human melanoma patients, the results of which will be instructive for future screens in the fish.

Because of developmental similarities between embryonic T-cell lymphoblasts and T-cell leukemia blasts, Ridges and Trede designed a screen to find suppressors of lymphoblast development that they posited would make therapeutics for T-cell leukemia (Ridges et al., 2012). Cross-testing against well characterized human T-cell leukemia cell lines revealed one potent hit they named lenaldekar which is active in human T-ALL mouse xenografts, without significant toxicity to the mice. Mechanistically, lenaldekar leads to decreased phosphorylation of downstream members of the PI3K-AKT-mTOR pathway, and identification of its direct target awaits further study. The inherent specificity of the screen combined with its potent activity makes this an exciting finding with potential for therapeutic utility in patients. Given that only 5-7% of molecules that enter phase I trials ever become useful therapeutics, screens such as this are likely to become models for future preclinical testing.

The field of chemical genetics in zebrafish is just emerging but its utility will be proven by the results of clinical trials in humans, which will become increasingly common. The advantages of using zebrafish for chemical screens must be counterbalanced by the reality that chemicals can have very divergent effects in different species, and not everything that works in a zebrafish will work in the human context. Moreover, the fish are “bathed” in the chemical, which

does not allow for establishment of tissue gradients that may be important for differential tissue effects. Finally, the majority of chemical screens are done in zebrafish embryos, not in adult animals, and thus the effects may not be completely relevant to adult cancer phenotypes. The ability to perform such screens in adults is limited by the larger size and complexity of handling thousands of adult zebrafish, and this has not yet been attempted in a systematic screening setting.

The next decade of zebrafish in cancer biology

Many of the technologies described above are reaching technical maturity, and are now widely available. The zebrafish is a unique model that has begun to shed light on cancer biology. The question for the field in the next ten years is: how does the zebrafish uniquely add to our knowledge of cancer biology in ways that are complementary, yet distinct, from more mainstream models? Below, we highlight areas that are likely to be particularly fruitful and of great interest to cancer biologists.

Large-scale reverse genetics to identify tumor suppressors

The majority of transgenic zebrafish models have relied on overexpression of dominant acting oncogenes. Comparatively fewer studies have interrogated tumor suppressor genes (TSGs; Choorapoikayil et al., 2012). However, many human cancer mutations occur in putative tumor suppressors, or in genes with unknown functions. Complicating this is the fact that many genes can have both tumor suppressor and oncogenic functions, depending on cellular context.

Loss-of-function studies using shRNA approaches in human cell culture and mouse models have developed rapidly in the past few years, but are hampered by the difficulties of studying a large number of candidate TSGs. This is one area in particular where zebrafish can

significantly contribute and can be achieved through two emerging technologies. First is the use of TAL-like effector nucleases (TALENs) and the Cas/CRISPr systems as extremely efficient and predictable methods of engineering genetic knockouts (Bedell et al., 2012; Dahlem et al., 2012). Second are advances in RNAi in the zebrafish (De Rienzo et al., 2012), using miR30-based approaches [G] now commonly employed in mouse shRNA studies (Premsrirut et al., 2011). This will allow tissue-specific and inducible knockdowns of virtually any candidate gene. Capitalizing on these two technologies, along with the thousands of potentially injectable embryos per day in the zebrafish, comprehensively testing hundreds or thousands of potential tumor suppressors, gleaned from human cancer sequencing studies, now seems possible. Since so many transgenic oncogene cancer models now exist, it will be straightforward to test these putative TSGs in those transgenic backgrounds.

Modeling multigenic changes in cancer

A second related issue is that cancer genomes harbor thousands or tens of thousands of mutations. The vast majority of mouse models study 1-4 genes at a time, although developments in creating targeted changes in embryonic stem cells and using these to generate chimeric animals holds promise for increasing this number (Premsrirut et al., 2011). Nonetheless, the simplicity of creating multigenic transgenic zebrafish models of cancer is unmatched. One can conceptualize creative extensions of the miniCoopR system to test not just two cooperating genes, but 5 or 10 or more. This is a critical missing piece of all current cancer models: the full spectrum of human cancer is not a 1-4 gene disease but a many gene disease, and *in vivo* models must begin to address this reality and embrace this complexity. The zebrafish is particularly well

suited to this challenge, and will begin to allow for a rational assessment of how complex genetic changes act together to mediate cancer initiation and progression.

Epigenetic modifications in cancer

Rapid progress in analyzing the epigenome of cancer is underway, assisted by the data that has emerged from the ENCODE consortium. There is little doubt that many cancers have an epigenetic component. Recent data in human leukemia suggests that genetic and epigenetic abnormalities are linked: somatic mutations in epigenetic regulators such as TET2, isocitrate dehydrogenase 1 (IDH1), IDH2, additional sex combs-like protein 1 (ASXL1), enhancer of zeste homologue 2 (EZH2) and DNA methyltransferase 3A (DNMT3A) highlight these complex interdependencies (reviewed in Shih et al., 2012). The ability to carry out high quality chromatin immunoprecipitation followed by deep sequencing (Ganis et al., 2012) as well as methylation profiling (Wu et al., 2011; Goll and Halpern, 2011) is rapidly emerging for zebrafish and will complement the work being done in mammalian systems. Moreover, the capacity for interrogating the phenotypic effects of knocking down or overexpressing epigenetic factors in transgenic cancer models will be a critical way to dissect, in an unbiased fashion, the roles of epigenomics in a variety of cancers.

Identifying cell intrinsic and microenvironmental regulators of metastasis

The combination of zebrafish imaging, genetics, small molecule screens and transgenics provides a novel method for interrogating both cell intrinsic and microenvironmental regulators of metastasis. Metastasis is an evolving, multistep process, necessitating better animal models. Large-scale, facile manipulation of tumor and microenvironment gives the zebrafish a unique

capability to study this process in vivo. Many zebrafish transplant studies have looked at how tumor cells interact with the vascular endothelium using the fli1-GFP line, but this cell type is only one of many in the microenviroment (Joyce et al., 2009). As transgenics that mark virtually any cell type are now available, it is easy to envision many investigations into how tumor cells interact with fibroblasts, macrophages, keratinocytes, epithelial cells, hematopoietic stem cells, osteoblasts, and others. For example, Feng and Martin (Feng et al., 2010) showed that induction of oncogenes such as HRAS in the melanocyte lineage leads to recruitment of endogenous myeloperoxidase-positive neutrophils, indicating that one of the earliest host responses to oncogene activation is an inflammatory reaction. This type of study exemplifies how transgenesis and *in vivo* imaging can come together in the zebrafish, and will become even more powerful as such studies are layered onto genetic mutants with defects in any of these cell types, in order to truly define which microenvironmental regulators are required for each step in metastasis.

Because of the heterogeneity of metastasis, our group has optimized a metastasis transplant assay using the casper zebrafish. Initial studies capitalized on the pigmented nature of zebrafish melanomas to visualize not only tumor growth at the transplant site, but also visualized single metastatic cells far from the transplant site. More recently, we have developed stable zebrafish melanoma cell lines marked by GFP that can be used for such transplant studies, and do not rely solely on pigmentation, which can vary widely amongst tumor cells (R. White, unpublished observations). Such lines can be applied to high-throughput assays to probe metastatic factors in vivo.

Final conclusions

The concept of using zebrafish as a cancer model, proposed just over a decade ago, has now begun to bear fruit. We are optimistic that the community of researchers using this system will continue to grow robustly. It is incumbent upon us to interact deeply with the mainstream cancer biology community who utilize human and mouse systems, so that there is a bilateral recognition that each model system offers a unique set of tools to understand tumor biology. Although the technologies described here are in varying stages of development, novel and unexpected tools will undoubtedly come to the forefront in the next decade, as the zebrafish community has a strong record of leading technological changes in biology.

Our lab has recently made great strides in the area of modeling melanoma using the zebrafish, specifically with the identification of *SETDB1* as a melanoma oncogene through the use of the miniCoopR system (Ceol et al., 2011). It is reasonable to hypothesize that the zebrafish could also be used to model uveal melanoma with the help of the miniCoopR system. Uveal melanoma is a rare disease with few treatment options and poor prognosis upon metastasis, and only in the last few years have discoveries been made as to some of the specific genetic aberrations that typify this disease. The identification of these common uveal melanoma mutations will assist with the establishment of more suitable animal models than were previously possible. A uveal melanoma animal model that accurately replicates some of the genetic signaling events in human uveal melanomas will be a powerful tool to better understand additional uveal melanoma genetics, as well as to study uveal melanoma pathogenesis, progression, and therapeutics discovery.

CHAPTER 2: Genetic drivers of uveal melanoma in zebrafish

Attributions

Leonard I. Zon and I conceived the project to study the induction of uveal melanoma by transgenesis in zebrafish. I performed the recombination reactions to generate miniCoopR plasmids used in transgenesis experiments. I performed the microinjection for the miniCoopR assays and surveilled the zebrafish for tumor formation, both with technical assistance from R. D. Fogley. I acquired photographs of live, anesthetized fish with uveal melanomas. I euthanized and preserved zebrafish prior to paraffin embedding, sectioning, and hematoxylin and eosin (H&E) staining being completed by the Brigham and Women's Hospital Pathology Core. I reviewed H&E slides for the presence of uveal melanomas, with consultation from Jon Aster (Brigham and Women's Hospital, Boston, MA) and Edwin Stone (University of Iowa, Iowa City, IA). I isolated zebrafish tumors and established tumor cell cultures. I performed statistical analysis of tumor onset rate and uveal melanoma incidence using MedCalc software. Additional cell line maintenance was provided by R. D. Fogley. I designed drug treatment experiments and performed the drug treatments and cell viability assays on cell lines with technical assistance by R. D. Fogley. I analyzed dose response data and generated dose response curves. I performed qPCR analysis of cell lines using primers provided by L. Jing. Western blots were performed by R. D. Fogley. R. D. Fogley extracted RNA from cell lines for RNAseq, processed the RNA, and prepared RNA libraries. RNAseq data was processed S. Yang, and this data was analyzed further by S. Yang, L. I. Zon, and me.

ABSTRACT

Uveal melanoma is a rare form of tumor that is difficult to treat and has a specific pattern of metastasis to the liver. Eighty-three percent of human uveal melanomas contain somatic mutations in GNAQ or GNA11, most commonly a Q209L mutation (van Raamsdonk et al., 2010). Many attempts have been made to establish a satisfactory animal model to effectively study uveal melanoma, a rare disease in humans. The spontaneous uveal melanomas that occasionally occur in some species are unpredictable, and various xenograft models require immunosuppression for tumor growth. In this work, I present the first animal model induced by a human uveal melanoma oncogene. I observed high rates of uveal melanoma formation by expressing the uveal melanoma oncogene GNA11 Q209L under the melanocyte-restricted *mitfa* promoter in Tg(*mitfa*:BRAF(V600E));*p53*-/-;*mitfa*-/- zebrafish. Cell culture methods allowed for the long-term propagation of a relatively purified population of zebrafish uveal tumor cells *in vitro*. RNAseq studies revealed induction of genes in the YAP and IGF-1 pathways by GNA11 Q209L in zebrafish uveal melanoma cells; these pathways have known functional roles in human uveal melanoma. A mini-screen of HOX genes led to a surprising induction of uveal melanomas. This work characterizes *in vivo* and *in vitro* zebrafish uveal melanoma models that advance the current tools available for the study of uveal melanoma pathogenesis, genetics, and therapeutics.

INTRODUCTION

Uveal melanoma is the cancer of the pigment-producing cells (melanocytes) of the iris, ciliary body, or choroid, which together make up the uvea of the eye. Although uveal melanoma is only diagnosed in about 5 people per million each year in the U.S., uveal melanoma is the most common primary intraocular tumor in adults (Kumar et al., 2009). Roughly half of uveal melanoma patients will develop metastases, primarily to the liver, with the metastatic disease having a poor prognosis of 87% mortality at one year (Gragoudas et al, 2003). Uveal melanoma is genetically and biologically distinct from cutaneous melanoma, and there is currently no effective treatment for the metastatic disease. Adding to the difficulty of studying the disease, no animal models have been developed to facilitate discoveries of new therapies.

Over eighty percent of uveal melanomas present with activating somatic mutations in the Gαq family members GNAQ and GNA11 (van Raamsdonk et al., 2010), specifically a constitutively activating GNAQ/11 Q209L mutation. These G-protein couple receptor (GPCR) α subunits have been shown to activate the MAP-kinase pathway, and canonical downstream signaling of Gαq family members includes protein kinase C (PKC) activation. While constitutively activated MAPK signaling has been shown to promote cellular growth, mutations in GNAQ on their own are insufficient to transform primary human melanocytes into melanomas (van Raamsdonk et al., 2009), and more work is needed to understand the genetic events downstream of GNAQ/11 activation in uveal melanoma. GNAQ mutations, which are mostly mutually exclusive with other common melanoma mutations (BRAF, KIT, etc.), appear to occur early in neoplastic transformation and cooperate with the loss of function in tumor suppressors such as p53 in order to promote tumorigenesis (Onken et al., 2008). Recent studies have indicated the ability of GNAQ/11 to stimulate YAP through Trio-Rho/Rac signaling circuitry

and independently of phospholipase C and canonical Hippo signaling (Feng et al., 2014). This GNAQ/11 signaling promotes YAP-dependent growth of uveal melanoma cells. However, the specific oncogenic signaling that arises from these constitutively activated Gαq family remembers is not fully understood.

Experimental models are critical for the assessment of novel diagnostic and therapeutic methods to prevent, detect early, or treat cancer. Animal models of uveal melanoma have previously consisted mainly of various orthotopic models, which have advanced my understanding of the morphology and immunohistochemistry of uveal melanomas (Dithmas et al., 2000; Diebold et al., 1997; Kan-Mitchell et al., 1989), but less so of the genetics of the disease. While these models benefit from tumors that develop in their natural microenvironment, immune suppression is necessary for tumor expansion in some models, and other models utilize melanoma cell lines of cutaneous origin. Virally-induced methods have also been used; the oncogenic RNA virus feline sarcoma virus induced uveal neoplasms when injected into the eyes of cats (Albert et al., 1981), and intraocular tumors with some similarities to uveal melanoma (e.g. a propensity to metastasize to the liver) were observed in mice expressing the simian virus 40 oncogene in pigment cells under the tyrosinase promoter (Bradl et al., 1981; Anand et al., 1994). Although proliferations of uveal origin have been biologically induced by these viral means, the presence of the virus in tumor cells and extraocular tumors forming from shed virus limit this model significantly as well. The area of animal models of uveal melanoma has lacked a transgenically induced model of uveal melanoma that reliably and consistently produces uveal tumors.

The zebrafish has recently gained much popularity for its use as a model organism for studying human cancers (White et al., 2013). As a vertebrate, the zebrafish genome shares

extensive similarity with the human genome, so many disease and developmental genes have counterparts in the zebrafish. Additionally, zebrafish are very genetically manipulated and are amenable to genetic analysis. The female zebrafish can lay up to 200 eggs per week, and this high fecundity is much more suited to broader genetic screens than may be possible in the mouse, for example. To date, cancers that have been modeled in zebrafish include, but are not limited to, melanoma, pancreatic cancer, T and B cell leukemia, liver cancer, and neuroblastoma.

My lab has previously developed a melanoma model in zebrafish wherein the human oncogenic BRAFV600E is expressed in a melanocyte-restricted manner and cooperates with p53 loss to generate melanoma (Patton et al., 2005). In this transgenic (*Tg*) zebrafish model, BRAFV600E is expressed under the control of the melanocyte-specific gene promoter *mitfa* on a *p53* null background (*p53-/-*). Melanocytes and melanomas that develop in *Tg(mitfa:BRAF(V600E)); p53−/−* zebrafish are suppressed by a *mitfa-/-* mutation and subsequently rescued by a transposon-based vector called miniCoopR (MCR) that drives the expression of a candidate gene in the rescued tissues. This model was used to identify a novel oncogene in melanoma, specifically the histone histone methyltransferase SETDB1 (Ceol et al., 2011).

Here, I have used this model to generate the first uveal melanomas induced by a human melanoma oncogene, GNA11 Q209L, in an animal model. A subsequent mini-screen of HOX genes using this model identified a novel role for HOXB7 in driving uveal melanoma formation. These uveal tumors were excised and cultured as cell lines that were used for genetic analysis by RNAseq, as well as to assess their response to MEK or PKC inhibition. My zebrafish uveal melanoma cells expressed YAP and glucocorticoid pathway signatures, and comparison of my cell lines to human uveal melanoma cell lines by RNAseq analysis revealed similarities between

zebrafish and human uveal melanoma genes. Additionally, GNA11 Q209L-overexpressing uveal melanomas were found to be sensitive to PKC inhibition. These genetic and drug-response features shared with human uveal melanomas support the validity of my model. This zebrafish uveal melanoma model will be a useful tool with unique benefits over currently available models for the study of uveal melanoma pathogenesis and the discovery of novel uveal melanoma therapies.

MATERIALS AND METHODS

miniCoopR assay

The miniCoopR (MCR) vector used was constructed as previously described (Ceol et al., 2011). Human GNA11 Q209L and HOXB7 cDNAs were purchased from the Harvard PlasmID Database and cloned into pENTR vectors with a pENTR/D-TOPO Cloning Kit (Life Technologies).MultiSite Gateway recombination reactions (Invitrogen) were utilized to create individual miniCoopR clones. MCR:EGFP was generously provided by Dr. Charles Kaufman (Childrens Hospital Boston, Boston, MA). One-cell zebrafish embryos were generated by incrosses of Tg(*mitfa*:BRAF(V600E));*p53*-/-;*mitfa*-/- zebrafish and these embryos were microinjected with 25 pg of each miniCoopR clone and 25 pg of Tol2 transposase mRNA. At 48 h post fertilization, the presence of rescued melanocytes was used as a readout to select transgenic animals. These animals were scored weekly for the presence of visible tumors. All fish were maintained at 28.5°C at a holding density of 15 fish/liter, and all procedures were approved by the local Institutional Animal Care and Use Committee. Survival analysis was performed using Kaplan-Meier life table analysis on MedCalc Software.

Histology

Fish were euthanized and fixed in 4% paraformaldehyde overnight at 4 C. They were then decalcified in 0.5 M ethylenediaminetetraacetic acid before paraffin embedding and sectioning. Staining was done according to the standard techniques by the Brigham and Women's Pathology Core.

Zebrafish tumor cell culture

Fish were euthanized on ice immediately prior to tumor dissection. The tumor was then placed into a dissection medium of 1:1 Dulbecco's Modified Eagle Medium and Ham's F-12 Nutrient Mixture (Life Technologies), with a final concentration of 1000 U/mL penicillin, 1000 mg/mL streptomycin, and 0.075 mg/mL liberase. The tumor was incubated in dissection medium for 30 minutes at room temperature with continual manual disaggregation by razor blade. Liberase is then inactivated by addition of a wash medium of 1:1 Dulbecco's Modified Eagle Medium and Ham's F-12 Nutrient Mixture (Life Technologies), with a final concentration of 1000 U/mL penicillin, 1000 mg/mL streptomycin, and 15% fetal bovine serum. The disaggregated tumor was then passed through a 40mm mesh filter, centrifuged at 500 rcf, and resuspended in a complete zebrafish medium (1:1 DMEM/Ham's 12, 15% FBS, 10ug/ml insulin, 10μg/ml holotransferrin, 1 x 10-8M selenous acid, 1/1000 chemically defined lipids, 1/1000 non-essential amino acids, 2mM glutamine (in addition the glutamine present in base media), 1/500 Primocin, 1/100 Penicillin-Streptomycin, 100uM sodium pyruvate, 1/1000 1M Hepes, and 10% zebrafish embryo extract) before plating on fibronectin-coated tissue-culture treated plastic. Cells were cultured at 28°C and passaged using 0.25% trypsin-EDTA until being weaned off of fibronectin and complete zebrafish media and onto tissue-culture treated plastic and DMEM with 10% FBS.

Drug treatments and cell viability

Cells were seeded at 30,000 cells per well in 96-well plates and treated for 48 h with the specified drugs at the indicated concentrations. Sotrastaurin (AEB071), vemurafenib, and trametinib were purchased from Sellek Chemicals (Houston, TX, USA) and reconstituted in DMSO. To quantitate ATP generated by metabolically active cells as a measure of cell viability, assays were performed using a CellTiter-Glo luminescent cell viability assay (Promega) per the manufacturer's instruction. After 48 h drug treatment, drug was removed from the assay plates by pipetting and was replaced by 50 μL untreated media and 50 μL Cell Titer Glo per well. Plates were agitated by shaking for 2 minutes to lyse cells and incubated at room temperature for 10 minutes to stabilize the luminescent signal. After incubation, the luminescent intensities of the wells were measured by using a BioTek Synergy 2 multi-well plate reader.

Western blot analyses

Western blots were performed with primary antibodies recognizing ERK1/2 (Cell Signaling Technology 9012), phospho-ERK1/2 (Cell Signaling Technology 4370), and PKC ε (BD Transduction Laboratories 61005). ERK1/2 primary antibody was diluted 1:1000, phosphor-ERK1/2 primary antibody was diluted 1:2000, and PKC ε primary antibody was diluted to a final concentration of 1 μg/mL. Secondary antibodies used were ECL Anti-Mouse IgG [HRP] (GE Healthcare), 1:10,000 dilution and ECL Anti-Rabbit IgG [HRP] (GE Healthcare), 1:10,000 dilution. All antibodies were diluted in 5% bovine serum albumen in phosphate buffered saline with 0.1% (v/v) Tween 20. All incubations were 1 h at room temperature, shaking. Twenty micrograms total protein was loaded per lane. All transfers were made using the iBlot Dry Blotting System (Life Technologies).

Real time PCR

RNA was extracted from zebrafish cell lines and cDNA was generated using the Superscript III First-Strand Synthesis System (Invitrogen) with oligo(dT) primers, per the manufacturer's instruction. Target gene expression was measured by quantitative PCR with SsoFast EvaGreen Supermix (Bio-Rad) with three technical replicates, per the manufacturer's optimized cycling conditions for Bio-Rad's CFX96 Real Time PCR System. Beta-actin was used as a control. Primer sequences are listed in **Supplementary Table S6**.

RNA collection and RNAseq data processing

Cells were lysed on ice using Buffer RLT Plus (Qiagen) and lysates were homogenized with QIAshredder columns (Qiagen) before total RNA was purified using the RNeasy Plus Mini Kit (Qiagen). Ribosomal RNAs were removed with Ribo-Zero rRNA removal kit (Illumina). RNA was sequenced on the HiSeq 2500 System (Illumina) with 40 million paired-end reads. Quality control of RNA-Seq datasets was performed by FastQC and Cutadapt to remove adaptor sequences and low quality regions. The high-quality reads were aligned to UCSC build hg19 of human genome or UCSC build danRer7 of zebrafish genome using Tophat 2.0.11 without novel splicing form calls. Transcript abundance and differential expression were calculated with Cufflinks 2.2.1. Principle component analysis by CummeRbund was used to find and exclude outliers. Sequences in exons were combined to form complete spliced messenger RNAs and these were counted to generate fragment per kilobase per million (FPKM) values. FPKM values were used to normalize and quantify transcripts; the resulting list of differential expressed genes are filtered by log fold change > 1 and q-value > 0.05.

Differential Expression analysis

Aiming to find out genes associated with different samples, two approaches were applied to the analysis of RNA-Seq data. First, the absolute expression levels (FPKM value) of each sample are compared. Top N expressed genes were compared among samples in a Venn diagram. The value for N was optimized to attain maximum overlaps within the Venn diagram. Second, the most differentially expressed genes (by log fold change) were derived from differential expression analysis. The combination of these two approaches resulted in highly expressed genes that are most differentially expressed between uveal and cutaneous melanoma. Heatmaps were used to show the relative expression levels of these selected genes among samples.

Pathway and Functional analysis

Gene Set Enrichment Analysis (GSEA) and Ingenuity Pathway Analysis (IPA) were used to uncover the biological pathways associated with the top differentially expressed genes. Gene Ontology enRIchment anaLysis and visuaLizAtion tool (GORILLA) relied on the GO term assignment of each gene to discover common GO terms enriched in gene lists. All of these analysis are based on pathway or GO annotation of human genes; zebrafish genes were associated to their orthologous human genes based on ZFIN annotation (ZFIN: The Zebrafish Model Organism Database; zfin.org).

RESULTS

GNA11 Q209L transgene produces uveal melanomas in zebrafish

In humans, it is has been found that as many as 83% of primary uveal melanomas harbor GNAQ/11 mutations and that these are early events in tumorigenesis (van Raamsdonk et al., 2010; Onken et al., 2008). To study the effect of GNA11 Q209L overexpression *in vivo*, I generated transgenic strains of zebrafish expressing GNA11 Q209L under the control of the melanocyte-restricted zebrafish *mitfa* promoter (**Figure 2.1A**). I utilized *Tg(mitfa:BRAF(V600E));p53-/-* zebrafish in which melanocytes and melanomas were suppressed by a *mitfa-/-* mutation. Melanocytes and melanomas were subsequently rescued by the transposon-based vector miniCoopR (MCR), which drives candidate gene expression in rescued tissues. Embryos were injected with the plasmid DNA at the one-cell stage and raised to adulthood. It was observed that fish injected with MCR:GNA11 Q209L frequently developed uveal melanomas, while EGFP-overexpressing control fish developed none in a 25 week period. Specifically, 31% of melanomas that arose in transient transgenic MCR:GNA11 Q209L fish were uveal in origin and the remainder were cutaneous (**Figure 2.1C, D**). These uveal tumors were commonly pigmented and unilateral (**Figure 2.1B**). When MCR:GNA11 Q209L fish were mated to *Tg(mitfa:BRAF(V600E));p53-/-;mitfa-/-* fish to identify germline transmission of the MCR:GNA11 Q209L transgene, the percentage of uveal melanomas remained stable in the F1 generation (**Figure 2.1D**). In MCR:GNA11 Q209L fish, uveal melanomas and cutaneous melanomas can occur in the same animal, and the rate of cutaneous melanoma onset in these fish is comparable to that seen in MCR:EGFP fish (**Figure 2.1E**). Overall melanoma onset, including cutaneous and uveal tumors, was significantly accelerated by GNA11 Q209L overexpression (**Figure 2.1F**). In this model, the stably inserted *mitfa:BRAF(V600E)* transgene was required for

all tumor formation (**Figure 2.1F**). My studies demonstrate that spontaneous uveal melanomas can be transgenically induced in an animal model using a human uveal melanoma oncogene.

Figure 2.1. GNA11 Q209L causes uveal melanomas in zebrafish. (**A**) Schematic representation of transgenes. (**B**) Animals injected with the GNA11 Q209L construct develop uveal melanomas (black arrow) (**C**). Uveal melanoma legion (red arrow) observed in the eye of GNA11 Q209L transgenic animal, intact retinal pigmented epithelium indicated with a black arrow. Left image at 10X magnification; right image is a zoom-in of the area boxed in red on the left image. (**D**) Relative incidences of uveal melanoma by transgene and generation. Significant increase in uveal melanoma incidence (compared to uveal melanoma incidence in MCR:EGFP animals) is marked by asterisks (*** $p<0.001$). The n values for each cohort of animals is as follows: MCR:EGFP, n = 42; MCR:GNA11 Q209L F0, n = 42; MCR:GNA11 Q209L F1, n = 50. (**E**) Rate of cutaneous melanoma formation in MCR:GNA11 Q209L and MCR:EGFP fish. (**F**) Percent overall melanoma-free survival in MCR:EGFP fish and MCR:GNA11 Q209L fish with and without *mitfa:BRAF(V600E)* transgene, with p-values indicated.

Figure 2.1 Continued.

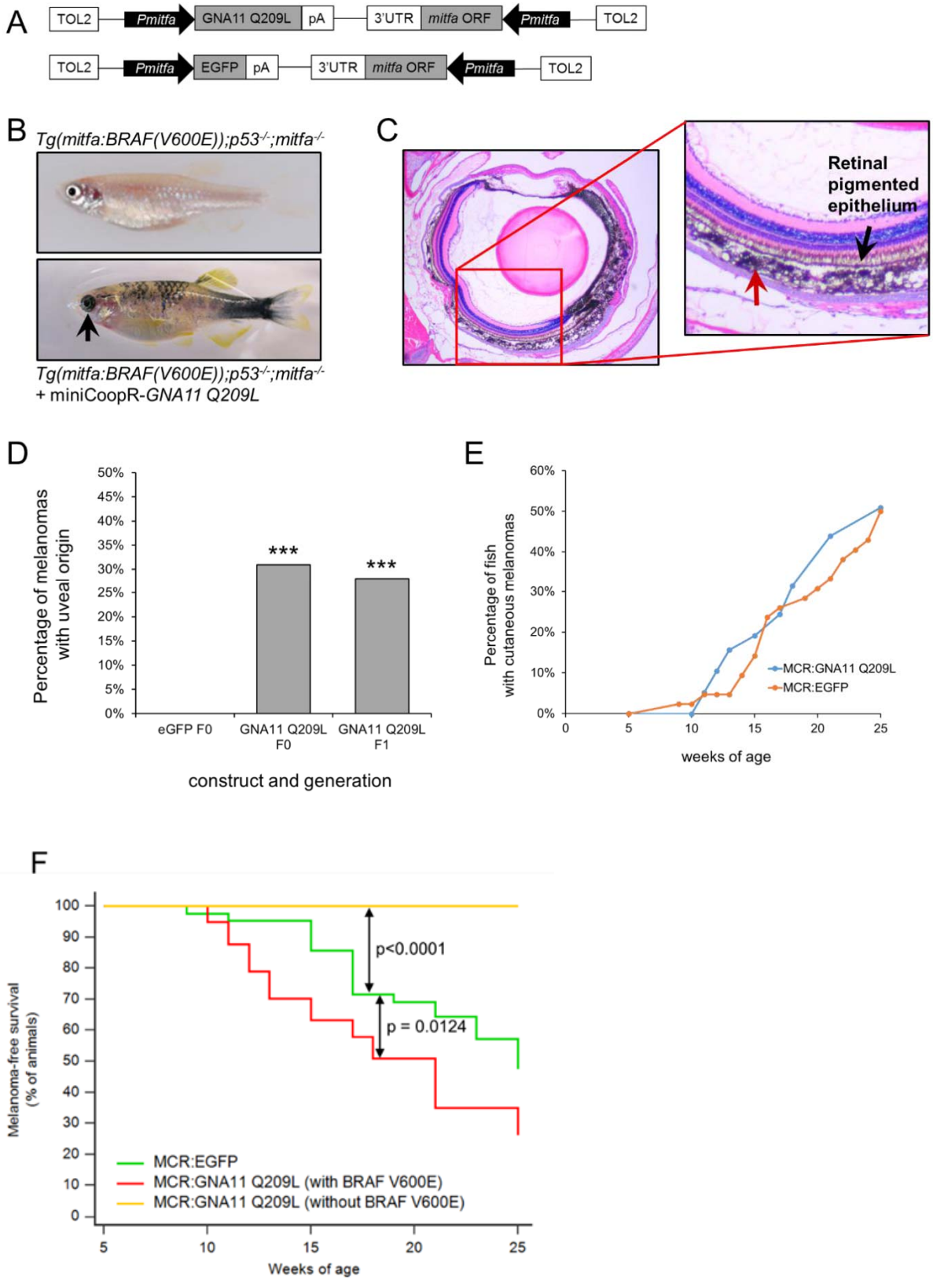

Zebrafish cell culture and sensitivity to PKC inhibition in GNA11 Q209L-overexpressing uveal melanoma cells

Challenges exist to studying the uveal melanoma cells of a zebrafish uveal melanoma tumor. Isolation of the tumor involves enucleation of the affected eye, and tumor tissue is grossly indistinguishable from normal eye tissue and stroma. Previous attempts to assess gene expression differences between uveal and cutaneous melanomas in both zebrafish and human datasets showed that uveal melanoma data was contaminated with eye-specification genes. To achieve a more pure uveal melanoma cell population, uveal tumors from MCR:GNA11 Q209L fish were excised and maintained in cell culture. This process involved euthanizing the fish followed by immediately dissecting the tumor, performing manual and chemical (by liberase treatment) disaggregation, filtering the cells, and then plating on fibronectin-coated tissue culture treated plastic in a cell medium containing zebrafish embryo extract and optimized for zebrafish cell growth. In addition to establishing MCR:GNA11 Q209L uveal tumor cell lines, I also applied this process to develop cutaneous melanoma cell lines from MCR:GNA11 Q209L and MCR:EGFP fish. After roughly two months in culture and about 10 cell passages, cell cultures were essentially uniform tumor cell populations and free of stromal cells. This is a recently developed system in my lab, and due to issues with low efficiency, I elected study one uveal or cutaneous cell line of each genotype.

PKC isoforms are known to be involved in GNAQ/GNA11-mediated activation of MAPK pathways (Hubbard et al., 2006; Naor et al., 2000). Specifically, GNAQ/GNA11 signals are propagated and amplified through activated PKCs which further activate ERK1/2 through the RAF/MAPK/ERK1/2 pathway (Naor et al., 2000). PKC inhibition has previously been shown to be an effective means of therapeutic targeting in uveal melanoma harboring GNAQ mutations,

both *in vitro* and in *in vivo* xenograft and allograft models (Wu and Zhu et al., 2012; Wu and Li et al., 2012; Chen et al., 2014). I sought to test the effects of PKC inhibition, MEK inhibition, or BRAF inhibition on my GNA11 Q209L-overexpressing zebrafish cutaneous and uveal melanoma cell lines, compared to an EGFP-overexpressing zebrafish cutaneous melanoma line as a control. This was done with the hypothesis that my GNA11 Q209L-overexpressing cell line would be sensitive to PKC inhibition, which would further establish the utility of my uveal melanoma model as being reflective of *de novo* human melanoma.

PKC inhibition was mediated by sotrastaurin (AEB071), BRAF inhibition was mediated by vemurafenib, and MEK inhibition was mediated by trametinib. AEB071 has proven effective at inhibiting growth of GNAQ-mutant uveal melanoma cells in *in vitro* and *in vivo* models (Wu et al., 2012; Chen et al. 2014), and trametinib has been used in Phase II trials for uveal melanoma patients (NCI #9445). BRAF-mutant uveal melanoma cells, while rare, have been shown to undergo cell cycle arrest with vemurafenib treatment (Mitsiades et al., 2011). GNA11 Q209L-overexpressing uveal melanoma cells were more sensitive to PKC inhibition than GNA11 Q209L- or EGFP-overexpressing cutaneous cell lines (**Figure 2.2A**). At 40 μM AEB071 treatment, cell viability of GNA11 Q209L-overexpressing uveal melanomas had dropped to 10%, compared to 81% and 70% in GNA11 Q209L- and EGFP-overexpressing cutaneous melanoma cells, respectively (**Figure 2.2A**). GNA11 Q209L overexpression in cutaneous or uveal melanoma cells also appeared to confer some resistance to BRAF or MEK inhibition compared to EGFP-overexpressing cutaneous cells (**Figure 2.2B, C**). BRAF/MEK inhibition had little effect on GNA11 Q209L-overexpressing uveal melanoma cells. These observations support the notion that PKC inhibition is a rational developmental therapeutic strategy in GNAQ/GNA11 uveal melanoma, and that my model is reflective of the human disease.

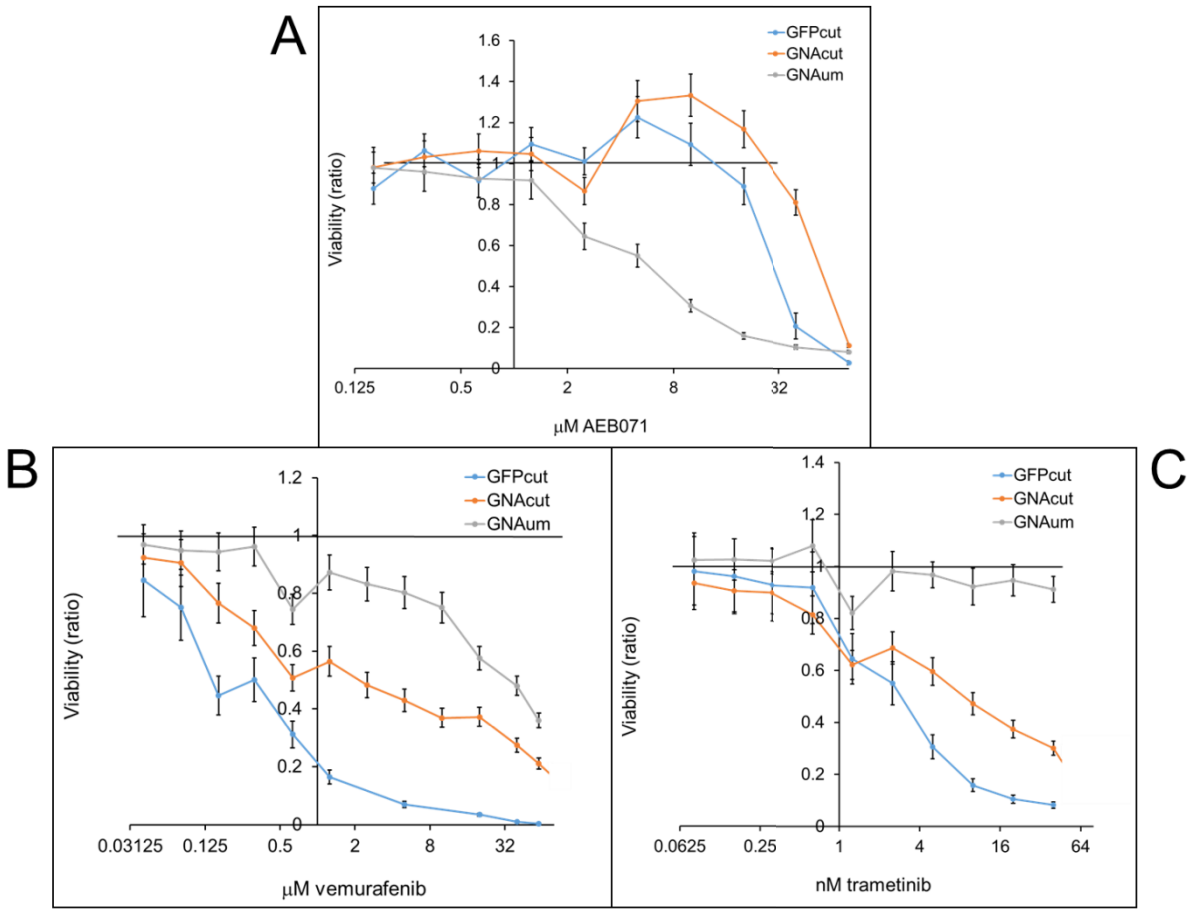

Figure 2.2. Effect of PKC, BRAF, or MEK inhibitor treatment on GNA11 Q209L-overexpressing zebrafish uveal melanoma and GNA11 209L- or EGFP-overexpressing cutaneous melanoma cell lines. AEB071 selectively reduced viability of zebrafish uveal melanoma cells overexpressing GNA11 Q209L. Cells were treated for 48 h with varying amounts of (**A**) AEB071, (**B**) vemurafenib, or (**C**) trametinib. GFPcut, EGFP-overexpressing cutaneous melanoma cells; GNAcut, GNA11 Q209L-overexpressing cutaneous melanoma cells; GNAum, GNA11 Q209L-overexpressing uveal melanoma cells. Data represent mean values ± s.e.m, performed on triplicate experiments.

A mini-screen for HOX genes in melanoma identifies HoxB7 as a regulator of uveal melanoma

I sought to test whether my zebrafish cancer model would be amenable to screening for novel genetic factors in uveal melanoma. A previous interest in the Hox genes had

been established in my lab when the miniCoopR assay was used to identify the novel melanoma oncogene SETDB1 (Ceol et al., 2011), and transcriptional dysregulation of the Hox genes was observed in SETDB1-overexpressing melanomas. I interrogated Hox expression in the Oncomine database (Rhodes et al., 2004) and found misexpressed Hox genes in a gene expression profile dataset of 63 uveal melanoma patients, reported by Laurent et al. in 2011, as well as in a gene expression profile dataset of 20 uveal melanoma patients, reported by Tschentscher et al. in 2003. I performed a proof of principle mini-screen of eight human Hox genes in my miniCoopR assay to test for a resultant increased incidence of uveal melanoma.

One Hox gene in particular, HoxB7, induced a striking rate of uveal melanoma formation in my zebrafish model (**Figure 2.3C-E**). In these animals, nearly half (47%) of melanomas were uveal (**Figure 2.3E**). Overall melanoma onset rate was accelerated by HOXB7 overexpression at a near-significant level ($p = 0.054$, logrank chi-squared test; **Figure 2.3F**). Interestingly, when MCR:HOXB7 fish were mated to *Tg(mitfa:BRAF(V600E));p53-/-;mitfa-/-* fish to generate stably transgenic animals, the rate of uveal melanomas in the F1 and F2 populations increased greatly to 74% and 80%, respectively (**Figure 2.3E**). While HoxB7 expression was low in the majority of the Tscentscher uveal melanoma samples in Oncomine (**Figure 2.3A**), this could be explained if HOXB7 function in my zebrafish uveal melanoma model is redundant with the function of other genes in human uveal melanomas. This is the first instance of HOXB7 being implicated in uveal melanoma.

Figure 2.3. HOXB7 overexpression induces uveal melanomas in zebrafish. (**A**) Misexpression of HOXB7 in 20 human uveal melanoma patient samples (Tschentscher et al., 2003); image downloaded from Oncomine. (**B**) Schematic representation of transgenes. (**C**). Animals injected with the HOXB7 construct develop uveal melanomas (black arrow). (**D**) Uveal melanoma legion (red arrow) observed in the eye of HOXB7 transgenic animal, intact retinal pigmented epithelium indicated with a black arrow; 10X magnification. (**E**) Relative incidences of uveal melanoma by transgene and generation. Significant increase in uveal melanoma incidence (compared to uveal melanoma incidence in MCR:EGFP animals) is marked by asterisks (**** $p<0.0001$, *** $p<0.001$). The n values for each cohort of animals is as follows: MCR:EGFP, n = 42; MCR:HOXB7 F0, n = 55; MCR:HOXB7 F1, n = 47; MCR:HOXB7 F2, n = 15; MCR:GNA11 Q209L F0, n = 42; MCR:GNA11 Q209L F1, n = 50. (**F**) Percent overall melanoma-free survival in MCR:EGFP, MCR:GNA11 Q209L, and MCR:HOXB7 fish, p-values indicated.

Figure 2.3 Continued.

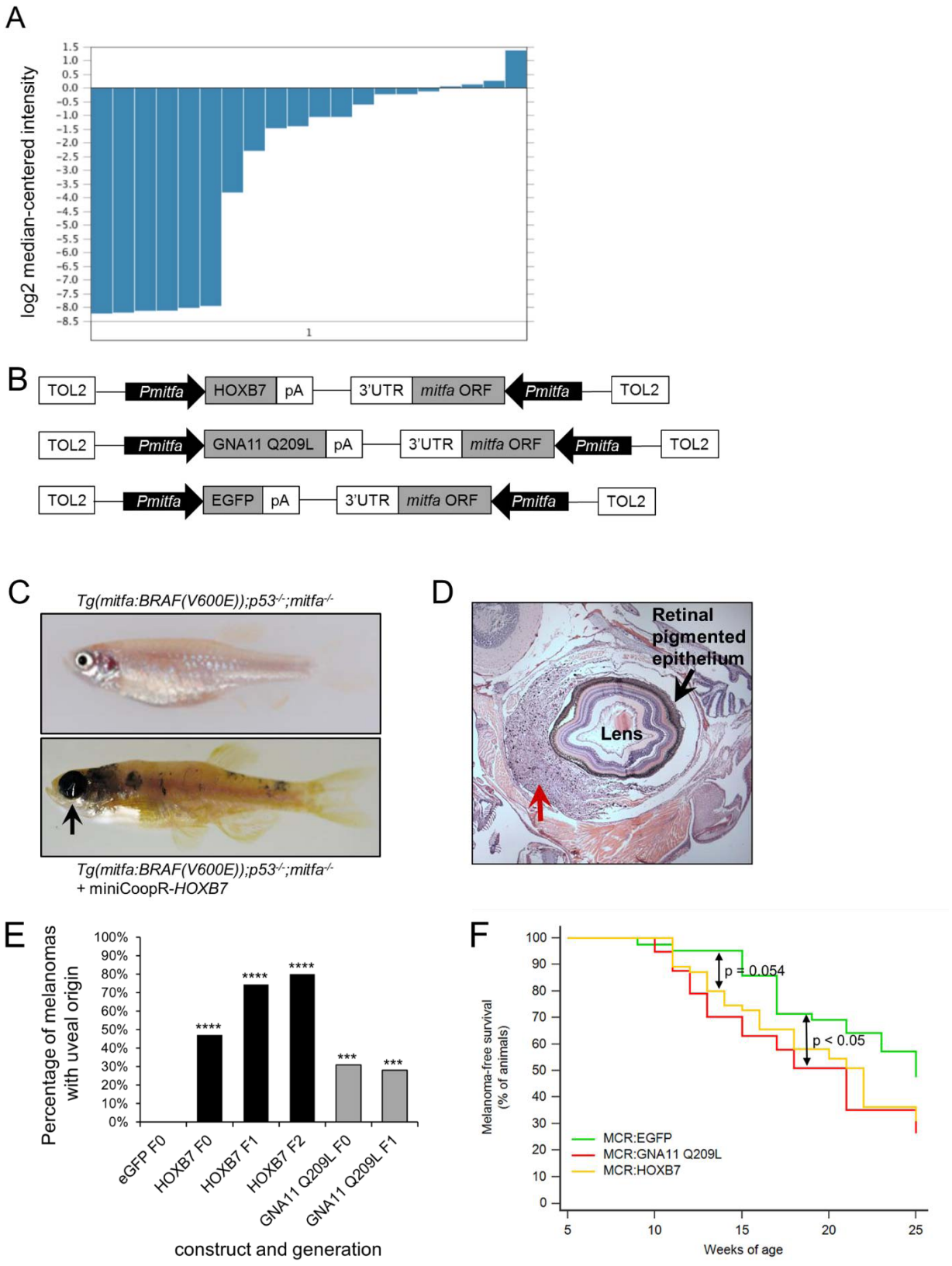

I established cell lines from cutaneous and uveal melanomas isolated from MCR:HOXB7 zebrafish, in the same manner mentioned previously. I sought to assess whether GNA11 Q209L or HOXB7 overexpression altered Hox gene expression, as was observed in Ceol et al.'s work and in the previously described Oncomine databases. In my cutaneous cell lines, qPCR analysis showed zebrafish *hox* gene expression to be altered by HOXB7 or GNA11 Q209L overexpression compared to EGFP overexpression (**Figure 2.4**). One *hox* gene that is suppressed by HOXB7 or GNA11 Q209L overexpression is *hoxb7a*, potentially suggesting that HOXB7 overexpression serves a function redundant with endogenous *hoxb7a* and that this function may also be served by GNA11 Q209L. Additionally, HOXB7 and GNA11 Q209L generally (for all but one *hox* gene assessed) had the same directional effect on *hox* expression; overexpression of HOXB7 or GNA11 Q209L both led to a decrease in most *hox* genes (**Figure 2.4**). Taken together, these findings validate my model as one that can be utilized as a screening system to find novel oncogenes in uveal melanoma.

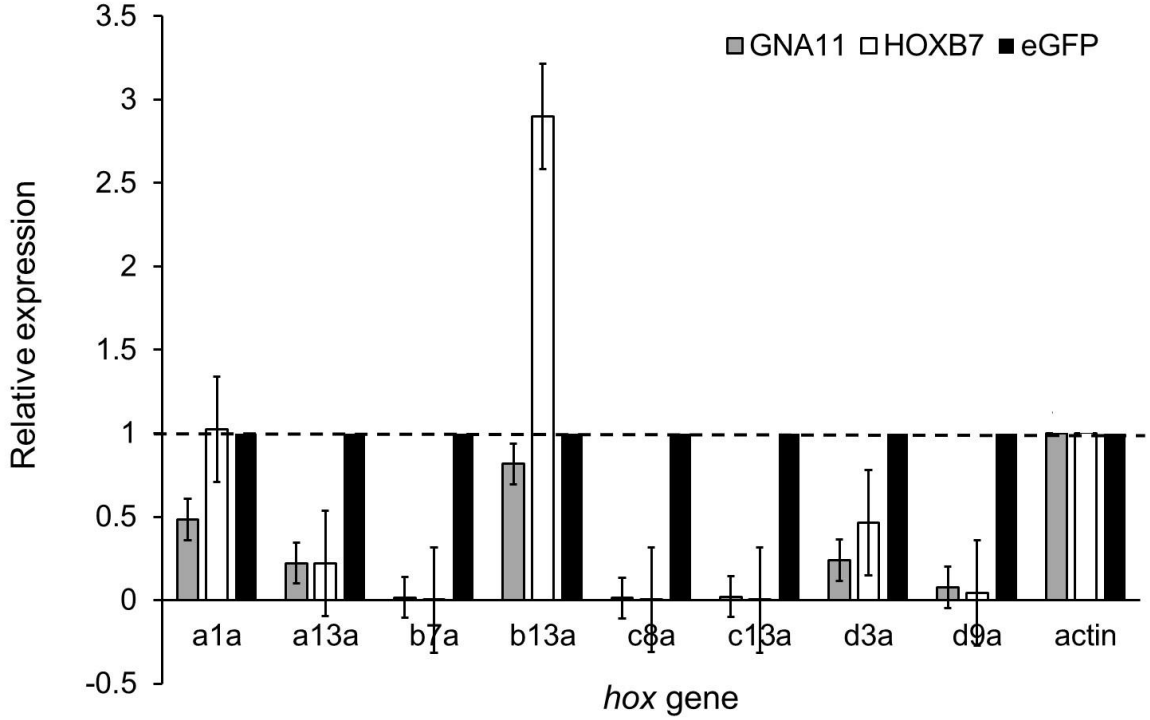

Figure 2.4. Hox gene expression in zebrafish cutaneous melanoma cell lines. Gene expression was determined by qPCR and expressed as a ratio of the amount of *hox* gene expression to the amount of expression of the housekeeping gene beta actin ("actin"), and expression levels in GNA11 Q209L- and HOXB7-overexpressing cells were normalized to expression levels in EGFP-overexpressing cells. Abbreviations are used for each *hox* gene shown on the x-axis such that, for example, *hoxa1a* is represented by 'a1a'. SE is represented by the error bars.

RNAseq and gene expression analysis reveal similarities between zebrafish and human uveal melanoma.

I sought to identify gene expression features which would confirm my zebrafish uveal melanoma model as a potentially useful tool for future uveal melanoma studies. RNA was isolated from GNA11 Q209L- and HOXB7-overexpressing zebrafish uveal and cutaneous melanoma cell lines, as well as from an EGFP-overexpressing zebrafish cutaneous melanoma cell line, and analyzed using RNA-seq technology to assess expression levels of coding mRNA transcripts. The top 1000 most highly expressed genes by sequence count in each of these five

cell lines were identified, and genes that fell into the top 1000 genes for two or more cell lines were used to generate gene lists representing overlaps in expression between cell lines (**Figure 2.5A**).

A "uveal melanoma signature" for my zebrafish melanoma cell lines was generated by identifying a list of 138 genes found in the top 1000 most highly expressed genes by both my HOXB7- and GNA11 Q209L-overexpressing uveal melanoma cell lines, but not found in the top 1000 most highly expressed genes of my EGFP-overexpressing cutaneous melanoma cell line (**Figure 2.5B**; **Supplementary Table S1**). This zebrafish uveal melanoma signature contained several genes whose human orthologs have known roles in human uveal melanoma and related biology. The YAP pathway genes *CYR61* and *CTGF* were present in the list of zebrafish uveal melanoma genes, and upregulation of these genes was recently used as a measure of the ability of GNAQ to induce YAP pathway genes (Feng et al., 2014). Additionally, *sparc*, an angioregulatory matricellular and pro-proliferative factor that is positively correlated with metastatic death in uveal melanoma (Ordonez et al., 2005; Maloney et al., 2009), was highly expressed in my uveal melanoma cell lines. Another gene linked to uveal melanoma metastasis, *capza1*, which has been used as one of fourteen genes whose protein expression discriminates uveal melanomas with metastatic potential from those without (Linge et al., 2012), was found on my uveal melanoma gene list. Invasion and metastasis in choroidal melanoma (of which uveal melanoma is a subset) are processes that involve increased expression of CTGF as well, also seen on this list (Mou et al., 2011). Other genes, like the proto-oncogene *jund* and the MAPK inhibitor *dusp1*, have roles more broadly in tumor and MAPK biology (Hirai et al., 1989; Sun et al., 1993). The identification of genes in my RNAseq studies that have known roles in human

uveal melanoma biology additionally adds credence to my model as an appropriate proxy for the human disease.

Gene Ontology (GO) terms and Ingenuity Pathway Analysis (IPA) were also used to investigate the nature of gene sets that were highly expressed in my zebrafish cell lines. GO terms analysis revealed four genes – *cdx4, pitx2, rx3,* and *aldh1a2* – that specified a significantly enriched camera-type eye morphogenesis program ($p = 7.86x10^{-6}$) in my uveal signature (**Supplementary Figure S1, Supplementary Table S2**), despite over a year in cell culture. By IPA analysis, the top upstream regulator in my uveal melanoma cell lines regulator was p53 (**Supplementary Table S3**); although the uveal melanoma cells in my model are p53 null, 34 genes from the uveal melanoma signature are classically regulated by p53 and would reasonably have expression changes in its absence. Interestingly, the top canonical pathway associated with the uveal melanoma signature by IPA analysis was glucocorticoid receptor signaling (**Supplementary Table S4**). Glucocorticoids have been shown to contribute to an adaptive immune privilege in the eye by suppressing the actions of immune cells (Kinsley et al., 1994). The zebrafish uveal melanoma signature contains genes that help to explain the biology of the zebrafish uveal melanomas in my model, and establish genetic parallels between my zebrafish uveal melanomas and human uveal melanomas.

Comparison of zebrafish and human uveal melanoma by gene expression analysis

To compare my zebrafish uveal melanoma gene signature with genes found in human uveal melanoma data sets, RNAseq data was gathered from 8 cutaneous melanoma cell lines by our lab, and 6 uveal melanoma cell lines by Levi Garraway's lab (Dana Farber Cancer Institute, Boston, MA; **Supplementary Table S5**). One way to establish a uveal melanoma signature from

this human RNAseq data was to isolate the significantly differentially expressed genes by fold change between all cutaneous cell lines and all uveal cell lines, and filter them for genes that are highly expressed in the uveal melanoma samples. As an example of this approach, a heat map was made showing genes with average fragment per kilobase per million (FPKM) values over 40 across uveal cell line samples, and whose log2 fold changes are greater than 3 on average in uveal melanoma cell lines compared to cutaneous melanoma cell lines. This produced a list of 50 genes that stratify well between human uveal and cutaneous melanomas (**Figure 2.5C**). This gene list included *CTGF* and *CYR61*, found in my zebrafish uveal melanoma signature and described above. Another relevant gene from this list is *GNAI1*, a Gαi subunit that, similarly to GNAQ/11, has constitutively active mutants found in a variety of cancers (O'Hayre et al., 2013). Additionally, analysis of matched patient normal and cancer DNA (The Cancer Genome Atlas, TGCA, http://cancergenome.nih.gov) shows *GNAI* ranking in the top 1% of genes for copy number gains in cancers of the central nervous system and kidney. Also present in this heat map was *ECM1*, Extracellular Matrix Protein 1, a marker for tumorigenesis that is correlated with invasiveness and poor prognosis in a variety of cancers; this gene has been shown to regulate metastasis and cancer stem cell-like properties through stabilization of β catenin (Lee et al., 2015).

I then sought to identify genes from my zebrafish uveal melanoma signature that were also found among the most significantly upregulated genes in human uveal melanoma versus cutaneous melanoma cell lines. Fifteen of the 138 zebrafish uveal melanoma signature genes had human orthologs among the significantly upregulated genes in human uveal melanoma cell lines. A heat map of these 15 genes across zebrafish cell lines showed that they stratify well by expression levels between cutaneous and uveal melanoma cells, and a heat map of the 13

orthologs of these genes in human cell lines showed a similar stratification (**Figure 2.5D**). The YAP pathway genes *CTGF* and *CYR61* appear on these lists, as well as *JUND* (mentioned above). Additionally, *NR4A1* was found on these lists, and this nuclear receptor has been shown to be highly expressed in many tumor types and has growth-promoting, angiogenic, and prosurvival activity in cancer (Lee et al., 2011). Because 11% (15/138) of the genes in the zebrafish uveal melanoma signature were also present among the genes most significantly upregulated in human uveal melanoma cell lines, I feel that my zebrafish uveal melanomas are suitable models of the *de novo* human disease.

Further probing of the human uveal melanoma cell line RNAseq data by gene set enrichment analysis (GSEA) provided biological insights into these cell lines. The third most enriched gene set in human uveal melanoma cells compared to cutaneous melanoma cells was that of vasopressin, a hormone involved in water retention and blood vessel constriction (**Figure 2.5E**). Interestingly, vasopressin acts through GPCRs that are selectively linked to GQ/G11 G-proteins (Schöneberg et al., 1998), the same class of G proteins whose activation plays a known role in uveal melanoma (van Raamsdonk et al., 2010). Additionally, the vasopressin-related gene list includes *ARHGDIA*, the Rho-GDP dissociation inhibitor whose homolog is found in my zebrafish uveal melanoma signature. *GNAS*, a stimulatory G-protein, is also in the vasopressin gene set. Another notable feature of the GSEA analysis of human uveal melanoma cell lines was the fact that four of the top 20 most enriched gene sets involved Notch signaling (**Figure 2.5F**). The Notch cascade has been shown to be active in uveal melanoma and its activity promotes tumor growth and invasion (Asnaghi et al., 2012). Enriched gene sets in human uveal melanoma revealed insights about the biology of human uveal melanoma and may have therapeutic implications for treatment of the disease.

Figure 2.5. RNAseq analysis of zebrafish and human uveal and cutaneous melanoma cell lines (**A**). Venn diagram of top 1000 most highly expressed genes by RNAseq FPKM values in all five zebrafish cell lines analyzed. Cut.GFP, EGFP-overexpressing cutaneous melanoma cells; cut.B7, HOXB7-overexpressing cutaneous melanoma cells; cut.GNA, GNA11 Q209L-overexpressing cutaneous melanoma cells; uveal.B7, HOXB7-overexpressing uveal melanoma cells, uveal.GNA, GNA11 Q209L-overexpressing uveal melanoma cells. (**B**) The 138 genes at the intersection of the most highly expressed genes by HOXB7- or GNA11 Q209L-overexpressing uveal melanoma cells (blue box), comprising a uveal signature. (**C**) Heat map of genes with average FPKM value greater than 40 in human uveal melanoma cell lines and whose log2 fold change is 3 or greater in human uveal melanoma vs human cutaneous melanoma cell lines. Cell line identities for each annotation are in **Supplementary Table S5**. JR1 and JF1-9 are human cutaneous melanoma cell lines, all "UMCL" cell lines are human uveal melanoma cell lines. (**D**) Heat maps showing (top) significantly upregulated genes in human uveal melanoma cells whose zebrafish orthologs are in the 138-gene zebrafish uveal melanoma signature, and (bottom) genes in the zebrafish uveal melanoma signature whose human orthologs are highly significantly upregulated in human uveal melanoma cells. (**E**) Gene set enrichment plot of the vasopressin gene set in human uveal melanoma cells. (**F**) Gene set enrichment plots of Notch-related gene sets in human uveal melanoma cells.

Figure 2.5 Continued.

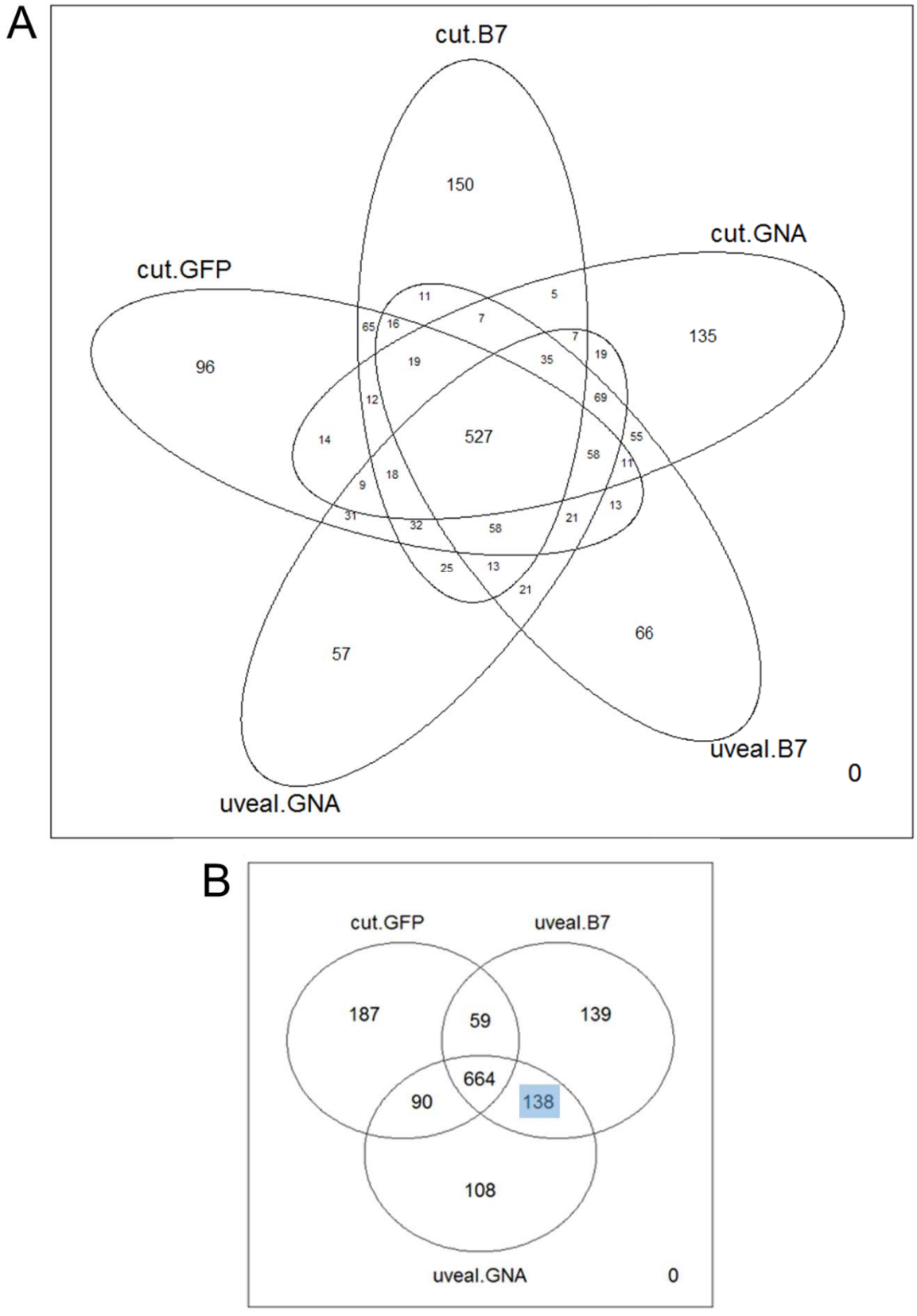

Figure 2.5 Continued.

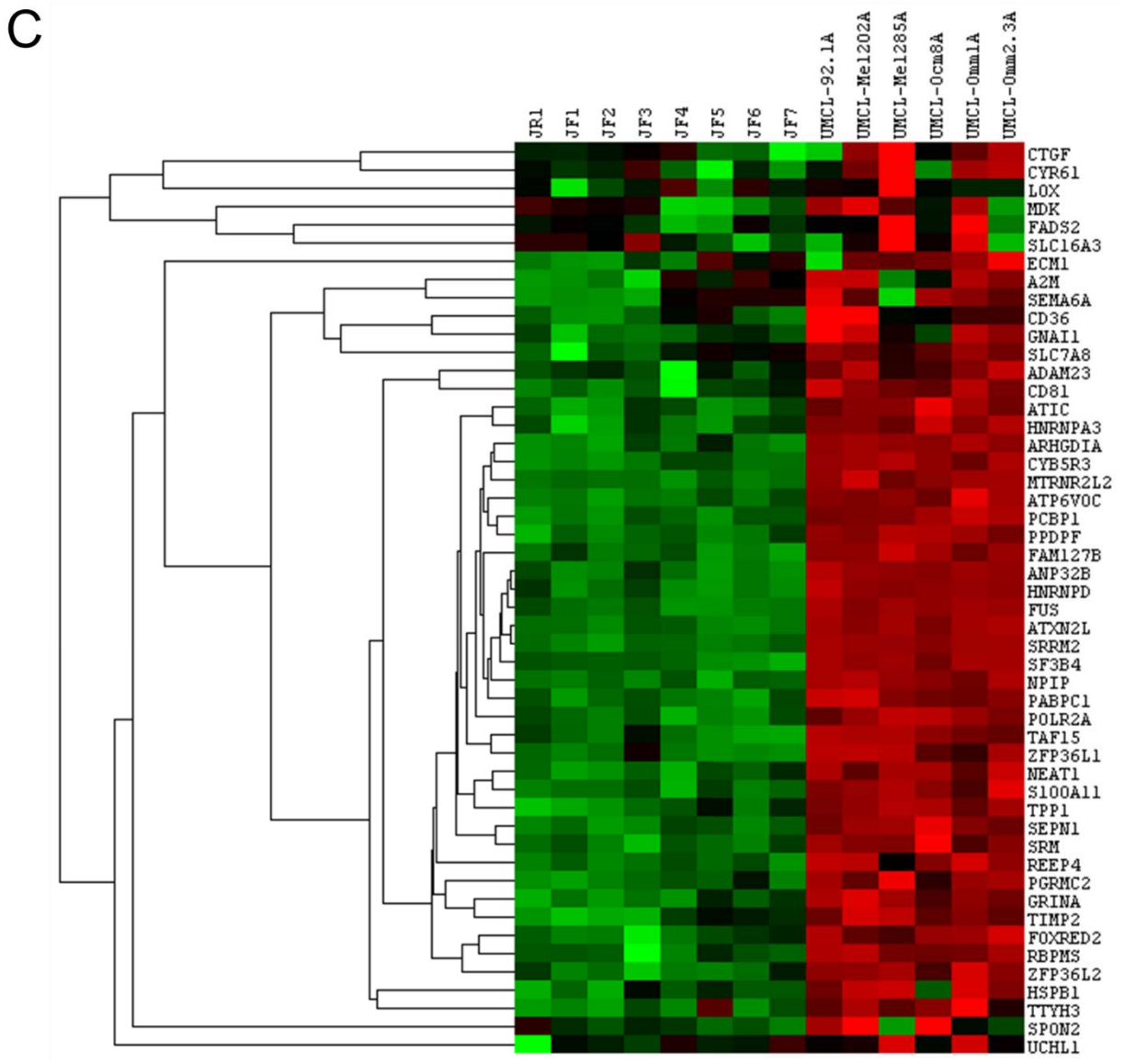

Figure 2.5 Continued.

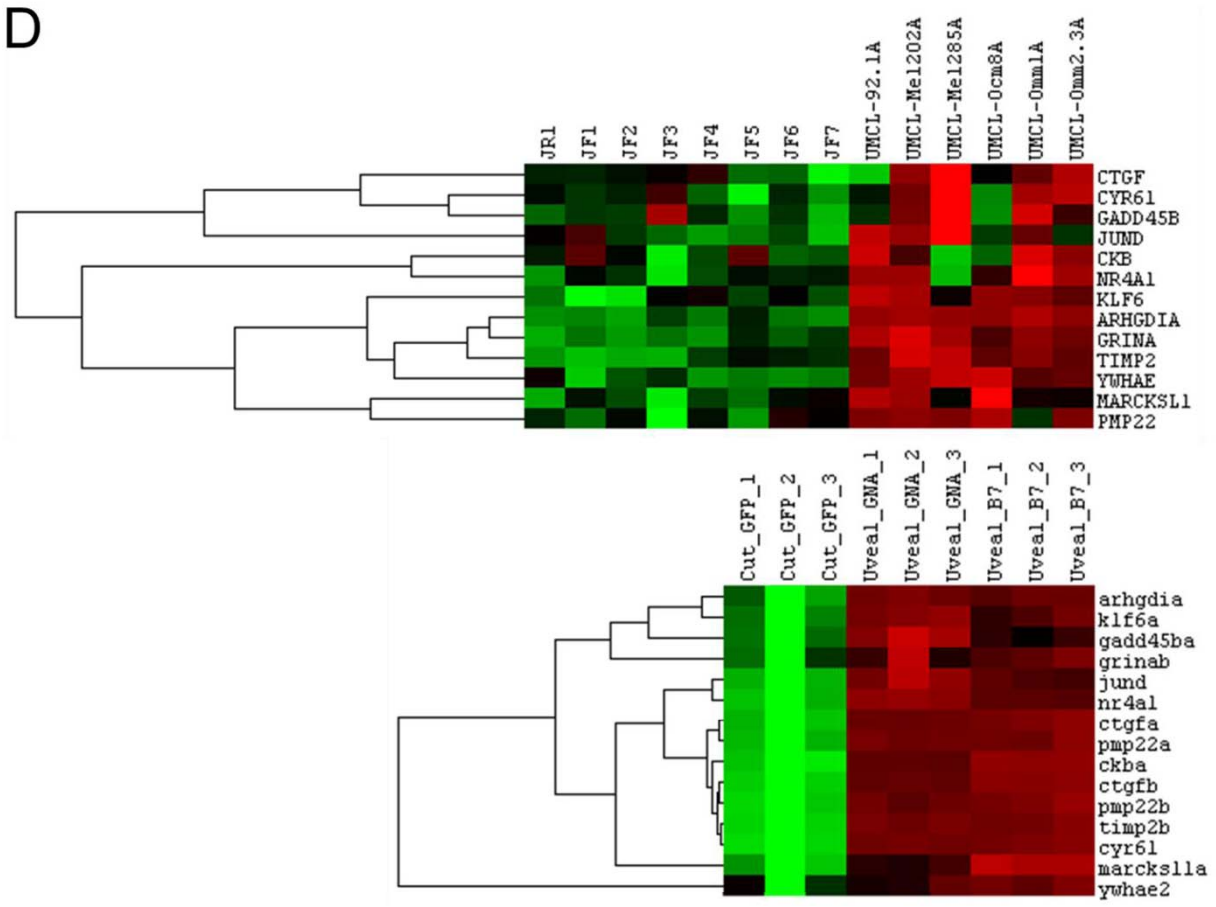

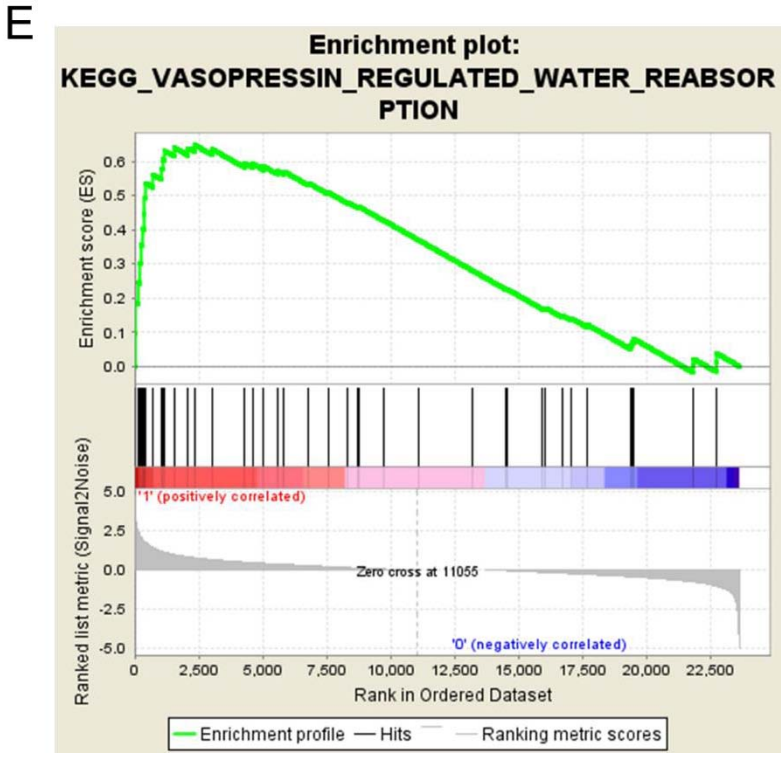

Figure 2.5 Continued.

F

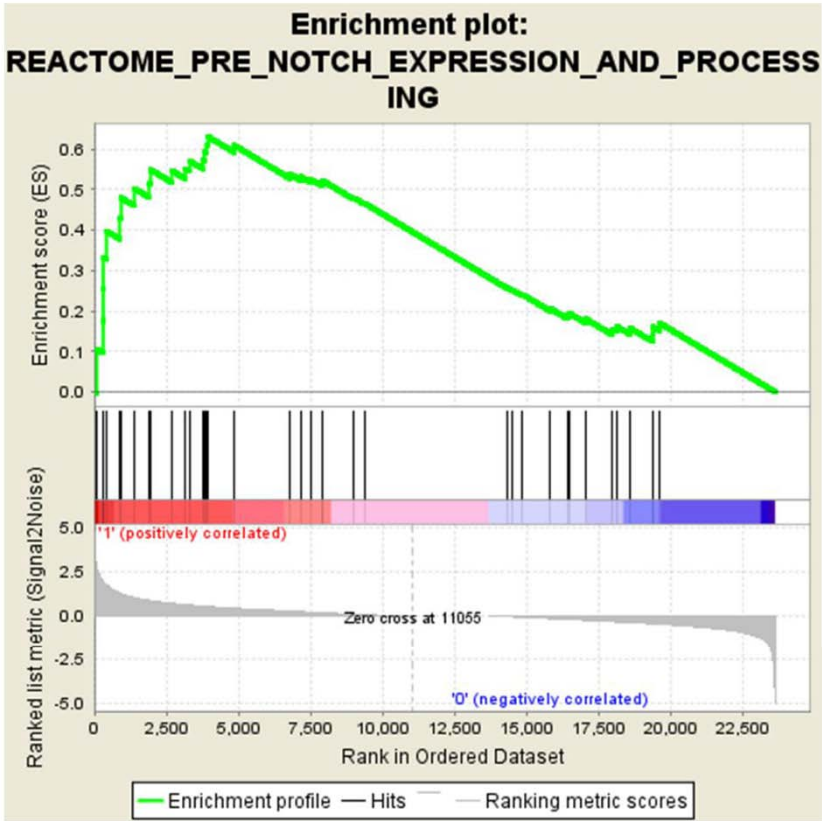

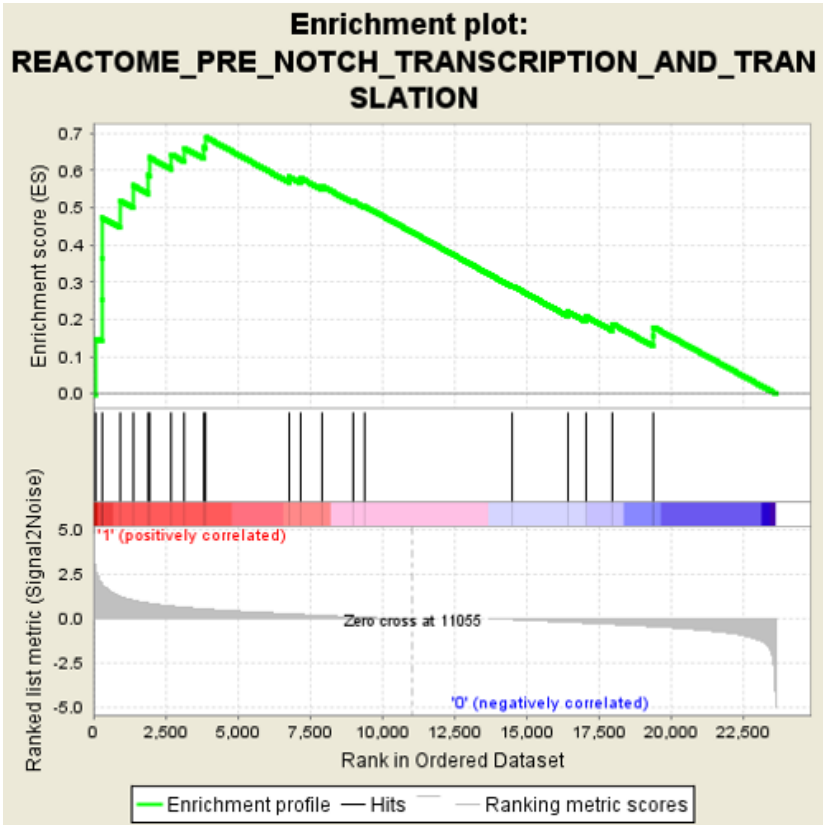

Figure 2.5 Continued.

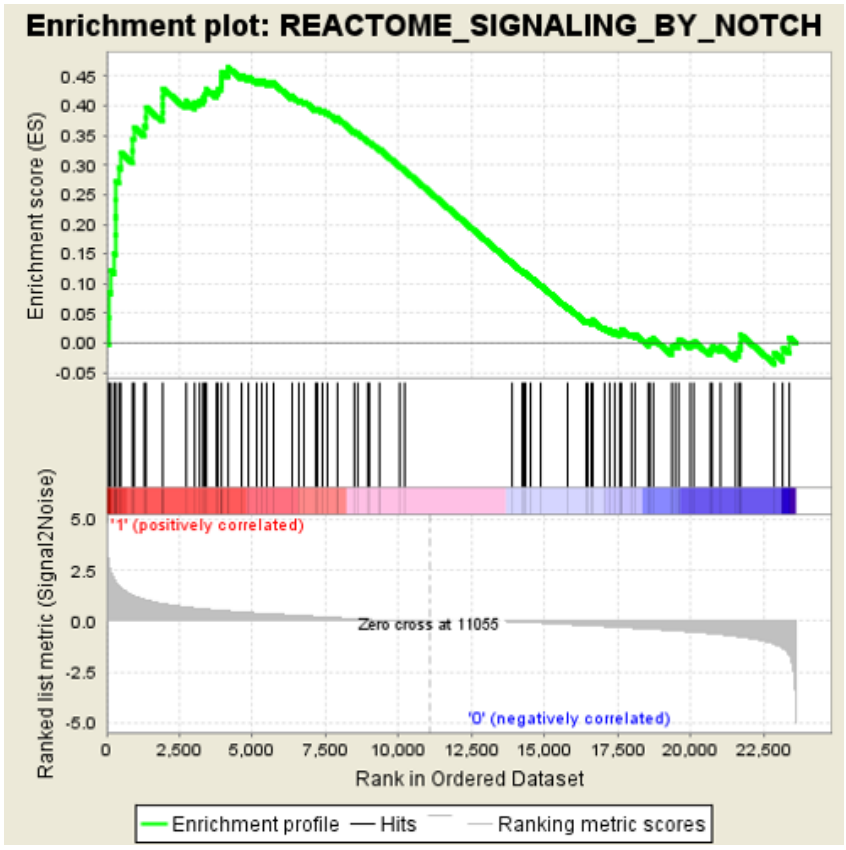

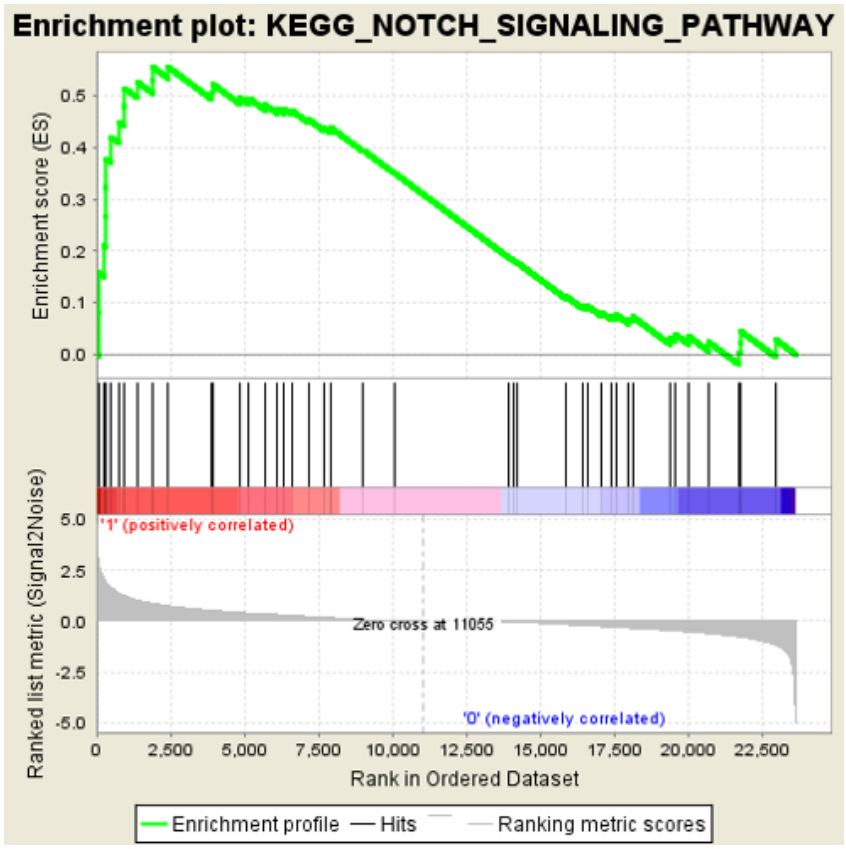

DISCUSSION

My study highlights a novel method of modeling uveal melanoma *in vivo* by transgenic induction, as well as an *in vitro* method for propagating this model long-term as purified uveal melanoma cells in cell culture. My model is, to the best of my knowledge, the first and only model to induce uveal melanoma by transgenesis with a uveal melanoma oncogene, in the case of GNA11 Q209L overexpression. This model has distinct advantages over existing models of uveal melanoma and is important in light of the limited availability of human uveal melanoma patient samples. My model circumvents certain disadvantages present in previous uveal melanoma animal models, such as xenograft models with uveal cells and hosts of different animal origins, and the requirement of immunosuppression. Two features of my zebrafish uveal melanoma model, sensitivity to PKC inhibition and gene expression characteristics similar to those observed in human uveal melanomas, suggest that my model could be valuable for future genetic and therapeutic studies of this rare disease Furthermore, the discovery of HOXB7 as an inducer of uveal melanoma in my model suggests a novel function for this gene in this disease, and confirms that my model is amenable to broader genetic screens to find new uveal melanoma oncogenes.

Previous studies could help to elucidate a potential mechanism for HOXB7 in my uveal melanoma model, as well as explain the near-significant acceleration of overall melanoma onset caused by HOXB7 expression. Notably, HOXB7 was shown to have oncogenic effects in melanoma cells where HOXB7 was observed to directly transactivate basic fibroblast growth factor (bFGF; Caré et al., 1996). Abrogation of HOXB7 binding to the bFGF promoter inhibited growth in melanoma cells (Caré et al., 1996). While it remains to be seen whether HOXB7 is acting upon bFGF in the same manner in my model, the work by Caré et al. provides additional

context for the pro-proliferative effects of HOXB7 in melanoma. Additionally, HOXB7 has been named as a prognostic indicator in several other cancers (Bitu et al., 2012; Agnelli et al., 2011; Liao et al., 2011; Chile et al., 2013), and has been found to induce the epidermal growth factor receptor (EGFR) and vascular endothelial growth factor (VEGF) pathways in breast cancer cells (Jin et al., 2012; Caré et al., 2001). Although HoxB7 expression was low in most samples in the Tschentscher uveal melanoma data set (**Figure 2.3A**), this could be explained by redundant functions and gene targets between HOXB7 in my uveal melanoma model and other oncogenes in the Tschentscher samples. In our model, the induction of growth factor pathways by HOXB7 could be one mechanism to explain the increased rate of tumor formation in MCR:HOXB7 animals, and could also be relevant to the uveal melanoma phenotype.

There are no drugs currently available to target the oncogenic GNAQ/GNA11 mutations that are frequently present in primary and metastatic uveal melanomas. It has been shown that the PKC inhibitor AEB071 holds novel therapeutic potential for uveal melanomas with GNAQ mutations (Wu et al., 2012). In my GNA11 Q209L-overexpressing zebrafish uveal melanoma cell line, the PKC ε isoform was sensitive to AEB071 treatment and showed a clear decrease in expression by Western blot upon treatment (**Supplementary Figure S2**). These cells were also markedly more sensitive to PKC inhibition than the other cell lines I assessed. This cell line could be used to identify other novel PKC inhibitors of therapeutic value in uveal melanoma by screening for decreased PKC ε expression alongside decreased cell viability.

BRAF V600E mutations are very rarely present in uveal melanoma (Zuidervaart et al., 2005). However, the genetic background of zebrafish used in the miniCoopR assay to identify GNA11 Q209L-driven uveal melanomas also overexpresses BRAF V600E. When MCR:GNA11 Q209L was used to rescue melanocytes in *p53-/-;mitfa-/-* (wild-type BRAF) zebrafish, no uveal

or cutaneous melanomas were observed in a 25-week study (**Figure 2.1F**). This would suggest that GNA11 Q209L mutations provide less MAPK activation than BRAF V600E mutations, considering that the use of MCR:EGFP (a fluorescent protein believed to have no influence on MAPK activity) to rescue melanomas in *Tg(mitfa:BRAF(V600E));p53-/-;mitfa-/-* zebrafish generates cutaneous melanomas in about half of all animals in the same time period (**Figure 2.1F**). Because GNA11 activation and p53 loss alone are insufficient for melanomagenesis in my model, I believe a threshold of MAPK activity is necessary as an early event in uveal melanoma. Also, because all fish in this study (EGFP-, HOXB7-, and GNA11 Q209L-overexpressing) contained the stably inserted BRAF V600E mutation, I do not believe this mutation influenced the differences in uveal and cutaneous melanoma rates observed between the fish genotypes.

The identification of particular genetic characteristics in my zebrafish uveal melanoma cells that have also been found in human uveal melanoma cells helps to validate the assertion that there is sufficient evolutionary conservation between these species for my zebrafish uveal melanoma model to serve as a compelling model for this disease. The high levels of expression of the YAP pathway genes *ctgfa/b* and *cyr61* in my zebrafish uveal melanoma cells is in keeping with recent studies showing that GNAQ activates YAP through Rho GTPase signaling circuitry in human uveal melanoma (Feng et al., 2014). Indeed, this indication of YAP pathway activity in the GNA11 Q209L-overexpressing uveal melanoma cells could explain the relative resistance of these cells to BRAF or MEK inhibition, as it has been demonstrated that YAP lends resistance to resistance to RAF- and MEK-targeted cancer therapies (Lin et al., 2015). These cell lines would likely also be sensitive to YAP inhibition. In addition, zebrafish uveal melanoma cells showed increase expression of *capza1*, a gene whose protein product has been used as a marker to identify uveal melanomas with metastatic potential (Linge et al., 2012), and *sparc*, an identified

pro-proliferative angioregulatory matricellular factor in uveal melanoma whose increased expression is correlated with uveal melanoma-related metastatic deaths (Ordonez et al., 2005; Maloney et al., 2009). The expression levels of *capza1* and *sparc* in these cells encourage future studies that would utilize my lab's previously published transparent adult zebrafish for *in vivo* transplantation analysis of the metastatic potential of these cells (White et al., 2008). The RNAseq analysis of human uveal melanoma cell lines allowed for the identification of genes that share expression patterns in zebrafish and human uveal melanoma data sets (**Figure 2.5D**), further validating my zebrafish uveal melanoma model as a meaningful representation of human uveal melanoma. The YAP pathway in particular seems to be involved in both human and zebrafish uveal melanoma cells, which helps to confirm that YAP pathway activation may be a downstream effect of GNAQ/11 activation, as well as a therapeutically exploitable target. Analysis of human uveal melanoma data also showed enrichment of biologically relevant pathways, such as vasopressin and Notch (**Figure 2.5E, F**), that could serve as targets in future uveal melanoma therapies.

In summary, this study has advanced the progression of *in vivo* and *in vitro* uveal melanoma animal models. I found that when expressed in a melanocyte-restricted manner, human oncogenic GNA11 Q209L cooperates with p53 loss to generate uveal melanomas, as does the transcription factor HOXB7, which currently has no published role in uveal melanoma. The similarity in drug responses and genetic features between zebrafish uveal melanoma cell lines and human uveal melanoma cell lines underscores both the importance and the utility of future zebrafish-based research of this disease. Further, the findings reported here should prove highly beneficial for understanding genetic events in uveal melanoma, as well as for providing advantageous *in vivo* and *in vitro* settings for identifying novel uveal melanoma therapies.

Chapter 3: Human BAP1 C91S accelerates melanoma onset in zebrafish

Attributions

Leonard I. Zon and I conceived the project to study the effect of BAP1 loss of function in zebrafish melanoma. I performed the microinjection for the miniCoopR assays and surveilled the zebrafish for tumor formation, both with technical assistance from E. C. Walsh. MCR:BAP1 C91S and MCR:BAP1 wild-type were provided generously by Y. Machida (Mayo Clinic, Rochester, Minnesota). I performed statistical analysis of tumor onset rate and uveal melanoma incidence using MedCalc software. Target sequences for CRISPR/Cas9-mediated gene knockout were selected by J. Ablain, and guide RNAs for these sequences were generated by J. Ablain. The T7E1 assay was performed by J. Ablain and E. C. Walsh. I performed the morpholino injections and subsequent *in situ* hybridizations and embryo scoring. Morpholino against *bap1* was provided by P. Li and *gna11* morpholino was purchased from Gene Tools, LLC. *In situ* probe for *hoxb7a* was provided by L. Jing.

ABSTRACT

Metastatic uveal melanoma, which mainly affects the liver, is a largely untreatable condition with a poor prognosis of over 80% mortality at one year. Poor prognosis in uveal melanoma is well-predicted by the presence of inactivating mutations in BRCA-1 associated protein 1 (BAP1), which is mutated in as many as 84% of uveal melanoma metastases. I sought to determine the *in vivo* effects of overexpression of the catalytically inactive human BAP1 C91S mutant in zebrafish. I found a significant acceleration of cutaneous melanomas in animals overexpressing mutant BAP1 ($p<0.05$), but not wild-type BAP1 ($p = 0.18$). However, no significant increase in uveal melanoma incidence was observed with either BAP C91S or wild-type BAP1 overexpression ($p = 0.46$ and $p = 0.65$, respectively). Morpholino experiments showed that knockdown of zebrafish *bap1* led to increased spatial expression of *hoxb7a*, and that *bap1* is epistatic to *gna11*. Efforts towards knocking out endogenous zebrafish *bap1* function have been made by designing guide RNAs against target sequences in the *bap1* locus, for use with CRISPR/Cas9 technology. Successful guide RNAs have been identified. These studies advance existing tools for studying BAP1 loss of function *in vivo*.

INTRODUCTION

Uveal melanoma is the most common primary intraocular tumor in adults, with about 1200-1500 new cases occurring per year in the U.S. (Chang et al., 1998; Singh and Topham, 2003). Although both uveal and cutaneous melanomas arise from melanocytes, uveal melanoma is biologically and genetically distinct from the more common cutaneous melanoma. In particular, uveal melanomas lack mutations in BRAF, NRAS, or KIT, unlike cutaneous melanoma (Saldanha et al., 2004; Zuidervaart et al., 2005; Davies et al., 2002; Pollock et al.,

2003). Instead, uveal melanomas frequently harbor activating mutations in the GPCR alpha subunits GNAQ or GNA11 (van Raamsdonk et al., 2010). Metastasis is a frequent occurrence in uveal melanoma, and outcomes are poor once distant spread occurs.

It is estimated that 40-50% of uveal melanoma patients will die of metastatic disease, even with early diagnosis, proper treatment, and close follow-up (Kujala et al., 2003). By far the most common site of metastasis is the liver, reported in 87% of metastasis cases (Roland et al., 1993). Inactivating somatic mutations in the gene encoding BRCA-1 associated protein 1 (BAP1) have been observed in as many as 84% of metastasizing uveal melanomas (Harbour et al., 2010). The frequency of BAP1 mutations in metastatic uveal tumors implicates BAP1 loss of function in uveal melanoma metastasis and suggests that targeting the BAP1 pathway could be a valuable therapeutic approach.

BAP1 is a deubiquitinating enzyme that mediates deubiquitination of histone H2A and host cell factor 1 (HCF-1; Scheuermann et al., 2010; Machida et al., 2009). BAP1 contains a ubiquitin carboxy-terminal hydrolase (UCH) domain and, when paired with the Polycomb group protein ASXL1, functions as the catalytic component of the Polycomb repressive deubiquitinase (PR-DUB) complex, which regulates homeobox genes by controlling H2A ubiquitination levels (Jensen et al., 1998; Scheuermann et al., 2010). Inactivation of BAP1 is the most important genetic alteration for predicting poor prognosis in uveal melanoma, and this occurs most often through mutation of one BAP1 allele followed by the loss of an entire copy of Chromosome 3 (Monosomy 3), unmasking the mutant allele (Harbour et al., 2010). Notably, there is no correlation between the GNAQ/11 mutations that are prevalent in primary uveal melanomas and the BAP1 mutations of metastatic uveal melanomas (Harbour et al., 2010). In several studies, a catalytically inactive form of BAP1 has been created by mutating the catalytic cysteine at codon

91 in the UCH domain to a serine (BAP1 C91S), and this has been shown to be a dominant negative mutant because of its ability to compete with wild-type BAP1 for the assembly of the same multiprotein complexes (Jensen et al., 1998; Mallery et al., 2002; Machida et al., 2009).

BAP1 mutations are not limited to uveal melanoma. Somatic mutations in BAP1 have been found in a few breast and lung cancer cell lines (Jensen et al., 1998), as well as in about 15% of clear cell renal cell carcinomas (CCRCC; Peña-Llopis et al., 2012). Interestingly, there is a novel familial cancer syndrome caused by germline BAP1 mutations; this BAP1 cancer syndrome is characterized by early-life benign melanocytic skin tumors, and later-life uveal melanomas, cutaneous melanomas, mesotheliomas, and potentially other cancers (Carbone et al., 2013). In a specific hereditary case of uveal melanoma, a BAP1 mutation was inherited that inserted a premature stop codon into the BAP1 UCH domain (Höiom et al., 2013). It has become evident that understanding the functions of BAP1 in various contexts would be beneficial for understanding the etiology of several types of cancers, and would further our knowledge of cancer biology as a whole.

Although recent years have seen many new discoveries about the role of BAP1 in uveal melanoma (and other cancers), more work is needed to elucidate the molecular mechanisms controlling BAP1 function in uveal melanoma and to determine potential treatment strategies based on such research efforts. Familial BAP1 studies are useful for understanding the effects of BAP1 mutations *in vivo* but are limited by small sample sizes and the potential confounding presence of other mutations. Animal models offer a controlled experimental setting to study BAP1 mutations; a full BAP1 knockout is lethal in mice, but heterozygous loss of BAP1 in mice leads to myeloid transformation (Dey et al., 2012) and accelerated development of malignant mesothelioma in response to environmental exposures (Xu et al., 2014). The field of uveal

melanoma research, however, lacks an animal model that incorporates BAP1 loss of function, and my work here attempts to build upon existing tools for studying BAP1 inactivation *in vivo* in uveal melanoma.

MATERIALS AND METHODS

miniCoopR assay

The miniCoopR (MCR) vector used was constructed as previously described (Ceol et al., 2011). BAP1 C91S and BAP1 wild-type constructs were generously provided in pcDNA3.1 vectors by Dr. Yuka Machida (Mayo Clinic, Rochester, Minnesota); human GNA11 Q209L and HOXB7 cDNAs were purchased from the Harvard PlasmID Database, and all were cloned into pENTR vectors with a pENTR/D-TOPO Cloning Kit (Life Technologies).MultiSite Gateway recombination reactions (Invitrogen) were utilized to create individual miniCoopR clones. MCR:EGFP was generated previously and used as a negative control (Ceol et al., 2011). One-cell zebrafish embryos were generated by incrosses of Tg(*mitfa*:BRAF(V600E));*p53*-/-;*mitfa*-/- zebrafish and these embryos were microinjected with 25 pg of each miniCoopR clone and 25 pg of Tol2 transposase mRNA. At 48 h post fertilization, the presence of rescued melanocytes was used as a readout to select transgenic animals. These animals were scored weekly for the presence of visible tumors. All fish were maintained at 28.5°C at a holding density of 15 fish/liter, and all procedures were approved by the local Institutional Animal Care and Use Committee.

Target sequence identification

Target sequences (**Table 3.1**) were selected by manually scanning early *bap1* exons for 20 bp sequences beginning with GG and followed immediately at the 3' end by NGG; these motifs are needed for Cas9 nuclease activity. Guide RNAs with regions complementary to these sequences were produced by *in vitro* transcription.

T7E1 assay

DNA was extracted from 8-10 embryos 48 h after injection using the HotSHOT method (Meeker et al., 2007). DNA extracted from uninjected embryos served as a control. The genomic region encompassing the *bap1* target site was amplified, melted, and annealed to form heteroduplex DNA. The primers used to amplify the target sites are listed in **Supplementary Table S7**. 200 ng of annealed DNA was treated with 10 units of T7E1 (New England BioLabs M0302L) for 30 minutes at 37°C. T7E1-treated DNA was immediately analyzed by agarose gel electrophoresis on a 2.5% agarose gel.

Morpholino injection

Morpholino oligonucleotides were microinjected into the yolk of single-cell embryos. The *bap1* morpholino (5'-CTAACTCCAGCCAACCTTTGTTCAT-3') was purchased from Gene Tools, LLC and the *gna11* morpholino was generously provided by Pulin Li (California Institute of Technology, Pasadena, CA, USA). A dose of 4 ng *bap1* morpholino and 3 ng *gna11* morpholino was used.

In situ hybridization

In situ hybridizations were performed as previously described (Schulte-Merker et al., 1994) with the modification that embryos were blocked in 10% heat-treated lamb serum. Antisense riboprobe labeled with digoxigenin was used and detected with antidigoxigenin antibody conjugated to alkaline phosphatase. In each case BCIP/NBT (5-bromo-4-chloro-3-indolyl phosphate p-toluidine salt/4-nitroblue tetrazolium chloride) was used as substrate to produce the purple colorimetric reaction. Digoxigenin-labeled antisense *hoxb7a* probe was obtained from Lili Jing (Boston Children's Hospital, Boston, MA, USA).

RESULTS

Transgenic overexpression of wild-type or catalytically inactive BAP1 in a zebrafish melanoma model

Inactivating mutations in the tumor suppressor BAP1 are common in metastatic uveal melanoma, and also causative of a familial cancer syndrome characterized by cutaneous and uveal melanoma, malignant mesothelioma, and other neoplasms (Harbour et al., 2010; Carbone et al. 2013). To study the effect of BAP1 inactivation *in vivo*, I generated transgenic zebrafish overexpressing either wild-type BAP1 or BAP1 C91S under the melanocyte-specific *mitfa* promoter (**Figure 3.1A**). I expected that the catalytically inactive BAP1 C91S, used previously to study BAP1 loss of function (Machida et al., 2009), would sequester zebrafish bap1 binding partners and act as a dominant negative mutant. This would ideally mimic human uveal melanomas where inactivating BAP1 mutations are unmasked by loss of heterozygosity via Monosomy 3 (Harbour et al., 2010), and BAP1 function is presumably lost.

Melanocytes and melanomas were rescued in *Tg(mitfa:BRAF(V600E)); p53-/-;mitfa-/-* zebrafish using the miniCoopR (MCR) vector to drive candidate gene expression in rescued tissues, as described in the previous chapter. Overall melanoma onset was significantly accelerated by BAP1 C91S overexpression compared to EGFP overexpression, and was unaffected by wild-type BAP1 overexpression (**Figure 3.1B**). Occasional uveal melanomas were observed in the cases of mutant or wild-type BAP1 overexpression, but these rates of occurrence were not significant ($p = 0.46$ and $p = 0.65$, respectively) and were negligible compared to rates seen previously with HOXB7 or GNA11 Q209L overexpression (**Figure 3.1C**).

Targeting endogenous *bap1* using the CRISPR/Cas9 system

The clustered regularly interspaced short palindromic repeats (CRISPR)-Cas9 system is a powerful gene editing tool. In zebrafish, this system takes advantage of the CRISPR/Cas prokaryotic immune defense system, and involves using small RNAs called guide RNAs (gRNAs) to direct the Cas9 endonuclease to modify or permanently disrupt genomic target sequences with high precision (Garneau et al., 2010; Jinek et al., 2012; Gasiunas et al., 2012). The gRNA/Cas9 complex is directed to a target sequence by complementary base pairing between the gRNA sequence and the target sequence in the genomic DNA. Double strand breaks introduced by Cas9 can be repaired by the error-prone non-homologous end joining pathway to result in random indel mutations that can lead to frameshifts and premature stop codons, causing gene knockout (Perez et al., 2008).

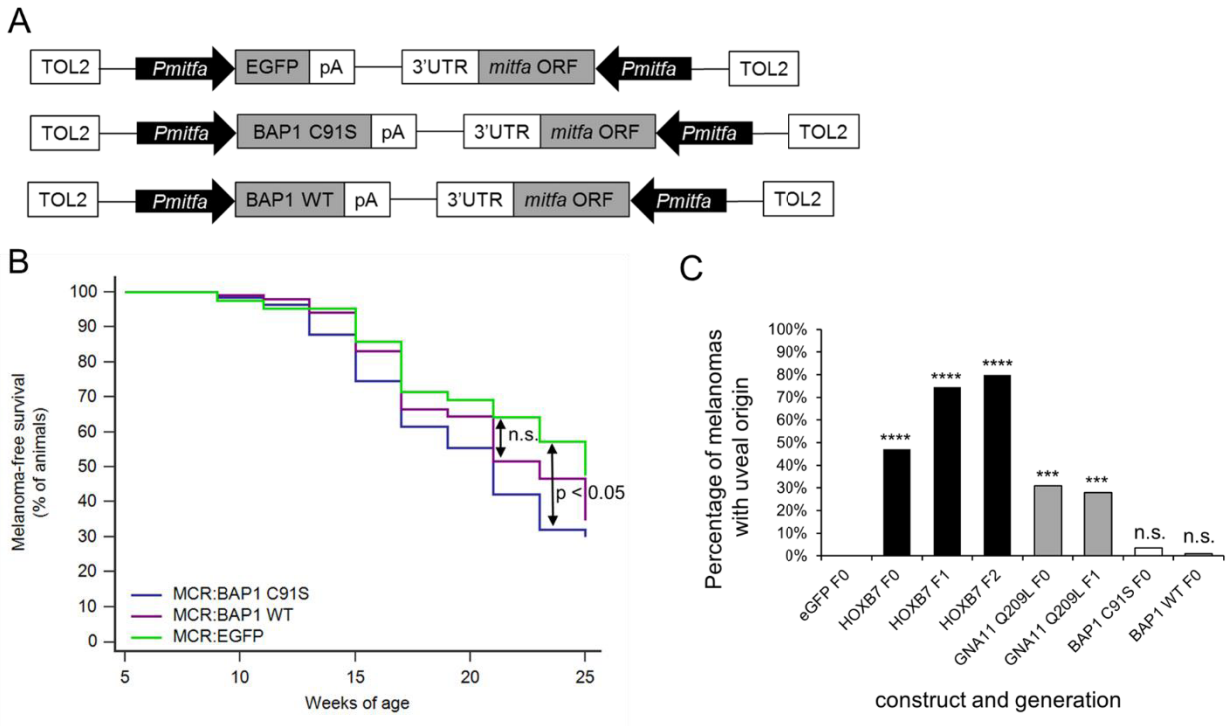

Figure 3.1. BAP1 C91S overexpression *in vivo*. (**A**) Schematic representation of transgenes. (**B**) Percent melanoma-free survival in EGFP-, BAP1 C91S-, or BAP1 wild-type (WT) overexpressing zebrafish, p-values indicated. (**C**) Relative incidences of uveal melanoma by transgene and generation. Significant increase in uveal melanoma incidence, compared to EGFP-overexpressing animals, is marked by asterisks (**** $p<0.0001$, *** $p<0.001$, n.s. = not significant). The n values for each cohort of animals is as follows: MCR:EGFP, n = 42; MCR:HOXB7 F0, n = 55; MCR:HOXB7 F1, n = 47; MCR:HOXB7 F2, n = 15; MCR:GNA11 Q209L F0, n = 42; MCR:GNA11 Q209L F1, n = 50; MCR:BAP1 C91S, n = 197; MCR:BAP1 WT, n = 101.

Because a targeted knockout of endogenous zebrafish *bap1* may provide a better representation of BAP1 loss of function than overexpression of the human dominant negative BAP1 in zebrafish, gRNAs have been designed to target sequences within the zebrafish *bap1* gene (**Table 3.1**). Three of the five gRNAs tested appear to show successful introduction of indel mutations to the endogenous *bap1* locus, as indicated by a T7 endonuclease 1 (T7E1) cleavage assay (**Figure 3.2B**). The T7E1 endonuclease is a mismatch-specific endonuclease that targets

and digests heteroduplex DNA, producing two or more smaller fragments in an enzymatic reaction (**Figure 3.2A**; Kim et al., 2009). The resolution and visualization of digested DNA fragments by agarose gel electrophoresis is a readout for indel mutations at loci targeted by guide RNAs. Guide RNAs were injected along with Cas9 mRNA into single-celled embryos to generate *bap1* mutant heterozygote founder animals that will transmit *bap1* mutations by germline when mated to wild-type fish. Heterozygous animals will be deep sequenced for mutations and bred for maintenance of a heterozygous mutant line, or generation of potential homozygous *bap1* mutants, although full Bap1 knockout is embryonic lethal in mice (Dey et al., 2012). Resulting *bap1* mutant fish could be used in future *in vivo* modeling of uveal melanoma, e.g. overexpression of GNA11 Q209L in melanocytes in this *bap1* mutant background may generate an aggressive and even metastatic uveal melanoma phenotype.

Table 3.1. Targeting sequences for CRISPR/Cas9-mediated knockout of *bap1*.

gRNA name	targeted gene	targeting sequence
bap1 gRNA1	bap1	GGATCGAGGAGCGAAGATCT (direct)
bap1 gRNA2	bap1	GGGCGTGTCTTCTGAAGAAG (reverse)
bap1 gRNA3	bap1	GGTGGTGGAGCGCCCCCTGC (reverse)
bap1 gRNA4	bap1	GGCTGGTAGACGCTGCACAA (reverse)
bap1 gRNA5	bap1	GGAGGATCTTGCTGCAGGTG (direct)

Figure 3.2. T7E1 assay indicates introduction of indel mutations to the *bap1* locus.
(**A**) Schematic overview of mismatch detection by T7E1 assay. Genomic DNA was purified from embryos injected with individual gRNAs and Cas9 endonuclease mRNA. DNA sequences encompassing the *bap1* target sites were PCR-amplified, and the DNA amplicons were melted and annealed. If amplicons contained both mutated and wild-type sequences, heteroduplexes would be formed. T7E1 binds and cleaves heteroduplexes, not homoduplexes. Agarose gel electrophoresis was used to assess DNA fragments; a schematic of an idealized gel is shown. Adapted from Kim et al., 2009. (**B**) Agarose gel electrophoresis shows PCR-amplified DNA containing the target regions in the *bap1* locus. "SX" corresponds to DNA amplified from embryos injected with gRNAX, where X = 1, 2, 3, 4, or 5. Where indicated, "SX' " is an additional independent injection of gRNAX. "CX" indicates DNA amplified from uninjected clutch control embryos. Red boxes indicate the presence of cleavage bands in gRNA/Cas9-treated embryos for which no cleavage bands are seen in uninjected clutch controls.

Figure 3.2 Continued.

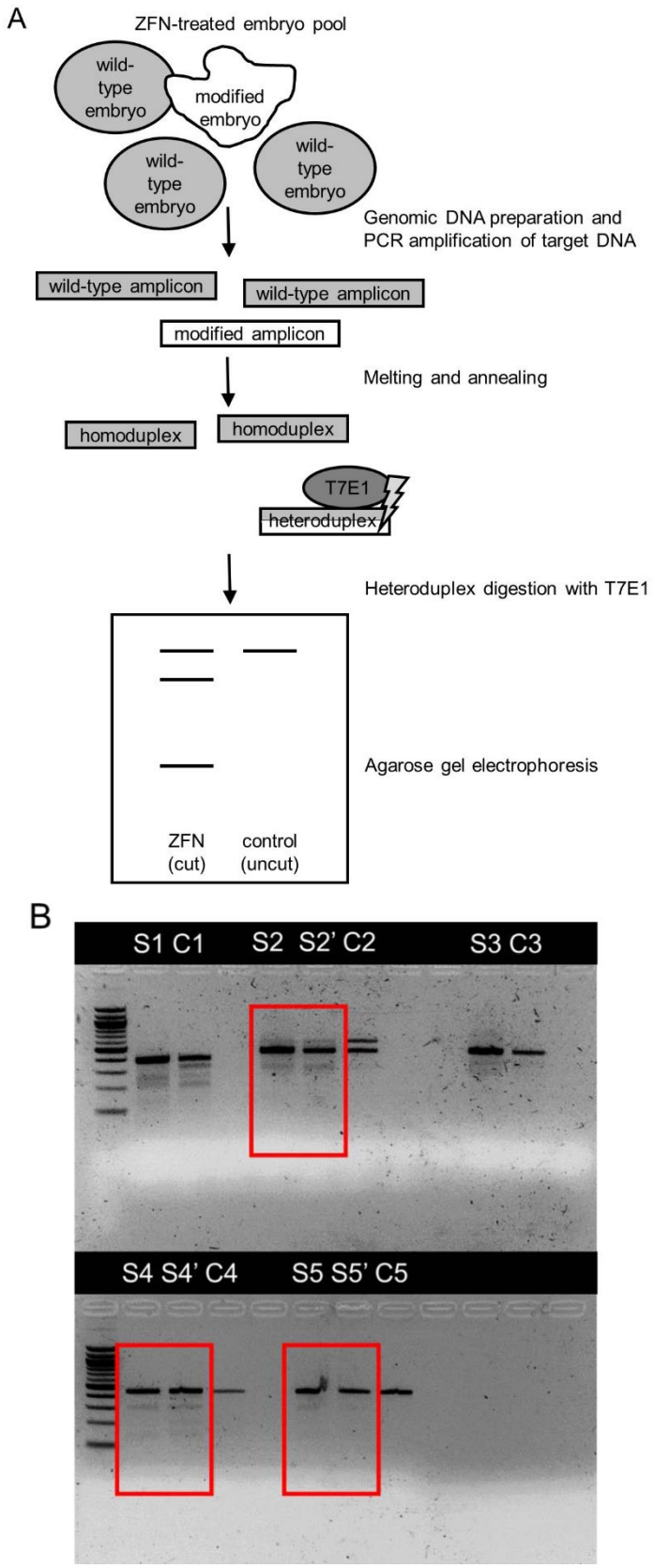

Zebrafish *bap1* influences *hoxb7a* levels and is epistatic to *gna11*

Although no correlation had previously been observed between GNAQ/11 and BAP1 mutation status in uveal melanoma (Harbour et al., 2010), I sought to explore potential interactions between zebrafish *bap1* and two genes whose human homologs proved to be of interest in my zebrafish uveal melanoma model (previous chapter): *gna11* and *hoxb7a.* I did this by injecting antisense morpholinos designed to block the ATG translation start site of *bap1* or of *gna11* into single-cell embryo yolks to block translation of each individually and in combination and then did *in situ* staining for *hoxb7a* at 24 hours post fertilization (hpf). I injected a 4 ng dose of *bap1* morpholino and a 3 ng dose of *gna11* morpholino for all experiments. Knockdown of *gna11* led to an ablation of *hoxb7a* expression by *in situ* (n = 16/16 embryos), while *bap1* knockdown led to an increase in the spatial expression of *hoxb7a* (n = 22/25 embryos; **Figure 3.3A-C**). Interestingly, injecting a combination of *gna11* and *bap1* morpholinos for a double knockdown showed the same phenotype of increased *hoxb7a* expression as was seen with *bap1* knockdown alone (n = 57/66 embryos; **Figure 3.3D**). This suggests that *bap1* is epistatic to *gna11*. Taken together, these morpholino experiments suggest an interaction between all three of these genes in zebrafish embryos.

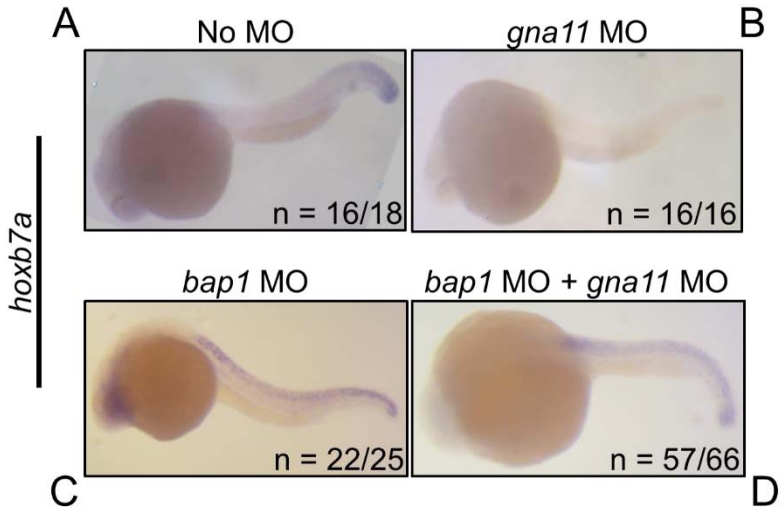

Figure 3.3. Morpholino experiments show *bap1* is epistatic to *gna11*. *In situ* hybridization staining for *hoxb7a* in 24 hpf embryos after receiving (**A**) no morpholino, (**B**) 3ng *gna11* morpholino, (**C**) 4ng *bap1* morpholino, or (**D**) 3ng *gna11* morpholino and 4ng *bap1* morpholino combined. n values are the number of embryos of the observed staining phenotype over the total number of embryos scored.

DISCUSSION

I sought to study the effects of BAP1 loss of function in melanocytes *in vivo* by transgenically overexpressing the catalytically inactive BAP1 C91S in zebrafish melanocytes. Our miniCoopR assay model is best suited to identify early, initiating mutations in melanoma, because candidate genes must be able to exert phenotypic changes in the presence of only *p53* loss and BRAF activation. Additionally, it is standard in my lab to track tumor formation for just 25 weeks, as most effects of candidate genes are noticeable by this time and tumor burden on the animals becomes a challenge. It is reasonable that with an assay of this stringency, BAP1 C91S overexpression did not significantly increase uveal melanoma incidence, because BAP1 loss of function mutations are overwhelmingly found in “class 2” metastatic uveal melanomas versus

non-metastatic “class 1” tumors (Harbour et al., 2010). Even the familial BAP1 cancer syndrome is rare, with only a small subset of hereditary uveal melanomas having *BAP1* as a candidate gene, suggesting contribution from other candidate genes (Abdel-Rahman et al., 2011). Interestingly, a small subset of atypical Spitz tumors, a type of benign melanocytic nevus, have been identified with BRAF V600E mutations and inactivation of BAP1 (Weisner et al., 2012); I did not observe such lesions and it may be beyond the scope of my model to identify these particular rare nevi in zebrafish.

Due to the tendency of *BAP1* mutations to occur later in uveal melanoma progression and to coincide with the onset of metastatic properties, it is logical that my model for finding early driver genes in uveal melanoma did not see great effect on uveal melanoma incidence from BAP1 C91S overexpression when compared to, for example, GNA11 Q209L overexpression (**Chapter 2**). My work suggests that inactivation of BAP1 is not functionally relevant to early uveal melanoma biology. An immediate future direction for this work is to combine overexpression of both the GNA11 Q209L and BAP1 C91S transgenes in zebrafish melanocytes in my model. I believe that this may result in a uveal melanoma phenotype with rapid onset and perhaps an aggressive, or even metastatic, tendency as well. This would be done by co-injection of MCR:GNA11 Q209L and MCR:BAP1 C91S constructs, with subsequent screening for animals expressing both transgenes in rescued melanocytes and melanomas. Notably, our model incorporates a *p53* null background, and I believe this is valuable in my efforts to model uveal melanomas as it has been shown that, although p53 expression is intact in most uveal melanomas, functional defects in the p53 pathway downstream of p53 activation are common (Sun et al., 2005).

We did observe that overexpression of BAP1 C91S led to a significant acceleration of overall melanoma onset, while overexpression of wild-type BAP1 did not (**Figure 3.1B**). This effect could be attributed to the identity of BAP1 as a tumor suppressor, with somatic BAP1 mutations occurring in mesothelioma, clear cell renal cell carcinoma, and cutaneous melanoma, in addition to uveal melanoma (Murali et al., 2013). BAP1 has been shown to be involved in transcription and DNA damage response, specifically through its ability to deubiquitinate the transcriptional regulator host cell factor 1 (HCF-1) to regulate cell growth (Machida et al., 2009), and through its interaction with BRCA1, which has roles in double-strand break repair, cell cycle checkpoints, and apoptosis (Nishikawa et al., 2009). Loss of function in BAP1, or introduction of a dominant negative BAP1 transgene, could disrupt wild-type BAP1 functions and promote a general tumorigenicity that would explain the acceleration of melanoma onset I observed in this study.

We have designed guide RNAs to direct Cas9-mediated disruption of the zebrafish endogenous *bap1* gene at the target sequences listed (**Table 3.1**). Guide RNAs and Cas9 mRNA were injected into one-celled embryos, which were subsequently screened for the presence of *bap1* indel mutations (**Figure 3.2B**). Ideally, I would breed heterozygous mutants together to establish homozygous *bap1* knockout fish, but the full knockout of this gene causes embryonic lethality in mice (Dey et al., 2012). If this is the case in zebrafish, I will maintain heterozygous *bap1* mutants by outcrossing. Additionally, my lab has recently published on a CRISPR/Cas9 vector system for tissue-specific gene disruption in zebrafish (Ablain et al., 2015), and this system is readily adaptable for establishing melanocyte-restricted *bap1* knockout zebrafish, circumventing any potential embryonic lethality in a whole-animal *bap1* knockout. Generation of a ubiquitously heterozygous or melanocyte-specific *bap1* knockout could be paired with

melanocyte-specific overexpression of GNA11 Q209L in hopes of producing an aggressive and even metastatic uveal melanoma phenotype. The use of CRISPR/Cas9-mediated knockout of endogenous *bap1* may be preferable to overexpression of human BAP1 C91S, because zebrafish *bap1* only shares 66% amino acid identity with its human ortholog (NCBI BLAST). It is possible that the human inactive BAP1 C91S, which has been shown to act as a dominant negative mutant in human cells (Machida et al., 2009), may not be able to bind with all endogenous zebrafish *bap1* binding partners. Successful disruption of the endogenous *bap1* by CRISPR/Cas9 serves as a more certain loss of bap1 function. The knockout of zebrafish *bap1* combined with overexpression of *mitfa*:GNA11 Q209L will be a potentially powerful tool to model the pathological and genetic effects of BAP1 loss of function in uveal melanoma.

We found that knocking down zebrafish *bap1* expression by morpholino resulted in a spatial increase in *hoxb7a* expression (**Figure 3.3C**). In Drosophila, BAP1 is encoded by the gene *calypso* and contains the catalytic activity of the Polycomb repressive deubiquitinase (PR-DUB), which removes monoubiquitin from histone 2A (Scheuermann et al., 2010). Scheuermann et al. showed that a mutation disrupting the catalytic activity of BAP1 (Calypso) led to the absence of HOX gene repression *in vivo*. In particular, expression of the HOX gene *Ubx* was affected by BAP1 loss of function. Interestingly, the vertebrate homolog of Ubx is HoxB7 (Scott MP, 1992), or hoxb7a in zebrafish. I demonstrate that the repressive relationship between Calypso and Ubx is conserved in zebrafish, as I expectedly saw increased *hoxb7a* expression in response to loss of *bap1* (via morpholino-mediated knock down; **Figure 3.3C**). I conclude from this that repression of HoxB7 by BAP1 is a well-conserved function, at least in the embryonic stages of life. Further studies could be useful to show whether HoxB7 is upregulated in BAP1 mutant metastatic uveal melanomas. In future studies, I would show that the wild-type *hoxb7a*

expression pattern (as in **Figure 3.3A**) could be rescued by injecting morpholinos together with the mRNA of the targeted gene (e.g. injection of *bap1* morpholino together with *bap1* mRNA). If wild-type *hoxb7a* expression patterns were restored, I would conclude that the morpholinos were specific in their targeting and that few if any off-target effects were incurred. Additionally, future experiments would include staining for other *hox* genes after *gna11* or *bap1* morpholino injection, to assess whether the effects observed with *hoxb7a* were specific or part of a more general effect on hox genes. This is particularly interesting given the role of BAP1 in Polycomb repression and regulation of Hox genes (Scheuermann et al., 2010), so I expect that other hox genes might show similar expression pattern changes in these morpholino experiments.

Lastly, I found *bap1* to be epistatic to *gna11* by a classic epistasis test using morpholinos (**Figure 3.3B-D**). Although there is no known correlation between GNAQ/11 and BAP1 mutations in uveal melanoma (Harbour et al., 2010), I observed that the zebrafish orthologs of these genes both seem to interact with *hoxb7a*. If this is true, I can reason that *bap1* should in fact be epistatic to *gna11*. As a chromatin factor, BAP1 would function in the nucleus, and loss of BAP1 (through mutation or knockdown) would immediately result in de-repression of genes, such as HoxB7. GNA11, however, as a GPCR alpha subunit would function at the cell surface, and would require a lengthier signaling cascade before its loss affected gene expression levels. There is no established genetic interaction between GNAQ/11 and the HOX genes, or between GNAQ/11 and BAP1, but my work suggests that there may be a relationship between these genes in embryos, namely one in which GNAQ/11 and BAP1 exert opposing effects on Hox gene expression.

Chapter 4: Concluding discussion and future directions

CONCLUDING DISCUSSION

Animal models of uveal melanoma

The use of experimental animal models of uveal melanoma is an important area of research for this rare disease. Many attempts have been made to establish a satisfactory animal model to effectively study the pathogenesis and therapy of uveal melanoma (Albert et al., 1981; Albert et al., 1968; Luyten et al., 1993; van der Ent et al., 2014; Hu et al., 1994; Blanco et al., 2005; Yang et al., 2008; Mueller et al., 2002; Ma et al., 1995). Suitable animal models are of immense value in a field where patients and patient samples are rare. While previous animal models have helped promote a better understanding of this disease, there are also caveats to these models that leave room for improvement. I believe that the model I have presented provides unique advantages for the study of uveal melanoma.

My MCR:GNA11 Q209L zebrafish constitute the first animal model of uveal melanoma that arises spontaneously as a result of transgenic overexpression of a human uveal melanoma oncogene. I observed a 31% uveal melanoma incidence in animals transiently overexpressing GNA11 Q209L in melanocytes (**Figure 2.1D**). Early attempts by others to induce uveal melanomas involved injecting oncogenic viruses into animal eye tissue, specifically feline sarcoma virus into cat eyes (Albert et al., 1981) and simian virus 40 into hamster eyes (Albert et al., 1968). The eye tumors that arose in cats had similar ultrastructural appearance to human eye tumors, but virus particles could be seen budding from the cell membrane, which is in stark contrast to human uveal melanoma. The hamster eye tumors were not of melanocytic origin, and therefore were non-melanoma ocular tumors. Both the cats and the hamsters experienced high mortality rates and required cautious handling due to the use of oncogenic viruses. My model is

not limited by the mortality of the animals, and is a closer match histologically and, I presume, genetically to human uveal melanoma than these early attempts.

Another method commonly used more recently to model uveal melanoma is to inoculate animal eyes (Hu et al., 1994; Blanco et al., 2005; Yang et al., 2008; Mueller et al., 2002; Ma et al., 1995) or embryos (Luyten et al., 1993; van der Ent et al., 2014) with human uveal melanoma cells. Although the uveal melanoma cells would often proliferate and even migrate in these studies, providing a better understanding of uveal melanoma pathology and metastasis, all of these xenograft models require immature or suppressed immune systems. This is a disadvantage due to some of the important functions of the innate and adaptive immune system in the tumor microenvironment, in addition to the fact that biological differences between the host and recipient species could confound the behavior of these tumors. Also, cultured cells may acquire adaptive changes while growing *in vitro* that distinguish them from tumor cells *in vivo*. In my model, these disadvantages do not exist because tumors initiate and proliferate in their native environment, and the adult zebrafish immune system is intact and functioning normally in MCR:GNA11 Q209L animals. It has been suggested that uveal melanomas may show increased numbers of CD3+ T lymphocytes and CD11b+ macrophages (De Waard-Siebinga et al., 1996); an interesting future study with my uveal melanoma model will be to compare the immune cell populations present in GNA11 Q209L-overexpressing uveal melanomas versus GNA11 Q209L-overexpressing cutaneous melanomas. This would help further our understanding of the immune response in uveal melanoma.

Another advantage of my uveal melanoma model over models utilizing genetic manipulation to induce uveal melanomas is that mine is the first to utilize a known human uveal melanoma oncogene. For instance, Tolleson and colleagues expressed activated human *HRAS* in

mouse melanocytes to induce uveal melanomas with a 15% incidence rate (Tolleson et al., 2005), but HRAS mutations are not observed in uveal melanoma (Zuidervaart et al., 2005). I observed uveal melanomas in mutant GNA11-overexpressing zebrafish twice as often (31% incidence, **Figure 2.1D**), and GNA11 is known to be genetically relevant in human uveal melanoma (van Raamsdonk et al., 2010). I hypothesize that my model would be more likely to accurately reflect signaling events that occur in human uveal melanoma. Evidence to support this hypothesis was found in the shared genes between my zebrafish uveal melanoma signature and highly differentially expressed genes in human uveal melanoma (**Figure 2.5C**). I believe that my model may be a more powerful tool than previous models for understanding uveal melanoma genetics and potentially uncovering novel therapeutic targets.

GNAQ/11 mutations in uveal melanoma

Somatic mutations in the GPCR alpha subunits GNAQ or GNA11 are present in over 80% of uveal melanomas (van Raamsdonk et al., 2010). The activating mutations in these genes lead to constitutive activation of downstream MAPK signaling, including the effectors MEK and ERK (Zuidervaart et al., 2005). These are the same downstream effectors that are activated in cutaneous melanomas by BRAF and NRAS mutations, and this redundancy helps to explain why BRAF and NRAS mutations are not found in uveal melanomas (Cruz et al., 2003). The upregulation of the MAPK pathway by GNAQ/11 appears to be a major contributor to the development of uveal melanoma, and MEK inhibitors have proven effective at inhibiting uveal melanoma growth *in vitro* and in clinical trials (von Euw et al., 2012; Kim et al., 2014).

Classic GNAQ/11 signaling involves the activation of downstream signaling through activation of phospholipase C (PLC), which will cleave phosphatidylinositol diphosphate into

inositol triphosphate and diacylglycerol (Lee et al., 1992; Wu et al., 1992). Protein kinase C (PKC) is one of the second messengers of inositol triphosphate and diacylglycerol signaling, and the phosphorylation of PKC activates the MAPK pathway (Rozengurt et al., 2007; Cobb et al., 1995). Knowing this, it is unsurprising that PKC inhibitors have shown efficacy at inducing apoptosis in GNAQ/11 mutant cell lines at a significantly higher rate than GNAQ/11 wild-type cell lines (Wu et al., 2012). I have generally corroborated this with my work, with the observation that cultured zebrafish uveal melanoma cells overexpressing GNA11 Q209L are sensitive to PKC inhibition when compared to EGFP-overexpressing cutaneous melanoma cells (**Figure 2.2A**). Interestingly, Wu and colleagues found that knockdown of PKC by shRNA or inhibition of PKC by the particular inhibitor used in my work (sotrastaurin) led to decreased NFκB signaling (Wu et al., 2012), suggesting an additional mechanism for PKC-mediated proliferation that is independent of the MAPK pathway.

With greater understanding of GNAQ/11 signaling comes additional opportunities for the development of therapeutic targets. In 2005, the first evidence was shown for upregulation of the well-known growth pathway stemming from the kinase cascade of phosphatidylinositol-3 kinase (PI3K) and Akt, which signal through the mammalian target of rapamycin (mTOR) and other effectors (Saraiva et al., 2005). Subsequently, combined MEK and PI3K/mTOR inhibition has been proven to synergistically inhibit cell growth in GNAQ/11 mutant uveal melanoma (Ho et al., 2012). More recently, GNAQ/11 has been shown to activate the YAP pathway in uveal melanoma (Feng et al., 2014). It is clear that combination treatments with MEK inhibitors and YAP inhibitors should be tested in uveal melanoma. Because YAP pathway genes were shown to be highly expressed in both my GNA11 Q209L- and HOXB7-overexpressing zebrafish uveal melanoma cell lines, I am hopeful that further probing of these cell lines would offer additional

genes or pathways of interest that may lend themselves to targeted therapies. Additionally, because PKC sensitivity was observed in my GNA11 Q209L-overexpressing uveal melanoma cells, my hope is that these cells would be appropriate for testing the efficacy of various singular and combination therapies that are suggested by future genetic studies of uveal melanoma.

A novel role for HOXB7

A mini-screen of HOX genes using the miniCoopR assay revealed that melanocyte-restricted overexpression of human HOXB7 induces uveal melanomas in zebrafish with an incidence of 47% in transiently transgenic animals (**Figure 2.3E**). No previously published studies suggest a role for HOXB7 in uveal melanoma. It is unclear at this time why the expression of HOXB7 in all melanocytes of the zebrafish biases towards the formation of uveal melanomas, just as it is unclear why GNAQ/11 mutations preferentially affect uveal melanomas. It is possible that a genetic program induced in the presence of HOXB7 overexpression creates a particularly pro-proliferative signal in the presence of factors specifically found in the uveal microenvironment. Uveal melanoma grows in one of the most capillary-rich tissues of the body and the development of blood vessels is necessary for tumor growth. Higher vascularity in these tumors predicts worse outcomes (Foss et al., 1996). Interestingly, HOXB7 has been observed in other cancer settings to induce pro-angiogenic factors including basic fibroblast growth factor (bFGF), vascular endothelial growth factor (VEGF), and epidermal growth factor receptor (EGFR; Caré et al., 1998; Caré et al., 2001; Jin et al., 2012). Two of these factors, the cytokines bFGF and VEGF, were found in one study to be expressed at the mRNA level in all 20 uveal melanoma samples tested (Boyd et al., 2002). An additional pro-angiogenic factor found among the top 1000 most highly expressed genes in HOXB7-overexpressing tumors in my study was

sparc (**Supplementary Table S1**), which has been found to have pro-proliferative effects in uveal melanoma (Maloney et al., 2009) and whose expression is correlated with poor prognosis in uveal melanoma (Ordonez et al., 2005). One theory explaining the induction of uveal melanomas by HOXB7 is that HOXB7 induces pro-angiogenic factors when expressed in zebrafish melanocytes, and that these factors are especially potent for promoting tumor growth in the highly vascularized eye, leading to a preferential formation of uveal tumors.

While my work is the first to implicate HOXB7 in uveal melanoma, previous work has shown roles for HOXB7 in cutaneous melanoma and other cancers; HOXB7 has particularly been found to be an oncogenic factor in cutaneous melanoma (Caré et al., 1998; Errico et al., 2013), which is in keeping with my result that HOXB7 overexpression accelerates the overall melanoma onset rate in zebrafish (**Figure 2.3F**). Caré et al. showed HOXB7 to be constitutively expressed in 25 melanoma cell lines, and that disrupting HOXB7 expression inhibited proliferation in these lines. HOXB7 was found to directly transactivate bFGF in this study, and this was thought to explain the pro-proliferative role of HOXB7 in these cells. Other studies have shown that disruption of HOXB7 binding to Pre-B-cell leukemia transcription factor 2 (PBX2) induces apoptosis in melanoma cells (Errico et al., 2013). These roles for HOXB7 in melanoma help to define a potential mechanism to explain the near-significant acceleration of overall melanoma onset by HOXB7 in my zebrafish model.

Tumorigenic effects of HOXB7 have been documented in a number of other cancer types. HOXB7 has been identified as a prognostic indicator in several cancers, including oral squamous cell carcinoma (Bitu et al., 2012), multiple myeloma (Agnelli et al., 2011; Storti et al., 2011), colorectal cancer (Liao et al., 2011), pancreatic adenoma carcinoma (Chile et al., 2013; Nguyen Kovochich et al., 2013), and breast cancer (Wu et al., 2006; Jin et al., 2012). Some of

the functional roles suggested for HOXB7 in these various cancer settings include direct transactivation of the EGFR promoter and activation of the EGFR pathway (Jin et al., 2012), activation of Ras and RhoA proteins via bFGF upregulation (Wu et al., 2006), and induction of pro-angiogenic genes including VEGF (Caré et al., 2001; Storti et al., 2011). Thus, while I propose a novel role for HOXB7 in uveal melanoma, evidence exists to support my observation of accelerated overall melanoma onset with HOXB7 overexpression, and to suggest hypotheses as to the functions of HOXB7 in my uveal and cutaneous zebrafish tumors. In particular, it is possible that HOXB7 is upregulating growth factor pathway activity via effects on bFGF, VEGF, and/or EGFR, as has been described above. It is reasonable to suggest that expression of HOXB7 under other tissue-specific promoters in zebrafish (such as the *ptf1a* promoter, which was used by Park et al. to drive activated KRAS in zebrafish exocrine pancreas to produce malignant pancreatic tumors) would provide new cancer models and a better understanding of HOXB7 function in cancer.

BAP1 as a tumor suppressor

Although I did not observe an increased incidence of uveal melanomas in BAP1 C91S-overexpressing zebrafish, I did see an acceleration of overall melanoma onset rate (**Figure 3.1**). The most likely reason I did not observe significant uveal melanomas is that BAP1 mutations are not early events in uveal melanoma, but are more of a hallmark of metastatic "class 2" uveal melanomas (Harbour et al., 2010). However, the acceleration of melanoma onset by BAP1 C91S overexpression is in keeping with the general role of BAP1 as a tumor suppressor. Specifically, BAP1 is able to deubiquitinate the transcriptional regulator host cell factor 1 (HCF-1), a process that regulates cell growth via HCF-1's roles in transcription and the DNA damage response

(Machida et al., 2009). Additionally, BAP1 was named for its association with BRCA1, which is known to influence cell cycle check points, double strand break repair, apoptosis, and other growth and death processes in the cell (Nishikawa et al., 2009). It is likely that I observed an increased onset rate of melanomas because I restricted BAP1 C91S overexpression to melanocytes, but it is reasonable that overexpression of this dominant negative protein in other tissues, or ubiquitous overexpression, would lead to significant production of other tumor types due to BAP1's role as a general tumor suppressor.

While overexpression of BAP1 C91S did significantly accelerate overall melanoma onset in my model, I did not see a significantly increased incidence of uveal melanomas, and I attributed this to the fact that BAP1 inactivation is not an early event in uveal melanomagenesis. However, other explanations could be relevant. First, BAP1 C91S may only serve as a dominant negative protein in human cells, and not in zebrafish cells. In fact, there is only a 66% shared identity between the amino acid sequences of zebrafish and human BAP1 (compared to, for example, a 91% identity between zebrafish and human GNA11; NCBI BLAST). It is possible that human BAP1 C91S is not fully able to sequester endogenous zebrafish bap1 binding partners, causing a partial loss of BAP1 tumor suppression that is sufficient for accelerating cutaneous melanomas, but is not equivalent to the loss of function observed in human uveal melanomas with Monosomy 3 and BAP1 inactivation. More work is needed to assess the function of human BAP1 C91S when expressed in zebrafish cells.

FUTURE DIRECTIONS

MCR assay to screen for uveal melanoma genes

In my work I identified a novel role for HOXB7 as an inducer of uveal melanoma in zebrafish, and I did so by screening several human HOX genes as candidate genes in our miniCoopR vector. These experiments served as a proof of principle that a miniCoopR-based assay can be used to discover novel uveal melanoma genes using zebrafish. Additionally, this method has previously been used in my lab to identify the novel cutaneous melanoma driver gene, SETDB1 (Ceol et al., 2011). Notably, the HOXB7- and GNA11 Q209L-overexpressing uveal melanoma models in this work develop uveal melanomas more frequently (47% and 31% incidence, respectively) than the dct:HRAS;Inf4/Arf-/- model described above (15% incidence). A successful miniCoopR based screen for uveal melanoma genes would reveal new potential therapeutic targets for this disease. Candidate genes to screen would include genes from my 138-gene "uveal signature" of genes that were found in the top 1000 most highly expressed genes in both GNA11 Q209L- and HOXB7-overexpressing uveal melanoma cells (**Supplementary Table S1**). For example, CTGF and CYR61, the YAP pathway genes found to be induced by GNAQ in uveal melanoma (Feng et al., 2010), would be ideal candidate genes from this list to test in miniCoopR. I hypothesize that I would see increase uveal melanoma incidence when overexpressing these genes in zebrafish melanocytes.

One caveat of my uveal melanoma model is the melanocyte-restricted stable expression of a BRAF V600E transgene, without which tumors were not observed (**Figure 2.1F**). However, in human uveal melanoma, GNAQ/11 mutations are mutually exclusive with BRAF mutations (Onken et al., 2008). In the future, it may be preferred to find a way to remove the BRAF mutation from my uveal melanoma model, but maintain a uveal melanoma phenotype. One

possibility is that the MCR:GNA11 Q209L fish in the *mitfa-/-;p53-/-* background without the BRAF mutation could form uveal melanomas on a sufficiently long timeline (e.g. 1 year), even though I did not observe any melanomas within 25 weeks. I would also perform a mutagenesis screen on *mitfa-/-;p53-/-;MCR:GNA11 Q209L* zebrafish to see if any mutations introduced by the mutagenesis synergize with GNA11 Q209L overexpression to produce a uveal melanoma phenotype. An additional option would be to overexpress multiple transgenes in the *mitfa-/-;p53-/-* background, specifically ones with uveal melanoma relevance. For example, co-injection of MCR:GNA11 Q209L and MCR:CTGF and/or MCR:CYR61 may cause uveal tumor formation. Any work to eliminate the BRAF V600E mutation from my model, while maintaining the uveal melanoma phenotype, will serve to move my model towards an even more genetically accurate model of human uveal melanoma. Until that time, the present model remains a valuable tool amongst uveal melanoma animal models by providing uveal melanomas for *in vivo* study, induced by a uveal melanoma oncogene.

Chemical screens in GNA11 Q209L fish and cell lines

My MCR:GNA11 Q209L zebrafish and uveal melanoma cell lines can be readily adapted to performing low-to-medium throughput chemical screens to identify drugs with potential efficacy in treating uveal melanoma. A chemical screen in adult animals with uveal melanomas would be more expensive and technically challenging than a screen in cell lines, but would benefit immensely from the *in vivo* context of the drug treatments, where systemic effects of the drug can be noted and the tumor microenvironment is intact; *in vivo* studies more accurately model the complexity of the human disease. Various approaches to delivering drugs include adding drugs directly to the water in the zebrafish tank, although some drugs will precipitate out

of the water, and it is generally difficult to control the amount of drug being received by the fish. More direct treatment methods include giving drug by gavage, a method currently being perfected in my lab that involves force-feeding drugs directly to the stomach, as well as the more traditional retro-orbital and intraperitoneal injection. Treatment dosage, frequency, and duration would be established and fish would be followed for shrinkage or growth inhibition of uveal melanomas. A potential positive control would be AEB071, the PKC inhibitor proven to inhibit uveal melanoma cells (Wu et al., 2012). This approach, because of the amount of time and precise technique required, would perhaps be better suited to validate drug candidates identified from an *in vitro* screen using cell lines.

I have shown that my MCR:GNA11 Q209L uveal melanoma cell line is sensitive to PKC inhibition (**Figure 2.2A**), just as human GNAQ-mutant uveal melanoma cell lines are (Wu et al., 2012). The potential to culture numerous zebrafish uveal tumors individually as cell lines is valuable in an area where human uveal melanomas are rare and human uveal melanoma cell lines are not as prolific as cell lines from other cancer types. Immediate future work with the MCR:GNA11 Q209L cell line would involve testing for synergistic inhibition of growth by MEK and YAP inhibitors. In the long term, this cell line and future zebrafish uveal melanoma-derived cell lines are readily adaptable to high-throughput chemical screening methods. Cells would be seeded in a 96- or 384-well formats for rapid screening of chemical libraries, and growth inhibition would be measured by cell viability assays like CellTiterGlo. Other readouts would include abrogation of PKC or MAPK signaling as measured by Western blot for PKC isoforms and phospho-ERK levels. While cell culture methods lose the tumor microenvironment and the interactions of several cell types that take place within and surrounding a tumor, this method of chemical screening is faster and less expensive than *in vivo* screens. Hits from this

screen would be tested further in adult zebrafish with uveal melanomas. Discovering effective therapies for treating primary uveal melanoma will be essential to inhibiting the disease before it takes on a more deadly and less treatable metastatic form.

Studying BAP1 inactivation in zebrafish

Expression of human BAP1 C91S in zebrafish melanocytes did not cause an increase in uveal melanoma incidence (**Figure 3.1C**), and it is unclear whether this is because BAP1 loss of function is not relevant to uveal melanoma initiation, or because human BAP1 may not interact with all zebrafish bap1 binding partners. In the future, a few measures would be taken to rule out or work around the latter caveat. One approach would be to co-immunoprecipitate human BAP1 along with its binding partners from zebrafish primary tumors or tumor cell lines, and establish by Western blot whether the human BAP1 is in fact bound to endogenous zebrafish proteins from the Polycomb-repressive deubiquitinase. Conversely, pull-down could be directed against zebrafish Asxl1 to check for binding of human BAP1. Another way to assess the function of human BAP1 in zebrafish cells is to do a chromatin immunoprecipitation (ChIP) experiment against the histone 2A lysine 119 monoubiquitin (H2AK119Ub) mark, which is antagonized by BAP1 (Scheuermann et al., 2013). I would expect a greater amount of H2AK119Ub in the presence of BAP1 C91S than wildtype BAP1 or no added transgene. Another approach would be to overexpress a catalytically inactive zebrafish bap1 mutant under the *mitfa* promoter in miniCoopR, to see whether I observe a similar phenotype to MCR:BAP1 C91S zebrafish. This would help to elucidate which aspects, if any, of the MCR:BAP1 C91S phenotype are due to an inability of the human protein to interact with zebrafish proteins.

Lastly, an approach currently ongoing in my lab is to use clustered regularly interspaced short palindromic repeats (CRISPRs) technology to knock out the endogenous zebrafish *bap1* gene. Briefly, the CRISPR/Cas9 system in zebrafish co-opts the CRISPR/Cas prokaryotic immune defense system and involves the design of guide RNAs that direct the Cas9 nuclease to cleave target genes. Guide RNAs targeting *bap1* have been designed and tested (**Table 3.1, Figure 3.2**), and my lab is exploring melanocyte-restricted expression of the Cas9 endonuclease, which would allow for *bap1* cleavage only in melanocytes (Ablain et al., 2015). This could help to promote cancer models of interest to us, such as uveal melanoma, as well as avoid presumed issues with embryonic lethality in a whole-organism *bap1* knockout (*Bap1-/-* is an embryonic lethal mutation in mice; Dey et al., 2012). Knockout of endogenous *bap1* by CRISPR may be a more accurate reflection of BAP1 loss of function than overexpression of the human BAP1 C91S, which may or may not fully sequester endogenous bap1 binding partners. I might also anticipate to observe myeloid transformation in systemic *bap1* mutants because systemic deletion of Bap1 in adult mice recapitulates features of human myelodysplastic syndrome (MDS; Dey et al., 2012). Systemic or tissue-restricted gene disruption using the CRISPR/Cas9 system in zebrafish is a relatively new tool that will be very powerful in my model and other studies.

Chemical screen for modifiers that bypass *bap1* deficiency

Metastatic uveal melanoma is largely untreatable and highly lethal (Gragoudas et al., 2003). A lack of BAP1 protein in uveal melanoma is correlated with increased risk of metastasis (Kalirai et al., 2014). When zebrafish *bap1* mutant heterozygotes are established (or homozygotes, depending on whether embryonic lethality is observed in homozygous mutants), I would perform a chemical screen for drugs that could bypass *bap1* deficiency. I hypothesize that

bap1 mutants would have increased ubiquination of histone 2A, due to the role of BAP1 as a deubiquitinase of H2A (Scheuermann et al., 2010). This would be confirmed by immunoprecipitation of zebrafish H2A from *bap1* mutant embryos, followed by Western blotting for H2A ubiquitination (H2AUb) marks and total H2A levels. I would expect the ratio of H2AUb to total H2A to be higher in *bap1* mutants than in wild-type embryos. If this is not the case in heterozygous mutants because of compensation by the wild-type copy of *bap1*, this screen could be performed following the use of a morpholino to transiently knock down *bap1* in embryos. Hits in a chemical screen for drugs that bypass *bap1* deficiency would be those chemicals that cause a reduction in the ratio of H2AUb to total H2A (to wild-type levels) in *bap1* mutant heterozygotes or *bap1*-morpholino treated embryos. Putative hits would be further analyzed by gene expression, either through microarray or RNAseq. I would assess for the restoration of wild-type gene signatures in drug-treated *bap1* mutants; for example, changes in *hox* gene expression may be expected in the presence of *bap1* loss of function, and this may be a signature to read out bap1 activity. Hits from this screen would be useful in the search for metastatic uveal melanoma therapies, specifically in metastatic uveal melanomas with BAP1 loss of function.

Identifying HOXB7 targets in uveal melanoma

The significant induction of uveal melanomas by HOXB7 was an unexpected result in my study. Published roles for HOXB7 include direct transactivation of bFGF in melanoma cells (Caré et al., 1996), of EGFR in breast cancer cells (Jin et al., 2012), and induction of VEGF in HOXB7-trasnduced breast cancer cells (Caré et al., 2001). While HOXB7 may be inducing any of these growth factor pathways in my uveal melanoma model, the involvement of HOXB7 in

uveal melanoma is novel and new functions could exist for this transcription factor in this context.

One way to broadly assess potential functions of HOXB7 in my uveal melanoma model would be through ChIP-seq analysis of HOXB7 targets. To this end, I have cloned a Myc- and FLAG-tagged HOXB7 construct into our miniCoopR vector. Chromatin immunoprecipitation with an antibody against the Myc or FLAG tags in primary uveal tumors or derived cell lines should allow for efficient pull-down of the HOXB7 transcription factor. Sequencing of bound DNA combined with RNAseq or microarray analysis for expression level changes would reveal which genes were putatively regulated by HOXB7 in these uveal melanomas. Candidates of interest, such as promoters of growth factor pathway genes, would be examined by qPCR and/or RNAseq, and these candidate genes would be tested for functional relevance by cloning them into miniCoopR and overexpressing them in zebrafish melanocytes to screen for a uveal melanoma phenotype. For example, MCR:bFGF, MCR:EGFR, and/or MCR:VEGF animals may exhibit and increased incidence of uveal melanomas. These experiments would help in understanding the particular mechanism of HOXB7 in my uveal melanoma model.

Metastasis studies in transparent adult *casper* fish

One of the hallmarks of uveal melanoma is its propensity to metastasize almost exclusively to the liver (Collaborative Ocular Melanoma Study Group, 2001). There is no cure for metastatic uveal melanoma, and the median survival time is six months or less (Gragoudas et al., 1991). Our method for testing candidate genes using the miniCoopR vector traditionally involves following fish for 25 weeks to observe tumor formation, and metastasis is typically not seen within this timeframe. However, my GNA11 Q209L or HOXB7 uveal melanoma models

would be greatly strengthened if I could demonstrate a preference for these tumors to metastasize to the zebrafish liver. One method to study this would be to utilize the transparent adult zebrafish *casper*, developed in my lab as a tool for *in vivo* transplantation and metastasis analysis.

Casper fish arise from a combination of two zebrafish pigment mutants – *nacre*, an *mitfa*-/- mutant lacking melanocytes, and *roy*, a mutant of unmapped genetic origin that lacks reflective iridophores, most melanocytes, and has translucent skin (White et al., 2008). Using this model, White et al. were able to visualize metastasis of Ras-mutant melanoma cells just five days after transplantation. I would transplant homogenized primary zebrafish uveal melanomas or cell line suspensions into *casper* zebrafish, and these cells would be transplanted in several locations, including intracardiac, intraperitoneal, retro-orbital, or subcutaneous sites (one transplant site per recipient). Preferential engraftment at one site over another would be of interest, in addition to whether or not liver metastases were observed. For example, if retro-orbital transplant sites show greater engraftment of donor cells, I would hypothesize that factors in the ocular microenvironment preferentially promote uveal melanoma proliferation. If these studies were to confirm a liver metastasis phenotype, as determined by histological analysis of the recipient liver post-transplantation, this work would be extended to test for chemical inhibitors of metastasis, either by treating cells pre-transplantation, or administering drugs to the recipient fish post-transplantation. Identification of uveal melanoma metastasis inhibitors would be a major triumph in this area where treatments are ineffective and mortality is high. Taken together, these experiments could provide much information about the importance of the zebrafish uveal melanoma niche, methods of uveal melanoma metastasis, and novel therapeutics for metastatic melanoma.

REFERENCES

1. Abdel-Rahman MH, Pilarski R, Cebulla CM, Massengill JB, Christopher BN, Boru G, Hovland P, Davidorf FH. Germline BAP1 mutation predisposes to uveal melanoma, lung adenocarcinoma, meningioma, and other cancers. *J Med Genet*. **48**, 856-9 (2011).

2. Ablain J, Durand EM, Yang S, Zhou Y, Zon LI. A CRISPR/Cas9 Vector System for Tissue-Specific Gene Disruption in Zebrafish. *Dev Cell*. **32**, 756-64 (2015).

3. Adatto, I., Lawrence, C., Thompson, M. & Zon, L.I. A new system for the rapid collection of large numbers of developmentally staged zebrafish embryos. *PLoS One* **6**, e21715 (2011).

4. Agnelli L, Storti P, Todoerti K, Sammarelli G, Dalla Palma B, Bolzoni M, Rocci A, Piazza F, Semenzato G, Palumbo A, Neri A, Giuliani N. Overexpression of HOXB7 and homeobox genes characterizes multiple myeloma patients lacking the major primary immunoglobulin heavy chain locus translocations. *Am J Hematol*. **86**, E64-6 (2011).

5. Albert DM, Rabson AS, Dalton AJ. In vitro neoplastic transformation of uveal and retinal tissue by oncogenic DNA viruses. *Invest Ophthalmol*. **7**, 357-65 (1968).

6. Albert DM, Shadduck JA, Craft JL, Niederkorn JY. Feline uveal melanoma model induced with feline sarcoma virus. *Invest Ophthalmol Vis Sci*. **20**, 606-24 (1981).

7. All-Ericsson C, Girnita L, Seregard S, Bartolazzi A, Jager MJ, Larsson O. Insulin-like growth factor-1 receptor in uveal melanoma: a predictor for metastatic disease and a potential therapeutic target. *Invest Ophthalmol Vis Sci*. **43**, 1-8 (2002).

8. Altschul, S.F. A protein alignment scoring system sensitive at all evolutionary distances. *J. Mol. Evol*. **36**, 290-300 (1993).

9. Anand R, Ma D, Alizadeh H, Comerford SA, Sambrook JF, Gething MJ, McLean IW, Niederkorn JY. Characterization of intraocular tumors arising in transgenic mice. *Invest Ophthalmol Vis Sci*. **35**, 3533-9 (1994).

10. Asnaghi L, Ebrahimi KB, Schreck KC, Bar EE, Coonfield ML, Bell WR, Handa J, Merbs SL, Harbour JW, Eberhart CG. Notch signaling promotes growth and invasion in uveal melanoma. *Clin Cancer Res*. **18**, 654-65 (2012).

11. Beckwith, L.G., Moore, J.L., Tsao-Wu, G.S., Harshbarger, J.C. & Cheng, K.C. Ethylnitrosourea induces neoplasia in zebrafish (Danio rerio). *Lab Invest* **80**, 379-85 (2000).

12. Bedell, V.M. et al. In vivo genome editing using a high-efficiency TALEN system. *Nature* **491**, 114-8 (2012).

13. Berghmans, S. et al. Making waves in cancer research: new models in the zebrafish. *Biotechniques* **39**, 227-37 (2005).

14. Berghmans, S. et al. tp53 mutant zebrafish develop malignant peripheral nerve sheath tumors. *Proc Natl Acad Sci U S A* **102**, 407-12 (2005).

15. Bitu CC, Carrera M, Lopes MA, Kowalski LP, Soares FA, Coletta RD. HOXB7 expression is a prognostic factor for oral squamous cell carcinoma. *Histopathology*. **60**, 662-5 (2012).

16. Blanco PL, Marshall JC, Antecka E, Callejo SA, Souza Filho JP, Saraiva V, Burnier MN Jr. Characterization of ocular and metastatic uveal melanoma in an animal model. *Invest Ophthalmol Vis Sci*. **46**, 4376-82 (2005).

17. Boyd SR, Tan DS, de Souza L, Neale MH, Myatt NE, Alexander RA, Robb M, Hungerford JL, Cree IA. Uveal melanomas express vascular endothelial growth factor and basic fibroblast growth factor and support endothelial cell growth. *Br J Ophthalmol*. **86**, 440-7 (2002).

18. Bradl M, Klein-Szanto A, Porter S, Mintz B. Malignant melanoma in transgenic mice. *Proc Natl Acad Sci U S A*. **88**, 164-8 (1991).

19. Carbone M, Yang H, Pass HI, Krausz T, Testa JR, Gaudino G. BAP1 and cancer. *Nat Rev Cancer*. **13**, 153-9 (2013).

20. Carè A, Felicetti F, Meccia E, Bottero L, Parenza M, Stoppacciaro A, Peschle C, Colombo MP. HOXB7: a key factor for tumor-associated angiogenic switch. *Cancer Res*. **61**, 6532-9 (2001).

21. Caré A, Silvani A, Meccia E, Mattia G, Stoppacciaro A, Parmiani G, Peschle C, Colombo MP. HOXB7 constitutively activates basic fibroblast growth factor in melanomas. *Mol Cell Biol*. **16**, 4842-51 (1996).

22. Ceol CJ, Houvras Y, Jane-Valbuena J, Bilodeau S, Orlando DA, Battisti V, Fritsch L, Lin WM, Hollmann TJ, Ferré F, Bourque C, Burke CJ, Turner L, Uong A, Johnson LA, Beroukhim R, Mermel CH, Loda M, Ait-Si-Ali S, Garraway LA, Young RA, Zon LI. The histone methyltransferase SETDB1 is recurrently amplified in melanoma and accelerates its onset. *Nature*. **471**, 513-7 (2011).

23. Chang AE, Karnell LH, Menck HR. The National Cancer Data Base report on cutaneous and noncutaneous melanoma: a summary of 84,836 cases from the past decade. The American College of Surgeons Commission on Cancer and the American Cancer Society. *Cancer*. **83**, 1664–78 (1998).

24. Chen X, Wu Q, Tan L, Porter D, Jager MJ, Emery C, Bastian BC. Combined PKC and MEK inhibition in uveal melanoma with GNAQ and GNA11 mutations. *Oncogene*. **33**, 4724-34 (2014).

25. Chile T, Fortes MA, Corrêa-Giannella ML, Brentani HP, Maria DA, Puga RD, de Paula Vde J, Kubrusly MS, Novak EM, Bacchella T, Giorgi RR. HOXB7 mRNA is overexpressed in pancreatic ductal adenocarcinomas and its knockdown induces cell cycle arrest and apoptosis. *BMC Cancer*. **13**, 451 (2013).

26. Choorapoikayil, S., Kuiper, R.V., de Bruin, A. & den Hertog, J. Haploinsufficiency of the genes encoding the tumor suppressor Pten predisposes zebrafish to hemangiosarcoma. *Dis Model Mech* **5**, 241-7 (2012).

27. Cobb MH, Goldsmith EJ. How MAP kinases are regulated. *J Biol Chem*. **270**, 14843–14846 (1995).

28. Collaborative Ocular Melanoma Study Group. Assessment of metastatic disease status at death in 435 patients with large choroidal melanoma in the Collaborative Ocular Melanoma Study (COMS): COMS report no. 15. *Arch Ophthalmol*. **119**, 670-6 (2001).

29. Cruz F 3rd, Rubin BP, Wilson D, Town A, Schroeder A, Haley A, Bainbridge T, Heinrich MC, Corless CL. Absence of BRAF and NRAS mutations in uveal melanoma. *Cancer Res*. **63**, 5761-6 (2003).

30. Dahlem, T.J. et al. Simple methods for generating and detecting locus-specific mutations induced with TALENs in the zebrafish genome. *PLoS Genet* **8**, e1002861 (2012).

31. Davies H, Bignell GR, Cox C, Stephens P, Edkins S, Clegg S, Teague J, Woffendin H, *et al*. Mutations of the BRAF gene in human cancer. *Nature*. **417**, 949-54 (2002).

32. De Rienzo, G., Gutzman, J.H. & Sive, H. Efficient shRNA-mediated inhibition of gene expression in zebrafish. *Zebrafish* **9**, 97-107 (2012).

33. De Waard-Siebinga I, Hilders CG, Hansen BE, van Delft JL, Jager MJ. HLA expression and tumor-infiltrating immune cells in uveal melanoma. *Graefes Arch Clin Exp Ophthalmol*. **234**, 34–42 (1996).

34. Dey A, Seshasayee D, Noubade R, French DM, Liu J, Chaurushiya MS, Kirkpatrick DS, Pham VC, Lill JR, Bakalarski CE, Wu J, Phu L, Katavolos P, LaFave LM, Abdel-Wahab O, Modrusan Z, Seshagiri S, Dong K, Lin Z, Balazs M, Suriben R, Newton K, Hymowitz S, Garcia-Manero G, Martin F, Levine RL, Dixit VM. Loss of the tumor suppressor BAP1 causes myeloid transformation. *Science*. **337**, 1541-6 (2012).

35. Diebold Y, Blanco G, Saornil MA, Fernández N, Lázaro MC. Morphologic and immunocytochemical characterization of four human uveal cell lines (melanoma- and melanocytes-derived). *Curr Eye Res*. **16**, 487-95 (1997).

36. Dimitrijevic, N. et al. Activation of the Xmrk proto-oncogene of Xiphophorus by overexpression and mutational alterations. *Oncogene* **16**, 1681-90 (1998).

37. Dithmar S, Albert DM, Grossniklaus HE. Animal models of uveal melanoma. *Melanoma Res.* **10**, 195-211 (2000).

38. Driever, W. et al. A genetic screen for mutations affecting embryogenesis in zebrafish. *Development* **123**, 37-46 (1996).

39. Errico MC, Felicetti F, Bottero L, Mattia G, Boe A, Felli N, Petrini M, Bellenghi M, Pandha HS, Calvaruso M, Tripodo C, Colombo MP, Morgan R, Carè A. The abrogation of the HOXB7/PBX2 complex induces apoptosis in melanoma through the miR-221&222-c-FOS pathway. *Int J Cancer*. **133**, 879-92 (2013).

40. Feng X, Degese MS, Iglesias-Bartolome R, Vaque JP, Molinolo AA, Rodrigues M, Zaidi MR, Ksander BR, Merlino G, Sodhi A, Chen Q, Gutkind JS. Hippo-independent activation of YAP by the GNAQ uveal melanoma oncogene through a trio-regulated rho GTPase signaling circuitry. *Cancer Cell*. **25**, 831-45 (2014).

41. Feng, Y., Santoriello, C., Mione, M., Hurlstone, A. & Martin, P. Live imaging of innate immune cell sensing of transformed cells in zebrafish larvae: parallels between tumor initiation and wound inflammation. *PLoS Biol* **8**, e1000562 (2010).

42. Foss AJ, Alexander RA, Jefferies LW, et al. Microvessel count predicts survival in uveal melanoma. *Cancer Res* **56**, 2900–3 (1996).

43. Ganis, J.J. et al. Zebrafish globin switching occurs in two developmental stages and is controlled by the LCR. *Dev Biol* **366**, 185-94 (2012).

44. Garneau JE, Dupuis MÈ, Villion M, Romero DA, Barrangou R, Boyaval P, Fremaux C, Horvath P, Magadán AH, Moineau S. The CRISPR/Cas bacterial immune system cleaves bacteriophage and plasmid DNA. *Nature*. **468**, 67-71 (2010).

45. Gasiunas G, Barrangou R, Horvath P, Siksnys V. Cas9-crRNA ribonucleoprotein complex mediates specific DNA cleavage for adaptive immunity in bacteria. *Proc Natl Acad Sci U S A*. **109**, E2579-86 (2012).

46. Golicki, D. et al. Leflunomide in monotherapy of rheumatoid arthritis: meta-analysis of randomized trials. *Pol Arch Med Wewn* **122**, 22-32 (2012).

47. Goll, M.G. & Halpern, M.E. DNA methylation in zebrafish. *Prog Mol Biol Transl Sci* **101**, 193-218 (2011).

48. Gragoudas ES, Egan KM, Seddon JM, Glynn RJ, Walsh SM, Finn SM, Munzenrider JE, Spar MD. Survival of patients with metastases from uveal melanoma. *Ophthalmology*. **98**, 383-9; discussion 390 (1991).

49. Haffter, P. et al. The identification of genes with unique and essential functions in the development of the zebrafish, Danio rerio. *Development* **123**, 1-36 (1996).

50. Harbour JW, Onken MD, Roberson ED, Duan S, Cao L, Worley LA, Council ML, Matatall KA, Helms C, Bowcock AM. Frequent mutation of BAP1 in metastasizing uveal melanomas. *Science*. **330**, 1410-3 (2010).

51. Hirai SI, Ryseck RP, Mechta F, Bravo R, Yaniv M. Characterization of junD: a new member of the jun proto-oncogene family. *EMBO J*. **8**, 1433-9 (1989).

52. Ho AL, Musi E, Ambrosini G, Nair JS, Deraje Vasudeva S, de Stanchina E, Schwartz GK. Impact of combined mTOR and MEK inhibition in uveal melanoma is driven by tumor genotype. *PLoS One*. **7**, e40439 (2012).

53. Höiom V, Edsgärd D, Helgadottir H, Eriksson H, All-Ericsson C, Tuominen R, Ivanova I, Lundeberg J, Emanuelsson O, Hansson J. Hereditary uveal melanoma: a report of a germline mutation in BAP1. *Genes Chromosomes Cancer*. **52**, 378-84 (2013).

54. Hong, S.K., Tsang, M. & Dawid, I.B. The mych gene is required for neural crest survival during zebrafish development. *PLoS One* **3**, e2029 (2008).

55. Hu LK, Huh K, Gragoudas ES, Young LH. Establishment of pigmented choroidal melanomas in a rabbit model. *Retina*. **14**, 264-9 (1994).

56. Hubbard KB, Hepler JR. Cell signalling diversity of the Gqalpha family of heterotrimeric G proteins. *Cell Signal*. **18**, 135–50 (2006).

57. Jensen DE, Proctor M, Marquis ST, Gardner HP, Ha SI, Chodosh LA, Ishov AM, Tommerup N, Vissing H, Sekido Y, Minna J, Borodovsky A, Schultz DC, Wilkinson KD, Maul GG, Barlev N, Berger SL, Prendergast GC, Rauscher FJ 3rd. BAP1: a novel ubiquitin hydrolase which binds to the BRCA1 RING finger and enhances BRCA1-mediated cell growth suppression. *Oncogene*. **16**, 1097-112 (1998).

58. Jin K, Kong X, Shah T, Penet MF, Wildes F, Sgroi DC, Ma XJ, Huang Y, Kallioniemi A, Landberg G, Bieche I, Wu X, Lobie PE, Davidson NE, Bhujwalla ZM, Zhu T, Sukumar S. The HOXB7 protein renders breast cancer cells resistant to tamoxifen through activation of the EGFR pathway. *Proc Natl Acad Sci U S A*. **109**, 2736-41 (2012).

59. Jinek M, Chylinski K, Fonfara I, Hauer M, Doudna JA, Charpentier E. A programmable dual-RNA-guided DNA endonuclease in adaptive bacterial immunity. *Science*. **337**, 816-21 (2012).

60. Joyce, J.A. & Pollard, J.W. Microenvironmental regulation of metastasis. *Nat Rev Cancer* **9**, 239-52 (2009).

61. Kalirai H, Dodson A, Faqir S, Damato BE, Coupland SE. Lack of BAP1 protein expression in uveal melanoma is associated with increased metastatic risk and has utility in routine prognostic testing. *Br J Cancer*. **111**, 1373-80 (2014).

62. Kan-Mitchell J, Mitchell MS, Rao N, Liggett PE. Characterization of uveal melanoma cell lines that grow as xenografts in rabbit eyes. *Invest Ophthalmol Vis Sci*. **30**, 829–834 (1989).

63. Kim DW, Patel SP. Profile of selumetinib and its potential in the treatment of melanoma. *Onco Targets Ther*. **7**, 1631-9 (2014).

64. Kim, H. J., Lee, H. J., Kim, H., Cho, S. W. & Kim, J. S. Targeted genome editing in human cells with zinc finger nucleases constructed via modular assembly. *Genome Res.* **19**, 1279-288 (2009).

65. Knisely TL, Hosoi J, Nazareno R, Granstein RD. The presence of biologically significant concentrations of glucocorticoids but little or no cortisol binding globulin within aqueous humor: relevance to immune privilege in the anterior chamber of the eye. *Invest Ophthalmol Vis Sci*. **35**, 3711-23 (1994).

66. Kujala E, Mäkitie T, Kivelä T. Very long-term prognosis of patients with malignant uveal melanoma. *Invest Ophthalmol Vis Sci*. **44**, 4651-9 (2003).

67. Kumar, Vinay. "Uvea: Neoplasms". *Robbins and Cotran Pathologic Basis of Disease, Professional Edition*. **8th ed**. (2009).

68. Langenau, D.M. et al. Myc-induced T cell leukemia in transgenic zebrafish. *Science* **299**, 887-90 (2003).

69. Laurent C, Valet F, Planque N, Silveri L, Maacha S, Anezo O, Hupe P, Plancher C, Reyes C, Albaud B, Rapinat A, Gentien D, Couturier J, Sastre-Garau X, Desjardins L, Thiery JP, Roman-Roman S, Asselain B, Barillot E, Piperno-Neumann S, Saule S. High PTP4A3 phosphatase expression correlates with metastatic risk in uveal melanoma patients. *Cancer Res*. **71**, 666-74 (2011).

70. Lee CH, Park D, Wu D, Rhee SG, Simon MI. Members of the Gq alpha subunit gene family activate phospholipase C beta isozymes. *J Biol Chem*. **267**, 16044–16047 (1992).

71. Lee KM *et al*. ECM1 regulates tumor metastasis and CSC-like property through stabilization of β-catenin. *Oncogene*. (2015). doi: 10.1038/onc.2015.54.

72. Lee SO, Li X, Khan S, Safe S. Targeting NR4A1 (TR3) in cancer cells and tumors. *Expert Opin Ther Targets*. **15**, 195-206 (2011).

73. Liao WT, Jiang D, Yuan J, Cui YM, Shi XW, Chen CM, Bian XW, Deng YJ, Ding YQ. HOXB7 as a prognostic factor and mediator of colorectal cancer progression. *Clin Cancer Res*. **17**, 3569-78 (2011).

74. Lin L, Sabnis AJ, Chan E1, Olivas V, Cade L, Pazarentzos E, Asthana S, Neel D, Yan JJ, Lu X, Pham L, Wang MM, Karachaliou N, Cao MG, Manzano JL, Ramirez JL5, Torres JM, Buttitta F, Rudin CM, Collisson EA, Algazi A, Robinson E, Osman I, Muñoz-Couselo E, Cortes J, Frederick DT, Cooper ZA, McMahon M, Marchetti A7, Rosell R, Flaherty KT, Wargo JA, Bivona TG. The Hippo effector YAP promotes resistance to RAF- and MEK-targeted cancer therapies. *Nat Genet*. **47**, 250-6 (2015).

75. Lin, W.M. et al. Modeling genomic diversity and tumor dependency in malignant melanoma. *Cancer Res* **68**, 664-73 (2008).

76. Linge A, Kennedy S, O'Flynn D, Beatty S, Moriarty P, Henry M, Clynes M, Larkin A, Meleady P. Differential expression of fourteen proteins between uveal melanoma from patients who subsequently developed distant metastases versus those who did not. *Invest Ophthalmol Vis Sci*. **53**, 4634-43 (2012).

77. Luyten GP, Mooy CM, De Jong PT, Hoogeveen AT, Luider TM. A chicken embryo model to study the growth of human uveal melanoma. *Biochem Biophys Res Commun*. **192**, 22-9 (1993).

78. Ma D, Luyten GP, Luider TM, Niederkorn JY. Relationship between natural killer cell susceptibility and metastasis of human uveal melanoma cells in a murine model. *Invest Ophthalmol Vis Sci*. **36**, 435-41 (1995).

79. Macgregor, S. et al. Genome-wide association study identifies a new melanoma susceptibility locus at 1q21.3. *Nat Genet* **43**, 1114-8 (2011).

80. Machida YJ, Machida Y, Vashisht AA, Wohlschlegel JA, Dutta A. The deubiquitinating enzyme BAP1 regulates cell growth via interaction with HCF-1. *J Biol Chem*. **284**, 34179-88 (2009).

81. Mallery DL, Vandenberg CJ, Hiom K. Activation of the E3 ligase function of the BRCA1/BARD1 complex by polyubiquitin chains. *EMBO J.* **21**, 6755-62 (2002).

82. Maloney SC, Marshall JC, Antecka E, Orellana ME, Fernandes BF, Martins C, Castiglione E, DI Cesare S, Logan P, Burnier MN Jr. SPARC is expressed in human uveal melanoma and its abrogation reduces tumor cell proliferation. *Anticancer Res*. **29**, 3059-64 (2009).

83. McCullough B, Schaller J, Shadduck JA, Yohn DS. Induction of malignant melanomas associated with fibrosarcomas in gnotobiotic cats inoculated with Gardner-feline fibrosarcoma virus. *J Natl Cancer Inst*. **48**, 1893-5 (1972).

84. Meeker ND, Hutchinson SA, Ho L, Trede NS. Method for isolation of PCR-ready genomic DNA from zebrafish tissues. *Biotechniques*. **43**, 610, 612, 614 (2007).

85. Mitsiades N, Chew SA, He B, Riechardt AI, Karadedou T, Kotoula V, Poulaki V. Genotype-dependent sensitivity of uveal melanoma cell lines to inhibition of B-Raf, MEK, and Akt kinases: rationale for personalized therapy. *Invest Ophthalmol Vis Sci*. **52**, 7248-55 (2011).

86. Mou YY, Zhao GQ, Lin JY, Zhao J, Lin H, Hu LT, Xu Q, Wang Q, Sun WR. Research of factors related to invasion and metastasis in choroidal melanoma. *Zhonghua Yan Ke Za Zhi*. **47**, 638-42 (2011).

87. Mueller AJ, Maniotis AJ, Freeman WR, Bartsch DU, Schaller UC, Bergeron-Lynn G, Cheng L, Taskintuna I, Chen X, Kan-Mitchell J, Folberg R. An orthotopic model for human uveal melanoma in SCID mice. *Microvasc Res.* **64**, 207-13 (2002).

88. Murali R, Wiesner T, Scolyer RA. Tumours associated with BAP1 mutations. *Pathology*. **45**, 116-26 (2013).

89. Naor Z, Benard O, Seger R. Activation of MAPK cascades by G-protein-coupled receptors: the case of gonadotropin-releasing hormone receptor. *Trends Endocrinol Metab*. **11**, 91–9 (2000).

90. Nguyen Kovochich A, Arensman M, Lay AR, Rao NP, Donahue T, Li X, French SW, Dawson DW. HOXB7 promotes invasion and predicts survival in pancreatic adenocarcinoma. *Cancer*. **119**, 529-39 (2013).

91. Nishikawa H, Wu W, Koike A, Kojima R, Gomi H, Fukuda M, Ohta T. BRCA1-associated protein 1 interferes with BRCA1/BARD1 RING heterodimer activity. *Cancer Res*. **69**, 111-9 (2009).

92. O'Hayre M, Vázquez-Prado J, Kufareva I, Stawiski EW, Handel TM, Seshagiri S, Gutkind JS. The emerging mutational landscape of G proteins and G-protein-coupled receptors in cancer. *Nat Rev Cancer*. **13**, 412-24 (2013).

93. Onken MD, Worley LA, Ehlers JP, Harbour JW. Gene expression profiling in uveal melanoma reveals two molecular classes and predicts metastatic death. *Cancer Res*. **64**, 7205-9 (2004).

94. Onken MD, Worley LA, Long MD, Duan S, Council ML, Bowcock AM, Harbour JW. Oncogenic mutations in GNAQ occur early in uveal melanoma. *Invest Ophthalmol Vis Sci.* **49,** 5230-4 (2008).

95. Ordonez JL, Paraoan L, Hiscott P, Gray D, García-Fiñana M, Grierson I, Damato B. Differential expression of angioregulatory matricellular proteins in posterior uveal melanoma. *Melanoma Res*. **15**, 495-502 (2005).

96. Park SW, Davison JM, Rhee J, Hruban RH, Maitra A, Leach SD. Oncogenic KRAS induces progenitor cell expansion and malignant transformation in zebrafish exocrine pancreas. *Gastroenterology*. **134**, 2080-90 (2008).

97. Patton EE *et al*. BRAF mutations are sufficient to promote nevi formation and cooperate with p53 in the genesis of melanoma. *Curr Biol*. **15**, 249-54 (2005).

98. Peña-Llopis S, Vega-Rubín-de-Celis S, Liao A, Leng N, Pavía-Jiménez A, Wang S, *et al.* BAP1 loss defines a new class of renal cell carcinoma. *Nat Genet*. **44**, 751-9 (2012).

99. Perez EE, Wang J, Miller JC, Jouvenot Y, Kim KA, Liu O, Wang N, Lee G, *et al*. Establishment of HIV-1 resistance in CD4+ T cells by genome editing using zinc-finger nucleases. *Nat Biotechnol*. **26**, 808-16 (2008).

100. Peterson, R.T., Link, B.A., Dowling, J.E. & Schreiber, S.L. Small molecule developmental screens reveal the logic and timing of vertebrate development. *Proc Natl Acad Sci U S A* **97**, 12965-9 (2000).

101. Pliss, G.B., Zabezhinski, M.A., Petrov, A.S. & Khudoley, V.V. Peculiarities of N-nitramines carcinogenic action. *Arch Geschwulstforsch* **52**, 629-34 (1982).

102. Pollock PM, Cohen-Solal K, Sood R, Namkoong J, Martino JJ, Koganti A, Zhu H *et al*. Melanoma mouse model implicates metabotropic glutamate signaling in melanocytic neoplasia. *Nat Genet*. **34**, 108-12 (2003).

103. Pollock PM, Harper UL, Hansen KS, Yudt LM, Stark M, Robbins CM, Moses TY, Hostetter G, Wagner U, Kakareka J, Salem G, Pohida T, Heenan P, Duray P, Kallioniemi O, Hayward NK, Trent JM, Meltzer PS. High frequency of BRAF mutations in nevi. *Nat Genet*. **33**, 19-20 (2003).

104. Premsrirut, P.K. et al. A rapid and scalable system for studying gene function in mice using conditional RNA interference. *Cell* **145**, 145-58 (2011).

105. Rhodes DR, Yu J, Shanker K, Deshpande N, Varambally R, Ghosh D, Barrette T, Pandey A, Chinnaiyan AM. ONCOMINE: a cancer microarray database and integrated data-mining platform. *Neoplasia*. **6**, 1-6 (2004).

106. Ridges, S. et al. Zebrafish screen identifies novel compound with selective toxicity against leukemia. *Blood* **119**, 5621-31 (2012).

107. Roland K, Hayungs J, Bronfeld N, Sauerwein W. Prognosis and Treatment of Disseminated Uveal Melanoma. *Cancer*. **72**, 2219-2223 (1993).

108. Rozengurt E. Mitogenic signaling pathways induced by G protein-coupled receptors. *J Cell Physiol*. **213**, 589–602 (2007).

109. Saldanha G, Purnell D, Fletcher A, Potter L, Gillies A, Pringle JH. High BRAF mutation frequency does not characterize all melanocytic tumor types. *Int J Cancer*. **111**, 705-10 (2004).

110. Saraiva VS, Caissie AL, Segal L, Edelstein C, Burnier MN Jr. Immunohistochemical expression of phospho-Akt in uveal melanoma. *Melanoma Res*. **15**, 245-50 (2005).

111. Saville, M.K. & Watson, R.J. B-Myb: a key regulator of the cell cycle. *Adv Cancer Res* **72**, 109-40 (1998).

112. Scheuermann JC, de Ayala Alonso AG, Oktaba K, Ly-Hartig N, McGinty RK, Fraterman S, Wilm M, Muir TW, Müller J. Histone H2A deubiquitinase activity of the Polycomb repressive complex PR-DUB. *Nature*. **465**, 243-7 (2010).

113. Schiffner S, Braunger BM, de Jel MM, Coupland SE, Tamm ER, Bosserhoff AK. Tg(Grm1) transgenic mice: a murine model that mimics spontaneous uveal melanoma in humans? *Exp Eye Res*. **127**:59-68 (2014).

114. Schöneberg T, Kostenis E, Liu J, Gudermann T, Wess J. Molecular aspects of vasopressin receptor function. *Adv Exp Med Biol*. **449**, 347-58 (1998).

115. Schulte-Merker S, van Eeden FJ, Halpern ME, Kimmel CB, Nüsslein-Volhard C. no tail (ntl) is the zebrafish homologue of the mouse T (Brachyury) gene. *Development*. **120**, 1009-15 (1994).

116. Scott MP. Vertebrate homeobox gene nomenclature. *Cell*. **71**, 551-3 (1992).

117. Shih, A.H., Abdel-Wahab, O., Patel, J.P. & Levine, R.L. The role of mutations in epigenetic regulators in myeloid malignancies. *Nat Rev Cancer* **12**, 599-612 (2012).

118. Singh AD, Topham A. Incidence of uveal melanoma in the United States: 1973–1997. *Ophthalmology*. **110**, 956–61 (2003).

119. Spitsbergen, J.M. *et al*. Neoplasia in zebrafish (Danio rerio) treated with 7,12-dimethylbenz[a]anthracene by two exposure routes at different developmental stages. *Toxicol Pathol* **28**, 705-15 (2000).

120. Spitsbergen, J.M. *et al*. Neoplasia in zebrafish (Danio rerio) treated with N-methyl-N'-nitro-N-nitrosoguanidine by three exposure routes at different developmental stages. *Toxicol Pathol* **28**, 716-25 (2000).

121. Stern, H.M. *et al*. Small molecules that delay S phase suppress a zebrafish bmyb mutant. *Nat Chem Biol* **1**, 366-70 (2005).

122. Stoletov, K. & Klemke, R. Catch of the day: zebrafish as a human cancer model. *Oncogene* **27**, 4509-20 (2008).

123. Storti P. *et al*. HOXB7 expression by myeloma cells regulates their pro-angiogenic properties in multiple myeloma patients. *Leukemia*. **25**, 527-37 (2011).

124. Sun H, Charles CH, Lau LF, Tonks NK. MKP-1 (3CH134), an immediate early gene product, is a dual specificity phosphatase that dephosphorylates MAP kinase in vivo. *Cell*. **75**, 487-93 (1993).

125. Sun Y, Tran BN, Worley LA, Delston RB, Harbour JW. Functional analysis of the p53 pathway in response to ionizing radiation in uveal melanoma. *Invest Ophthalmol Vis Sci*. **46**, 1561-4 (2005).

126. Tolleson WH, Doss JC, Latendresse J, Warbritton AR, Melchior WB Jr, Chin L, Dubielzig RR, Albert DM. Spontaneous uveal amelanotic melanoma in transgenic Tyr-RAS+ Ink4a/Arf-/- mice. *Arch Ophthalmol*. **123**, 1088-94 (2005).

127. Tschentscher F, Hüsing J, Hölter T, Kruse E, Dresen IG, Jöckel KH, Anastassiou G, Schilling H, Bornfeld N, Horsthemke B, Lohmann DR, Zeschnigk M. Tumor classification based on gene expression profiling shows that uveal melanomas with and without monosomy 3 represent two distinct entities. *Cancer Res*. **63**, 2578-84 (2003).

128. Van der Ent W, Burrello C, Teunisse AF, Ksander BR, van der Velden PA, Jager MJ, Jochemsen AG, Snaar-Jagalska BE. Modeling of human uveal melanoma in zebrafish xenograft embryos. *Invest Ophthalmol Vis Sci.* **55**, 6612-22 (2014).

129. Van Leeuwen, C.J., Grootelaar, E.M. & Niebeek, G. Fish embryos as teratogenicity screens: a comparison of embryotoxicity between fish and birds. *Ecotoxicol Environ Saf* **20**, 42-52 (1990).

130. Van Raamsdonk CD, Bezrookove V, Green G, Bauer J, Gaugler L, O'Brien JM, Simpson EM, Barsh GS, Bastian BC. Frequent somatic mutations of GNAQ in uveal melanoma and blue naevi. *Nature*. **457**, 599-602 (2009).

131. Van Raamsdonk CD, Griewank KG, Crosby MB, Garrido MC, Vemula S, Wiesner T, Obenauf AC, Wackernagel W, Green G, Bouvier N, Sozen MM, Baimukanova G, Roy R, Heguy A, Dolgalev I, Khanin R, Busam K, Speicher MR, O'Brien J, Bastian BC. Mutations in GNA11 in uveal melanoma. *N Engl J Med.* **363**, 2191-9 (2010).

132. von Euw E, Atefi M, Attar N, Chu C, Zachariah S, Burgess BL, Mok S, Ng C, Wong DJ, Chmielowski B, Lichter DI, Koya RC, McCannel TA, Izmailova E, Ribas A. Antitumor effects of the investigational selective MEK inhibitor TAK733 against cutaneous and uveal melanoma cell lines. *Mol Cancer*. **11**, 22 (2012).

133. White R, Rose K, Zon L. Zebrafish cancer: the state of the art and the path forward. *Nat Rev Cancer*. **13**, 624-36 (2013).

134. White RM, Cech J, Ratanasirintrawoot S, Lin CY, Rahl PB, Burke CJ, Langdon E, Tomlinson ML, Mosher J, Kaufman C, Chen F, Long HK, Kramer M, Datta S, Neuberg D, Granter S, Young RA, Morrison S, Wheeler GN, Zon LI. DHODH modulates transcriptional elongation in the neural crest and melanoma. *Nature*. **471**, 518-22 (2011).

135. White RM, Sessa A, Burke C, Bowman T, LeBlanc J, Ceol C, Bourque C, Dovey M, Goessling W, Burns CE, Zon LI. Transparent adult zebrafish as a tool for in vivo transplantation analysis. *Cell Stem Cell*. **2**, 183-9 (2008).

136. Wiesner T, Murali R, Fried I, Cerroni L, Busam K, Kutzner H, Bastian BC. A distinct subset of atypical Spitz tumors is characterized by BRAF mutation and loss of BAP1 expression. *Am J Surg Pathol*. **36**, 818-30 (2012).

137. Wu DQ, Lee CH, Rhee SG, Simon MI. Activation of phospholipase C by the alpha subunits of the Gq and G11 proteins in transfected Cos-7 cells. *J Biol Chem*. **267**, 1811–1817 (1992).

138. Wu X, Chen H, Parker B, Rubin E, Zhu T, Lee JS, Argani P, Sukumar S. HOXB7, a homeodomain protein, is overexpressed in breast cancer and confers epithelial-mesenchymal transition. *Cancer Res*. **66**, 9527-34 (2006).

139. Wu X, Li J, Zhu M, Fletcher JA, Hodi FS. Protein kinase C inhibitor AEB071 targets ocular melanoma harboring GNAQ mutations via effects on the PKC/Erk1/2 and PKC/NF-κB pathways. *Mol Cancer Ther*. **11**, 1905-14 (2012).

140. Wu X, Zhu M, Fletcher JA, Giobbie-Hurder A, Hodi FS. The protein kinase C inhibitor enzastaurin exhibits antitumor activity against uveal melanoma. *PLoS One*. **7**, e29622 (2012).

141. Wu, S.F. et al. DNA methylation profiling in zebrafish. *Methods Cell Biol* **104**, 327-39 (2011).

142. Xu J, Kadariya Y, Cheung M, Pei J, Talarchek J, Sementino E, Tan Y, Menges CW, Cai KQ, Litwin S, Peng H, Karar J, Rauscher FJ, Testa JR. Germline mutation of Bap1 accelerates development of asbestos-induced malignant mesothelioma. *Cancer Res*. **74**, 4388-97 (2014).

143. Yang H, Fang G, Huang X, Yu J, Hsieh CL, Grossniklaus HE. In-vivo xenograft murine human uveal melanoma model develops hepatic micrometastases. *Melanoma Res*. **18**, 95-103 (2008).

144. Zuidervaart W, van Nieuwpoort F, Stark M, Dijkman R, Packer L, Borgstein AM, Pavey S, van der Velden P, Out C, Jager MJ, Hayward NK, Gruis NA. Activation of the MAPK pathway is a common event in uveal melanomas although it rarely occurs through mutation of BRAF or RAS. *Br J Cancer*. **92**, 2032-8 (2005).

Appendix

SUPPLEMENTARY FIGURES AND TABLES

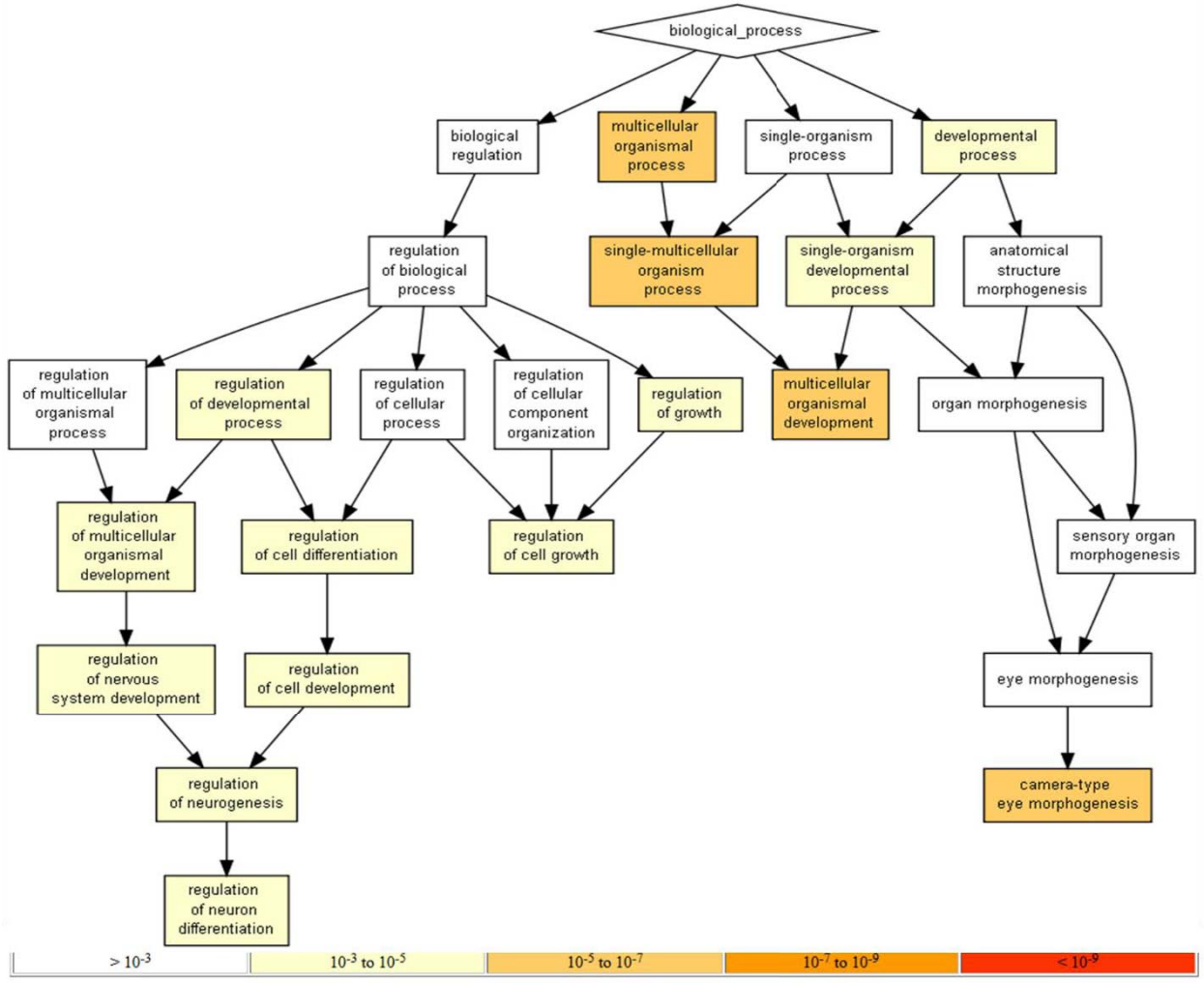

Supplementary Figure S1. Enriched Gene Ontology (GO) terms in zebrafish uveal melanoma gene signature.

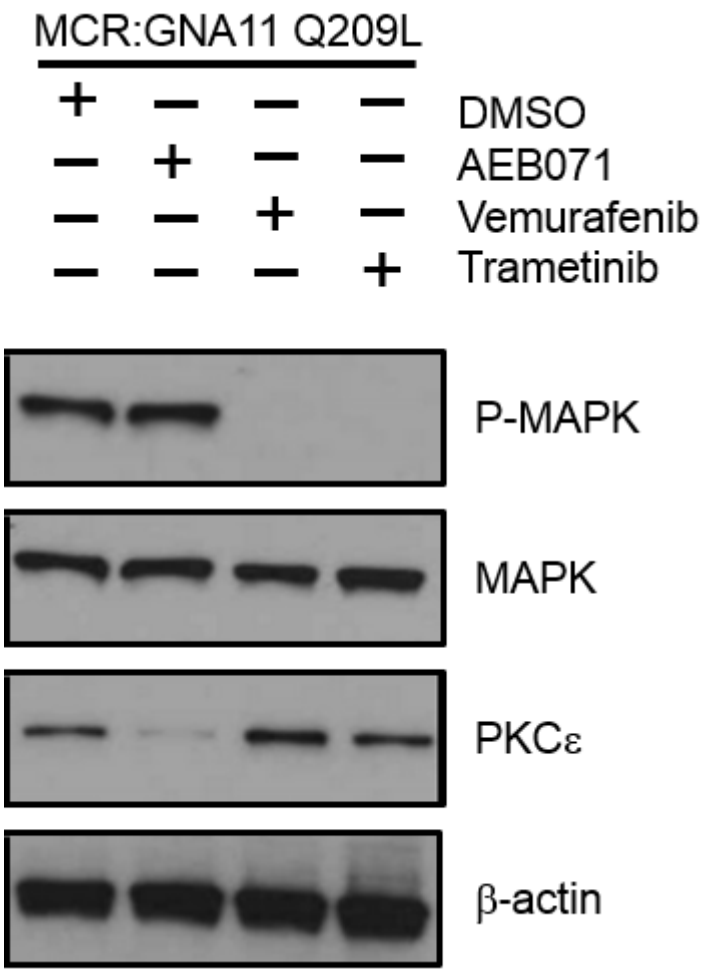

Supplementary Figure S2. The effect of PKC, BRAF, or MEK inhibition on target proteins in GNA11 Q209L-overexpressing uveal melanoma cells. MAPK (ERK1/2), P-MAPK (phosphor-ERK1/2) and PKC ε expression were visualized through Western blot analysis in cells treated for 48 h with DMSO, 5 μM AEB071, 20 μM vemurafenib, or 0.1 μM trametinib.

Supplementary Table S1. Human orthologs of genes in zebrafish uveal melanoma signature.

ADIPOR2	DDIT3	KDELR2	POLR2L	YWHAE
AIP	DDX3X	KLF6	PRRX1	YWHAQ
ALAS1	DDX3X	KRT18	PSMC2	
ANXA1	DHCR24	LASP1	PTP4A1	
ANXA11	DUSP1	LDHA	RAP1B	
ANXA2	EFEMP2	LMO4	RPLP0	
AP1S2	EIF2S2	LSM4	RPS7	
AP2M1	EIF4G2	LSS	SEC13	
ARHGDIA	EMILIN1	MAFK	SERPINE1	
ARL6IP5	EZR	MANF	SGK1	
ATP5I	F3	MARCKSL1	SLC25A22	
BRK1	FAM20A	MEIS1	SLC38A2	
BUD31	FBL	MMP2	SLMO2	
CALM1	FHL1	MTDH	SOCS3	
CAPN2	GADD45B	MYL9	SPARC	
CAPNS1	GJA1	NDUFA11	SRSF5	
CAPZA1	GLTSCR2	NDUFB5	SSB	
CD9	GLUL	NDUFS1	STC2	
CDC42SE1	GRINA	NHP2	SUMO1	
CKB	HARS	NME3	TAX1BP3	
CNN2	HAS1	NOP58	TCEB2	
COPG2	HN1	NR4A1	TIMP2	
CPNE1	HSP90AB1	PA2G4	TMBIM1	
CSRNP1	HSP90B1	PFDN5	TMEM256	
CTGF	ID3	PFDN6	TOMM20	
CTGF	IER5	PIM1	TPMT	
CTHRC1	IRF2BP2	PLEC	TRIB3	
CTSK	JAM3	PMP22	TXNDC9	
CYR61	JUNB	PMP22	WDR1	
DCTN2	JUND	POLR2E	WLS	

Supplementary Table S2. Gene Ontology terms for camera-type eye morphogenesis in zebrafish uveal melanoma signature.

GO term Description	P-value	FDR q-value	Enrichment	# of genes	Genes
camera-type eye morphogenesis	7.86E-06	1.15E-02	24.39	4	[cdh4, pitx2, rx3, aldh1a2]

Supplementary Table S3. Top upstream regulators by IPA analysis of zebrafish uveal melanoma signature genes.

Upstream Regulator	Molecule Type	p-value of c
TP53	transcription regulator	6.39E-19
PDGF BB	complex	2.87E-17
TGFB1	growth factor	7.72E-14
CTNNB1	transcription regulator	1.35E-12
beta-estradiol	chemical - endogenous mammalian	3.00E-12
FOS	transcription regulator	3.06E-12
MYC	transcription regulator	5.98E-12
dexamethasone	chemical drug	1.14E-11
forskolin	chemical toxicant	1.20E-11
PD98059	chemical - kinase inhibitor	4.44E-11
LY294002	chemical - kinase inhibitor	8.73E-11
lipopolysaccharide	chemical drug	1.39E-10
TNF	cytokine	2.41E-10
IPMK	kinase	2.55E-10
JUN	transcription regulator	6.43E-10
IL1B	cytokine	6.83E-10
HGF	growth factor	1.09E-09
SB203580	chemical - kinase inhibitor	1.18E-09
VEGFA	growth factor	1.41E-09
hydrogen peroxide	chemical - endogenous mammalian	1.86E-09
LDL	complex	2.57E-09
TNFSF11	cytokine	4.74E-09
Pkc(s)	group	4.77E-09
HRAS	enzyme	5.88E-09
P38 MAPK	group	8.54E-09
PTEN	phosphatase	1.55E-08
tanespimycin	chemical drug	1.60E-08
NME1	kinase	1.95E-08
tretinoin	chemical - endogenous mammalian	1.98E-08
epigallocatechin-gallate	chemical drug	2.12E-08
U0126	chemical - kinase inhibitor	4.58E-08
Jnk	group	4.75E-08
EGF	growth factor	5.06E-08
FSH	complex	5.11E-08
EPAS1	transcription regulator	5.23E-08
F2R	g-protein coupled receptor	9.95E-08
carbon tetrachloride	chemical toxicant	1.08E-07
D-glucose	chemical - endogenous mammalian	1.19E-07
simvastatin	chemical drug	1.22E-07
INSR	kinase	1.29E-07

Supplementary Table S4. Top canonical pathways associated with zebrafish uveal melanoma signature genes by IPA analysis.

Ingenuity Canonical Pathways	Molecules
Glucocorticoid Receptor Signaling	POLR2L,DUSP1,SGK1,HSP90B1,POLR2E,SERPINE1,HSP90AB1,ANXA1
nNOS Signaling in Neurons	CALM1 (includes others),GRINA,CAPNS1,CAPN2
Amyotrophic Lateral Sclerosis Signaling	GLUL,GRINA,CAPNS1,CAPN2
Oxidative Phosphorylation	NDUFA11,NDUFB5,ATP5I,NDUFS1
Hepatic Fibrosis / Hepatic Stellate Cell Activation	MMP2,KLF6,CTGF,MYL9,SERPINE1
Corticotropin Releasing Hormone Signaling	JUND,CALM1 (includes others),NR4A1,RAP1B
Regulation of Cellular Mechanics by Calpain Protease	EZR,CAPNS1,CAPN2
PCP pathway	JUND,CTHRC1,JUNB
Glutamate Receptor Signaling	GLUL,CALM1 (includes others),GRINA
Hypoxia Signaling in the Cardiovascular System	HSP90B1,LDHA,HSP90AB1
Calcium-induced T Lymphocyte Apoptosis	CALM1 (includes others),NR4A1,CAPN2
Endoplasmic Reticulum Stress Pathway	HSP90B1,DDIT3
Huntington's Disease Signaling	POLR2L,SGK1,POLR2E,CAPNS1,CAPN2
Aldosterone Signaling in Epithelial Cells	DUSP1,SGK1,HSP90B1,HSP90AB1
Prostate Cancer Signaling	HSP90B1,PA2G4,HSP90AB1
PPAR Signaling	AIP,HSP90B1,HSP90AB1
Protein Kinase A Signaling	CALM1 (includes others),DUSP1,KDELR2,PTP4A1,RAP1B,MYL9
PPARα/RXRα Activation	AIP,HSP90B1,ADIPOR2,HSP90AB1
Calcium Signaling	CALM1 (includes others),GRINA,RAP1B,MYL9
Mitochondrial Dysfunction	NDUFA11,NDUFB5,ATP5I,NDUFS1
EIF2 Signaling	EIF2S2,RPS7,RPLP0,EIF4G2
Coagulation System	F3,SERPINE1
Nucleotide Excision Repair Pathway	POLR2L,POLR2E
Agranulocyte Adhesion and Diapedesis	MMP2,EZR,MYL9,JAM3
Integrin Signaling	RAP1B,MYL9,CAPNS1,CAPN2
Cholesterol Biosynthesis I	LSS,DHCR24
Cholesterol Biosynthesis II (via 24,25-dihydrolanosterol)	LSS,DHCR24
Cholesterol Biosynthesis III (via Desmosterol)	LSS,DHCR24
Lanosterol Biosynthesis	LSS
Leukocyte Extravasation Signaling	MMP2,EZR,RAP1B,JAM3

Supplementary Figure S5. Cutaneous and uveal melanoma cell lines analyzed by RNAseq.

Cell line Annotation	Cell line ID	origin
JR1	A375	cutaneous
RF1	CJM	cutaneous
RF2	COLO	cutaneous
RF3	LOXIMVI	cutaneous
RF4	SKMEL2	cutaneous
RF5	SKMEL5	cutaneous
RF6	SKMEL30	cutaneous
RF7	UACC	cutaneous
UMCL-92.1	92.1	uveal
UMCL-Mel1202A	Mel1202A	uveal
UMCL-Mel1285A	Mel1285A	uveal
UMCL-Ocm8A	Ocm8A	uveal
UMCL-Omm1A	Omm1A	uveal
UMCL-Omm2.3A	Omm2.3A	uveal

Supplementary Table S6. Primer sequences for qRT-PCR analysis of Hox genes.

Target ger	Primer ID	Sequence (5'-3')
hoxa1a	Forward	tggatgaaggttaaacgcaa
	Reverse	cgaaaaattggtgcgtacag
hoxa13a	Forward	tgtggaagtcgtcaatacca
	Reverse	ggtatatggaacacgtttctt
hoxb7a	Forward	cgaaaacaacctccgaatct
	Reverse	gtctgacggcctcttttcc
hoxb13a	Forward	ctaacggatggggtagtcag
	Reverse	tggtgggccacaacatct
hoxc8a	Forward	agcctcatgttcccttggat
	Reverse	gctgtatgtctgccttccatt
hoxc13a	Forward	tggaaatctccctttccaga
	Reverse	ccacgtcgataactgctgac
hoxd3a	Forward	agcagaaaagcaccaactg
	Reverse	caggcggactcttgtcatc
hoxd9a	Forward	acggtgagcctaaagacga
	Reverse	ttcttgttgatctcgcatgg

Supplementary Table S7. Sequences of primers used to amplify *bap1* target sites for T7E1 assay.

Target sequence 1: GGATCGAGGAGCGAAGATCT (direct)
FW : GTACACACATTTACACAAGT (Tm=57°C)
RV : GGGTTAAGGCTTCATTTTGT (Tm=59°C)
381 bp amplicon (250 + 130)
Target sequence 2: GGGCGTGTCTTCTGAAGAAG (reverse)
FW : GAGTATTAGGCTACCTGTGA (Tm=58°C)
RV: GACAACAGCAGTTATTCGCT (Tm=61°C)
446 bp amplicon (310 + 130)
Target sequence 3 : GGTGGTGGAGCGCCCCCTGC (reverse)
FW : GCAATGACCTTTAAGTCAAA (Tm=57°C)
RV : CTCCTCCTCTTCATCATCAT (Tm=59°C)
453 bp amplicon (290 + 160)
Target sequence 4: GGCTGGTAGACGCTGCACAA (reverse)
FW : CATCAGAAACTCAAGAAGGT (Tm=58°C)
RV : GGAGATTTGTTACAACGACA (Tm=59°C)
438 bp amplicon (310 + 130)
Target sequence 5: GGAGGATCTTGCTGCAGGTG (direct)
FW : CATCAGAAACTCAAGAAGGT (Tm=58°C)
RV : GGAGATTTGTTACAACGACA (Tm=59°C)
438 bp amplicon (300 + 140)
FW = forward primer sequence
RV = reverse primer sequence
Tm = melting temperature of primer